Anisotropic Molecular Orientation and Enhanced Thermal Stability in Vapor-Deposited Glasses of Organic Semiconductors

By

Diane M. Walters

A dissertation submitted in partial fulfillment of

the requirements for the degree of

Doctor of Philosophy

(Chemistry)

at the

UNIVERSITY OF WISCONSIN-MADISON

2017

Date of final oral examination: 05/11/2017

The dissertation is approved by the following members of the Final Oral Committee:

Mark D. Ediger, Professor, Chemistry
Lian Yu, Professor, Pharmaceutical Sciences
Gilbert Nathanson, Professor, Chemistry
Paul Voyles, Professor, Materials Science and Engineering
Arun Yethiraj, Professor, Chemistry

Acknowledgements

First and foremost, I would like to thank my advisor, Prof. Mark Ediger. Mark, you embody everything I ever hoped to be as a scientist. I admire your poise, careful thinking, and constant effort to listen and learn in order to grow as a researcher and advisor. Thank you for all of the time you have spent mentoring me. I feel every conversation with you makes me want to be a better scientist and a better person. I am honored to have worked with you.

I would like to thank the entire Ediger group, past and present. You taught me that my passion lies in doing science with other people, and I could not have chosen a better group to join. Shakeel Dalal, thank you for mentoring me when I joined the group. You designed an entire short course for teaching Ankit and me the fundamentals of ellipsometry, and it is something I use to this day to train others. Maddy Beasley, thank you for organizing the group and doing fantastic science to boot. Your bravery in tackling climate issues and creating an inclusive environment are a big part of why this group is so fantastic. Yue Qui, Camille Bishop, and Marie Fiori, you are incredibly thoughtful, talented scientists, and I know I am leaving the ellipsometer in good hands. Ankit Gujral, we joined the group together and it has been a fantastic five years working with you. Noah Johnson, I am so fortunate to have worked with such a talented undergraduate and I am excited to hear about your future work in Sydney, Chicago, and beyond. Travis Powell, thank you figuring out transparent substrates with me when I needed someone to work with the most. Your careful science and perseverance facing problems was reenergizing. Mike Tylinski, your enthusiasm for science and life was infectious and made every conversation with you enlightening. Thanks for being a great labmate. Kelly

Hebert and Jartiza Gomez, thank you so much for your friendship and support my last few years of graduate school and during my job search. I look forward to joining you at Intel! Katie Whitaker, Alfonso Sepúlveda, Ben Bending, Josh Ricci, Jing Jiang, Aundrey Laventure, Yeong Zen Chua, Trevor Bennin, Kushal Bagchi, Niko Van den Brande, and Ben Kasting: thank you for being such fantastic colleagues!

The UW Madison chemistry department has an incredible staff that makes the place run. I would like to thank April Sonnentag, Cheri Stephens, Kristi Heming, Sue Martin, Bruce Goldade, and Chad Skemp who have helped me navigate purchases, going to conferences, and organizing seminars. Bill Goebel in the electronic shop and Kendall Schneider and Steve Meyers in the machine shop instilled in me the confidence that, with their incredible design and machining skills backing me up, I could build or fix any equipment. I would particularly like to thank Arrietta Clauss for her tireless work connecting students with the outside world, whether that is navigating the graduate school's regulations or interviewing with potential employers. She made a stressful job hunt immensely much more bearable.

I would like to thank the UW Madison Writing Center and Dr. John Puentes. If you are reading this and have a thesis to write, I cannot urge you enough to go to the Writing Center. You will find a community of writers waiting to advise and support you.

I have been fortunate enough to have many influential teachers in my life, but none more so than Prof. Daniela Kohen, my undergraduate research advisor at Carleton College. Dani opened a spot in her lab to me when I was not sure what "research" entailed; I just knew I wanted to dive deeper into chemistry. She taught me the value of a good presentation and

clear communication, introduced me to UW Madison, and taught me that graduate school was about so much more than just taking classes.

My family has been my bedrock throughout my time in graduate school. Mom, Dad, and Scott, words fail to express my love and gratitude for you. Our regular phone calls are so enjoyable and I appreciate you constant support. Our family has had so many milestones the past few years: graduations, new jobs, retirement, cross-country moves. I look forward to all of the ones still to come.

My friends in Madison have been essential to my happiness and success in graduate school. Mary Van Vleet, I have learned as much from you as I have in earning my PhD. Thank you for being such an amazing friend. Adam Denny, Britta Johnson, Tom McDonough, Aaron Wright, Trevor Kuehl: you can turn cooking dinner on a weekday evening into a festive occasion with good conservation, music, and board games. Every slow food, bike ride, and game night was such fun with you there. Thank you for being fantastic friends! I would also like to thank my entire physical chemistry cohort. Corn mazes, problem sets in the TA office, Hirschfelder dinners, game nights at Barriques, Sailor Moon costumes, swants, TBOs, RPs, and now defenses… I cannot imagine a more fun and talented group of chemists to be my colleagues and friends. Thank you!

Finally, I would like to thank the Madison Ultimate Frisbee community, particularly the chemistry department teams. I am honored to have been your “Captain Diane.”

Table of Contents

Abstract

Vapor deposition is commonly used to prepare active layers in organic electronic devices. For model systems, vapor-deposited glasses have shown extraordinary properties such as enhanced thermal stability, high density, low enthalpy, and increased photostability. When annealed above T_g, the glass transition temperature, vapor-deposited glasses transform via fronts initiated at the free surface or other interfaces with high mobility, a mechanism only seen in vapor-deposited glasses due to their exceptionally high stability. These properties are attributed to enhanced equilibration on the glass surface allowing molecules to find more stable, lower energy packing configurations during the deposition process. However, it is unclear if this mechanism is general for systems used in organic electronics. Additionally, enhanced equilibration alone cannot explain the anisotropic packing seen in vapor-deposited glasses of both model glassformers and organic semiconductors. Anisotropic molecular orientation enhances the performance of active layers, but controlling this property is a challenge in amorphous materials.

In this thesis, I present my studies of the thermal stability and anisotropic molecular orientation in vapor-deposited glasses for six molecules used as organic semiconductors and emitters. I use a high-throughput sample preparation protocol to simultaneously deposit many glasses with different substrate temperatures. I characterize them using spectroscopic ellipsometry. For all the systems studied, I find that a wide range of substrate temperatures can prepare glasses with enhanced thermal stability. For one organic semiconductor, I study the transformation behavior when it is annealed above T_g and observe that it transforms via a front mechanism. By developing a high throughput annealing protocol, I establish that the front

velocity is independently determined by the mobility of the transformed liquid at the annealing temperature and the structure of the vapor-deposited glass.

Additionally, all the systems studied show anisotropic molecular orientation when vapor-deposited with a wide range of substrate temperatures. Molecules with similar molecular shapes show similar trends in molecular orientation when the substrate temperature is normalized by T_g. However, rod- and disk-shaped molecules have different trends in molecular orientation. Simulations of the equilibrium liquid show anisotropic molecular orientation near the surface, and rod- and disk-shaped molecules have different trends in this anisotropic structure. Coarse-grained models of the rod- and disk-shaped molecules are constructed, and the equilibrium liquid of these systems with simple shapes and lacking specific interactions also show anisotropic molecular orientation. Furthermore, simulations of the vapor-deposition process for a coarse-grained rod reproduce the trends in the experiments and suggest an orientation mechanism.

We propose that enhanced thermal stability and anisotropic molecular orientation in vapor-deposited glasses are due to enhanced equilibration at the glass surface during the deposition. Molecules on the surface equilibrate to more stable structures and obtain molecular orientations favorable near the free surface of the equilibrium liquid. These configurations are then trapped by subsequent deposition, resulting in a bulk glass that is stable and has anisotropic molecular orientation otherwise only seen at the free surface. I show this mechanism is general for different molecular shapes. Establishing a general mechanism for stability and molecular orientation could inform the choice of materials and deposition conditions for active layers and improve the performance of organic electronic devices.

Chapter 1

Introduction

Glasses are materials that lack periodicity. Unlike crystals that have a well-defined unit cell that repeats in all directions within the material, a glass is more disordered and has a structure that more closely resembles a liquid. In our everyday lives, the term “glass” is primarily used to describe silicate oxide glasses that make-up objects like windows and cups. However, glasses of organic or metallic materials are also all around us. Polymer glasses are used in products ranging from polystyrene plastic cutlery to Kevlar body armor. Molecular glasses are seen in foods, like Lifesavers or fudge, and many pharmaceuticals have amorphous states, such as indomethacin, an anti-inflammatory. Metallic glasses can be found in sporting equipment like golf club faces. Understanding and controlling the properties of these ubiquitous materials that lack a uniform structure is one of the primary challenges of glass science.

In the work presented here, I study how molecular structure and preparation conditions can influence the properties of vapor-deposited glasses. Vapor deposition has been shown to prepare glasses with exceptional properties such as enhanced thermal stability and anisotropic molecular orientation. For the first time, I characterize these features for molecules with different molecular shapes deposited over a wide range of substrate temperatures. Using primarily spectroscopic ellipsometry, I find the thermal stability and molecular orientation are tunable with substrate temperatures and molecular orientation differs for molecules with different molecular shapes. The glasses transform by a front-based mechanism only seen in highly stable vapor-deposited glasses. I explain these results in terms of enhanced equilibration

at the glass surface during the deposition and, for the first time, offer a general explanation for both thermal stability and anisotropic molecular orientation for vapor-deposited glasses of a wide variety of molecules. The organic molecules studied here have been used in hole-transport and emitting layers in organic electronic devices, and my thesis seeks to bridge the divide between research on the fundamental properties of glasses and applications-based research on organic semiconductors and emitters.

This chapter will provide context and background for the content of my thesis. Section 1 defines a glass in greater detail and describes fundamental properties of supercooled liquids and glasses. Section 2 explains how vapor deposition can be used to prepare glass films and the extraordinary properties of these films. Section 3 describes the mechanism for how vapor-deposited glasses transform to the supercooled liquid when heated. Section 4 gives a brief history of the characterization of molecular orientation in amorphous material and summarizes what was known before my thesis work on the anisotropic molecular orientation in vapor-deposited glass films. Section 5 gives an overview on spectroscopic ellipsometry, a key tool in characterizing thin films and the primary technique I used to measure molecular orientation and stability in vapor-deposited glasses for the work presented in this thesis. Section 6 provides an overview of the major contributions of my thesis to the general body of knowledge.

1.1. Supercooled Liquids and Glasses

One of the most common methods of preparing a glass is by cooling a liquid. As illustrated in Figure 1.1, a material has a high enthalpy, entropy, and specific volume as a liquid. On cooling, the material thermally contracts and its enthalpy and entropy decreases. At T_m, the

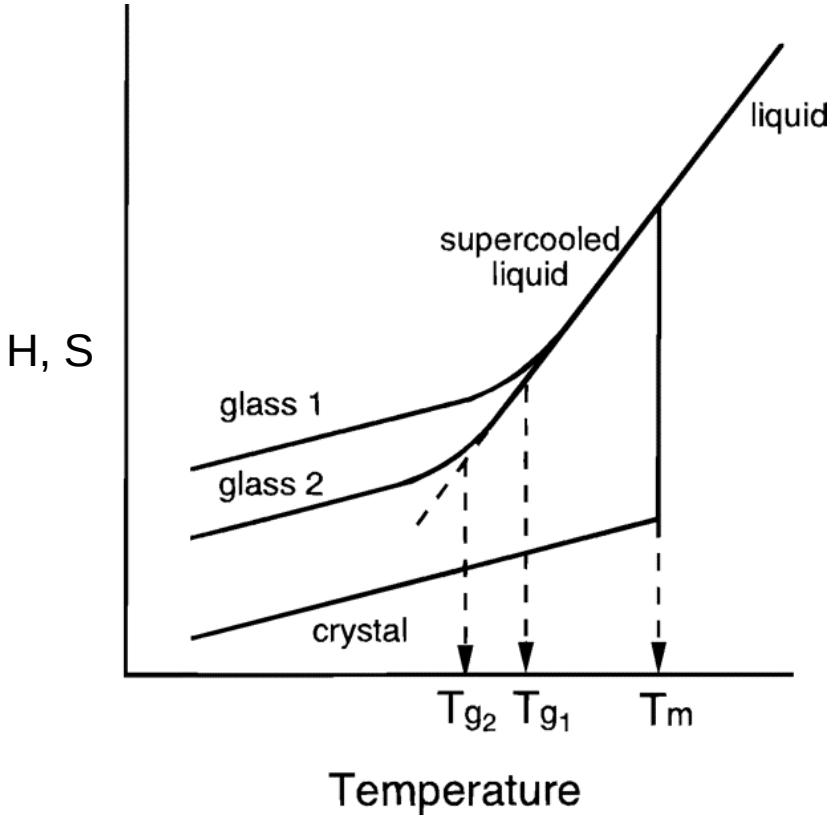

Figure 1.1. A schematic illustration of the properties of glasses and liquids. The enthalpy, H, and entropy, S, depends on the temperature and state of matter. The material can undergo a first or second order transition from a liquid to a crystal or glass, respectively. Modified with permission from reference 1. Copyright 1996 American Chemical Society.

material's melting or crystallization temperature, it may undergo a first-order transition and form a crystal. If the material avoids crystallization, it is considered a supercooled liquid. As the material cools further, molecules move slower and slower and the relaxation time of the material increases.[1–6] Eventually, molecules move too slowly to maintain equilibrium. At this point the material falls out of equilibrium and becomes a glass. This occurs at the glass transition temperature, T_g. A glass has a lower thermal expansion coefficient than a liquid and on further cooling the specific volume decreases at a slower rate than for the liquid.

Glasses are non-equilibrium materials and their properties are influenced by the method of preparation. For instance, T_g depends on the cooling rate.[1–4] If the material is cooled at a slower rate, molecules have high enough mobility to stay in equilibrium to lower temperatures. This results in a lower T_g, such as what is seen for glass 2 in Figure 1.1. The properties of a glass also change with time through a process called aging.[1,3,7] Molecules in glasses continuously rearrange and approach the more thermodynamically stable equilibrium state, the supercooled liquid. Given sufficient time and mobility, glasses with lower specific volume, higher density, and higher kinetic stability can be prepared. Under the right conditions, glasses can obtain the properties of a supercooled liquid below T_g. As shown in Figure 1.1, at lower temperatures there is a larger difference between the properties of the glass and the supercooled liquid. This means the glass is farther from equilibrium and has a larger thermodynamic driving force for approaching the equilibrium supercooled liquid. On the other hand, at higher temperatures the glass has higher mobility and is better able to equilibrate. In this way, the properties of the glass are determined by kinetics, specifically the molecular mobility and equilibration time, and thermodynamics, the driving force for equilibration.

The non-equilibrium nature of glasses makes them both desirable and challenging materials. Unlike crystals which may only have a few different types of unit cells and structures, called polymorphs, glasses can have a wide variety of packing arrangements. The packing can be tuned to gain desired properties.[8,9] Additionally, macroscopically homogenous materials can be made that are free of defects and grain-boundaries. However, glasses are inherently less ordered than a crystal which can decrease charge mobility and hinder performance in organic electronic devices.[8] Glasses are also less stable than crystals and their properties can evolve over time or with changes in temperature.[1,3,7,8] Developing glasses with controlled packing and enhanced stability would combine the most useful properties of both glasses and crystals.

1.2. Vapor-deposited glasses

There are many different methods of preparing glasses. Cooling a liquid, as discussed above, is one of the most common methods. A liquid can be rapidly quenched to avoid crystallization. For instance, metallic glass films can be prepared by flowing a liquid melt onto a chilled, spinning belt.[10] The liquid metal rapidly cools on contact with the belt and forms a glassy, metallic ribbon. Liquid cooled glasses are typically isotropic, smooth, and easy to characterize.

Spin-coating is another commonly used technique to prepare organic glasses. In this method, the organic material of interest is dissolved in a solvent with high concentrations. The solution is placed on a substrate and the substrate is rapidly spun. The centrifugal force causes the solution to spread out, covering the substrate. The solvent evaporates during the spinning, leaving behind a glassy film. The film can then be annealed or placed in a vacuum to ensure full removal of the solvent. Spin-coating is advantageous because it can easily process a wide

variety of organic materials, but it is difficult to produce films on a large scale. Additionally, solvents may dissolve underlying organic layers limiting the choice of substrate. Slot coating is a similar, emerging technique where a solution is dispensed on a moving belt to form glasses on an industrial scale.[11,12]

Vapor-deposition is an important technique for preparing small molecule and metallic glasses. In particular, it is used to prepare the active layers, such as hole-transport layers and insulting layers, in electronic device. Unlike the techniques described above, vapor-deposition builds a film by slowing depositing molecules in a vacuum chamber rather than preparing a bulk material all at once. This can result in extraordinary properties such as enhanced thermal stability and anisotropic molecular orientation.[13–15] Understanding these properties is the focus of my thesis. This section will describe the vapor-deposited process, properties of vapor-deposited films, and how surface mobility was understood to influence vapor-deposited glass formation prior to my work.

1.2.1. What is vapor deposition?

There are several different types of vapor deposition techniques. The techniques are similar in that they involve attaining the vapor phase of the desired material under vacuum and allowing it to condense on a substrate to grow a film, as illustrate in Figure 1.2. In the physical vapor-deposition, molecules simply adsorb onto the substrate. In chemical vapor deposition, a reaction occurs on the substrate surface resulting in the formation of the film. The reaction by-products are typically gasses that can be pumped away. The depositions are done under vacuum to prevent other materials and gasses from being incorporated in the film and ensure

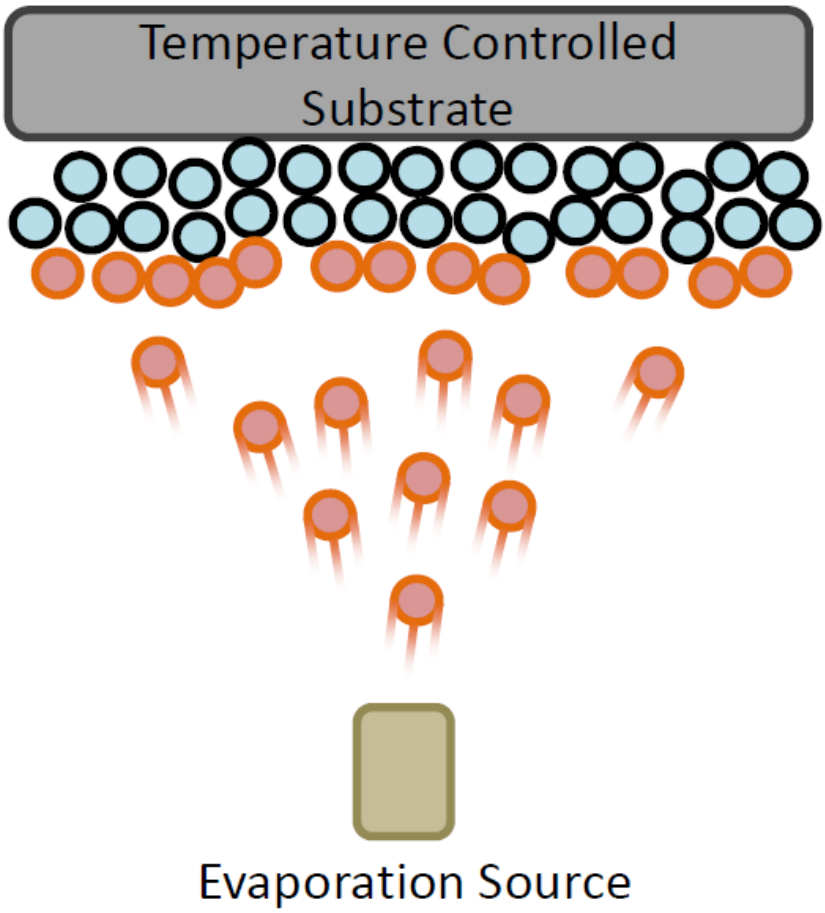

Figure 1.2. A schematic illustration of physical vapor deposition. Molecules are evaporated or sublimed in a vacuum from a crucible and condense to form a glass on a substrate. Molecules on the surface of the glass are highly mobile compared to molecules buried in the bulk of the glass. The substrate temperature can be controlled to tune the mobility on the surface of the glass during the deposition.

film purity. This section will focus on describing the physical vapor deposition process used in this thesis.

Depending on the vapor pressure and stability of the source material, the material can be introduced in the vapor phase in different ways. Small organic molecules can be thermally heated so they evaporate or sublime, as is done in this thesis. Metallic materials have vapor pressures too low to evaporate on heating, but are robust enough to deposit by sputtering. In sputtering, a concentrated ion beam is directed at a target of the source material. Incoming ions cause atoms from the target to break off and be introduced in the gas phase. Recently, a new technique called MAPLE (Matrix Assisted Pulsed Laser Evaporation) was developed for the deposition of polymers.[16] Polymers have vapor pressures too low for thermal evaporation and degrade on traditional sputtering. In this technique, molecules are placed in a solvent matrix. A pulsed laser beam introduces small pieces of the matrix into the gas phase. The solvent evaporates, and molecules can deposit on a substrate.

Material in the vapor phase has high mobility and effective temperature. When a molecule or atom encounters a substrate, it rapidly cools and can form a glass. At a typical deposition rate of 2 Å/s for organic molecules, material on the surface has about two seconds to equilibrate before being buried by subsequent deposition and a glassy film is grown. As discussed in detail below, molecules on the surface of a glass are highly mobile compared to the bulk. That mobility can be tuned by changing the substrate temperature during the deposition. Constructing a bulk film from highly mobile molecules that all had a chance to equilibrate near

the free surface before being buried results in glasses with extraordinary properties described below.

1.2.2. Extraordinary properties of vapor deposited glasses

Glasses prepared by physical vapor deposition can have remarkable properties like high density,[17,18] low heat capacity,[13,14,19,20] enhanced thermal and photochemical stability,[13,21–23] increased sound velocity,[24] and anisotropic molecular orientation and packing.[15,25,26] A few of these properties are demonstrated in Figure 1.3 for a vapor-deposited glass of indomethacin, a pharmaceutical commonly studied due to its industrial relevance and glassforming ability. On heating, a vapor-deposited glass transforms to the supercooled liquid at a temperature 18 K higher than T_g for a glass ramped at 1 K/min. Additionally, the vapor-deposited films is nearly 1.2% thinner than the liquid cooled glass. Due to the thin film geometry, the area of the film stays the same and only the height of the film contracts and expands on temperature ramping, so changes in film thickness are inversely proportional with changes in density. These results illustrate enhanced thermal stability and high density in the vapor-deposited glass. Similar temperature ramping experiments can be done with differential scanning calorimetry (DSC) and nanocalorimetry. These methods observe decreased heat capacity and enthalpy as well as increased T_{Onset}.[13,14,19]

Glasses with equivalent density and stability have not been prepared by any other method on laboratory timescales other than by vapor deposition. An ordinary glass would need to be aged for over a thousand years to prepare a glass of similar stability.[27] Similarly, Figure 1.3

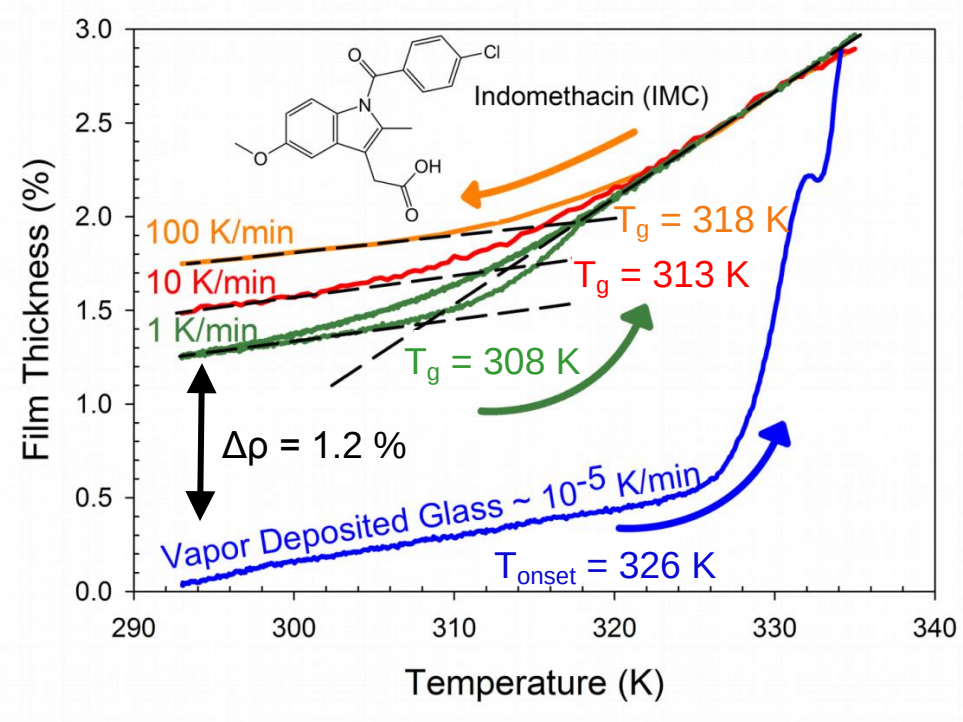

Figure 1.3. Thickness of indomethacin films as measured by spectroscopic ellipsometry during temperature ramping. The glass transition temperature, T_g, is measured for films cooled at 100, 10, and 1 K/min. A vapor-deposited glass is heated at 1 K/min and the onset of the transformation to the supercooled liquid, T_{onset}, is measured. T_{onset} is 18 K higher than T_g for a glass ramped at 1 K/min and the vapor-deposited films is nearly 1.3% thicker, indicating enhanced thermal stability and high density. A film of equivalent density would need to be cooled at a rate of about 10^{-5} K/min. Inset: the molecular structure of indomethacin. Adapted from work provided by Dr. Shakeel Dalal.

illustrates that a liquid would need to be cooled at a rate of 10^{-5} K/min to prepare a glass of equivalent density. Due to their high stability, vapor-deposited glasses heated above T_g transform to the supercooled liquid by a different mechanism than liquid cooled glasses. While glasses prepared by other methods transform via a macroscopically homogenous bulk mechanism, vapor-deposited glasses transform heterogeneously via a front initiated at an interface.[28] The transformation behavior of vapor-deposited glasses is described in detail in Section 3 and is characterized for an organic semiconductor for the first time in Chapter 3 of this thesis.

The extraordinary properties of vapor-deposited glasses described above are tunable with substrate temperature and deposition rate. This is the result of vapor deposited glass properties arising from high mobility on the free surface of the glass during deposition process, described in detail below. Molecules are able to partially equilibrate and adopt more favorable positions and orientations. Decreasing the deposition rate increases the amount of time molecules have on the surface to equilibrate before being buried by subsequent deposition, and increasing the substrate temperature increases the mobility molecules have on the surface. Generally, the most stable vapor-deposited glasses are generated when the substrate temperature is near 0.85 Tg when depositing at a rate of 2 Å/s.[29]

The properties of vapor-deposited glasses can be tuned by the preparation conditions. Dalal et. al. summarizes the properties of vapor-deposited glasses of indomethacin prepared over a wide range of substrate temperatures in Figure 1.4.[29] At substrate temperatures just below T_g, 315 K, glasses are prepared with the same macroscopic properties as the supercooled liquid,

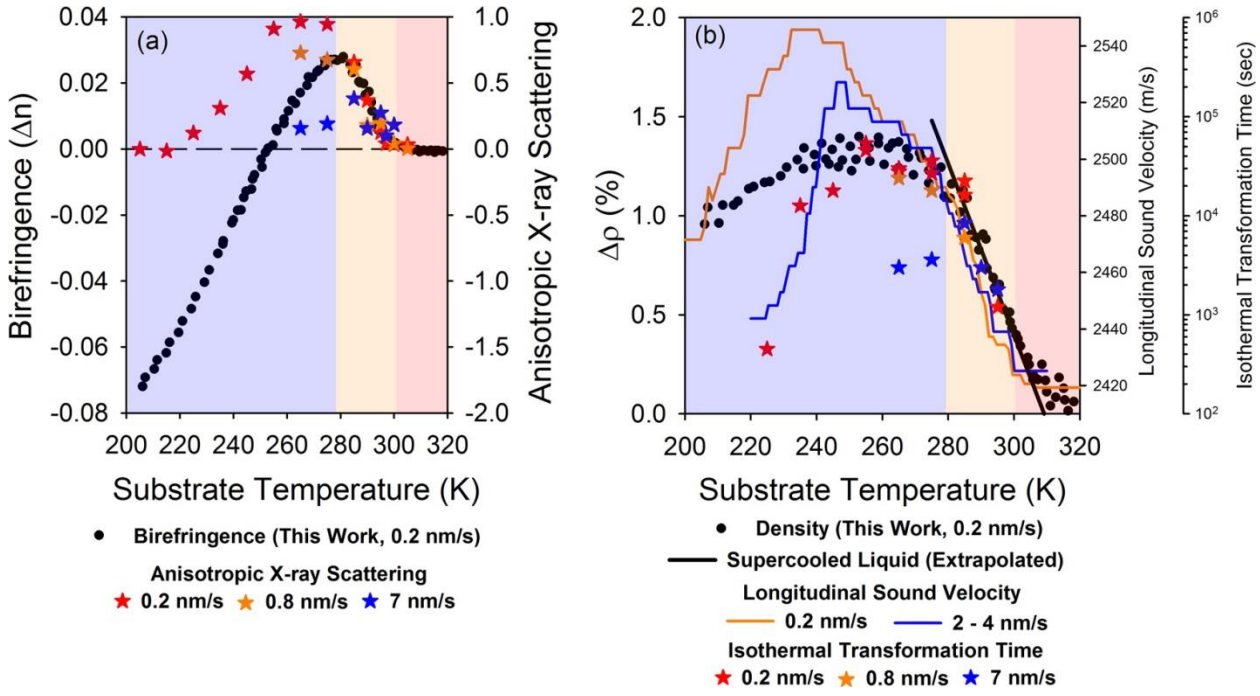

Figure 1.4. The properties of vapor-deposited glasses of indomethacin prepared over a wide range of substrate temperatures. Shaded regions indicate the regime: equilibrium (red), quasi-equilibrium (orange), and kinetically controlled (blue). (a) Properties describing the microscopic structure of the glasses, specifically the birefringence and anisotropic x-ray scattering. (b) Macroscopic properties such as the density relative to the supercooled liquid, sound velocity, and transformation times. Reproduced with permission from reference 29. Copyright 2013 American Chemical Society.

such as the density and sound velocity. (Figure 1.4b) This temperature range has been referred to as the "quasi-equilibrium" regime because the macroscopic properties of vapor-deposited glasses resemble that of equilibrium supercooled liquid and can be explained by heightened surface mobility allowing for better equilibration. However, indomethacin glasses are birefringent and have anisotropic packing in this regime while the equilibrium supercooled liquid is isotropic, so the materials have different microscopic structures. (Figure 1.4a) At lower substrate temperatures, the vapor deposited glasses no longer share the same macroscopic properties as the supercooled liquid. The glass properties are understood to be kinetically controlled as mobility decreases with substrate temperature. Generally the macroscopic properties of vapor-deposited glasses such as density, T_{Onset}, photochemical stability, and sound velocity have a maximum value near 0.85 T_g and their enhancement can be explained by heightened surface mobility allowing for better equilibration. However, vapor-deposited glasses can be anisotropic and surface mobility alone cannot explain the observed anisotropic molecular orientation packing. This is the central focus of Chapters 2 and 4 of this thesis, and background on anisotropy in vapor-deposited glasses is described in Section 4.

Vapor deposition can prepare highly stable glasses for a wide variety of materials. For instance, stable glass formation has been seen in pharmaceuticals such as indomethacin and nifedipine,[14] model organic glassformers like o-terphenyl[30] and ethylbenzene[19], and similar sputtering techniques prepare stable glasses of copper and zirconium alloys.[22,31] Simulations of highly stable glasses predict some of the features seen in vapor-deposited glasses, such as transformation via surface initiated fronts. Molecular dynamic simulations of the vapor deposition process have even been developed and produce glasses with low potential energy,

high kinetic stability, high density, and even anisotropy resembling experimentally prepared systems. Stable glass behavior is even captured by polymer glasses deposited via MAPLE (Matrix Assisted Pulsed Laser Evaporation), such as enhanced thermal stability. However, because MAPLE glasses are deposited as small clusters instead of single molecules they have lower density and rough surfaces compared to small molecule films.[16]

Materials used as hole-transport layers and emitter layers in organic electronic devices such as OLEDs and OPVs are prepared by vapor-deposition. These materials likely form highly stable glasses, but before my work few studies had been done to systematically compare the properties of vapor-deposited glasses to their liquid-cooled counterparts. In Chapters 2 and 4 of this thesis, I show that vapor deposition of molecules relevant for organic electronics can lead to anisotropic glasses with high thermal stability.

1.2.3. Surface mobility as a mechanism behind vapor-deposited glass properties

The free surface of a glass has significantly higher mobility than the bulk. This is due to molecules near the free surface having a lower barrier for rearrangement due to a decrease in the number of neighboring molecules at the free surface. Zhu et. al. calculated the diffusion constants for indomethacin at the free surface.[32] They prepared indomethacin films on a sinusoidal grating and monitored the flattening of the film using AFM and light scattering to extract a diffusion coefficient. Comparing their results with the diffusion coefficients for the bulk shown in Figure 1.5, they find that dynamics near the free surface are at least six orders of magnitude faster than in the bulk. High surface mobility persists far below T_g. Enhanced surface mobility has been demonstrated for a wide variety of organic systems. Surface diffusion was

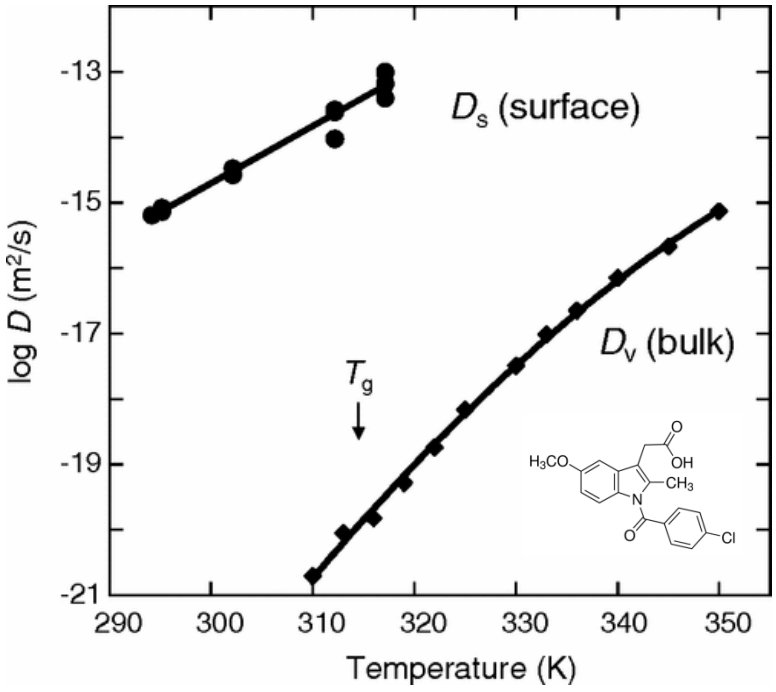

Figure 1.5. The diffusion coefficients for indomethacin at the free surface (circles) and in the bulk (diamonds). At T_g, 315 K, diffusion at the surface is at least six orders of magnitude faster than in the bulk. Adapted with permission from reference 32. Copyright 2011 American Physcial Society.

lower for systems with hydrogen bonding capability, such as nifedipine and indomethacin, and for large molecules, such as polystyrene with a molecular weight of 1.1 K or 1.7 K.[33–35] However mobility was several orders of magnitude higher at the free surface than in the bulk for even the slowest of these systems.

Enhanced mobility at the surface of a glass during vapor deposition is believed to increase equilibration near the glass surface and give rise to the extraordinary properties of vapor-deposited glasses. Surface diffusion measurements described above show there is heightened diffusion at the surface of a glass, suggesting high mobility. Previous work has also shown that surface mobility is not influenced by the stability of the underlying glass; surface diffusion was the same for a glass prepared by liquid cooling and a highly stable vapor-deposited glass.[36] This provides further evidence that there is high mobility at the surface during the vapor deposition process. Surface mobility during the deposition was probed experimentally by depositing alternating layers of deuterated and protonated α,α,β-tris-naphthylbenzene and using neutron reflectivity to probe the mixing at the interface of the layers.[13] The authors found that significant mixing occurred over a wide range of substrate temperatures, and the degree of mixing increased with the deposition temperature. Finally, simulations of the vapor deposition process show heightened mobility near the free surface and variable arrest depths depending on the substrate temperature during the deposition.[37–39]

Low surface mobility is expected to inhibit stable glass formation by limiting equilibration at a glass surface. For instance, hydrogen bonding has been shown to decrease mobility on the surface of a glass.[33] Vapor-deposited glasses of triazine derivatives showed that the material

with the most hydrogen bonding had the lowest thermal stability.[40] Another study of a series of small alcohols showed these systems had significantly lower kinetic stability than previously studied systems without hydrogen bonding.[41] However, the triazine derivatives still exhibited high density and benzyl alcohol showed unexpectedly high stability despite the presence of hydrogen bonding. Further work is still needed to predict stable glassforming ability.

Enhanced surface mobility during vapor deposition cannot by itself explain anisotropic molecular orientation and packing in vapor-deposited glasses.[29] Equilibration near the surface explains the thermal stability of vapor-deposited glasses and other observed features, such as the change in stability with changes in substrate temperature and deposition rate. However, it is unclear why equilibration near the surface would induce anisotropic structure because the equilibrium liquid is believed to be isotropic. The anisotropic structure in vapor-deposited glasses is discussed more fully in Section 4 below. Establishing a mechanism for explaining both thermal stability and anisotropic molecular orientation is one of the main accomplishments of this thesis and is explained in Chapters 2 and 4.

1.3. Transformation Mechanisms in Vapor-Deposited Glasses

Vapor deposition can prepare glasses with high thermal stability. As illustrated in Figure 1.3, vapor-deposited glasses can be heated far above the typical glass transition temperature before they transform into the supercooled liquid. Enhanced thermal stability is valuable for a variety of applications of vapor-deposited glasses. For instances, vapor-deposited films are used as active layers in organic electronic devices. In contrast, low thermal stability can lead to pin-hole formation or the loss of useful anisotropic molecular orientation and packing, resulting in

decreased device performance.[42–44] Understanding the transformation behavior of vapor-deposited glasses is important for improving device lifetimes and efficiency.

Vapor-deposited glasses transform to the supercooled liquid by a different mechanism than glass prepared by other techniques. Typically, a glass transforms via a bulk mechanism that is macroscopically homogenous.[1,3] In contrast, vapor-deposited glasses transform via a heterogeneous mechanism initiated at the free surface or another interface.[28,45–47] Molecules near the interface have increased mobility and are able to transform to the supercooled liquid on heating. Then, subsequent molecules bordering the supercooled liquid can have higher mobility and transform. In this way enhanced mobility propagates through the film, resulting in a transformation front. The velocity of the transformation front dictates the stability of the vapor-deposited film. This section describes experiments and theoretical descriptions of the transformation mechanism for vapor-deposited glasses.

1.3.1. Experimental Observations of Transformation Front Behavior

The heterogeneous transformation mechanism of vapor-deposited glasses can be directly observed by secondary ion mass spectroscopy (SIMS). In work by Sepúlveda, et. al. shown in Figure 1.6, thin layers of alternating deuterated and protonated indomethacin were vapor-deposited.[45,48] The films were then annealed above T_g and SIMS was used to characterize ion concentration at different depths throughout the film. Mixing of the deuterated and protonated layers caused a change in ion concentration and revealed regions with high mobility. The authors observe that molecules initially mix near the free surface. This region of enhanced mobility propagates linearly as a front and initiates transformation in the bulk of the

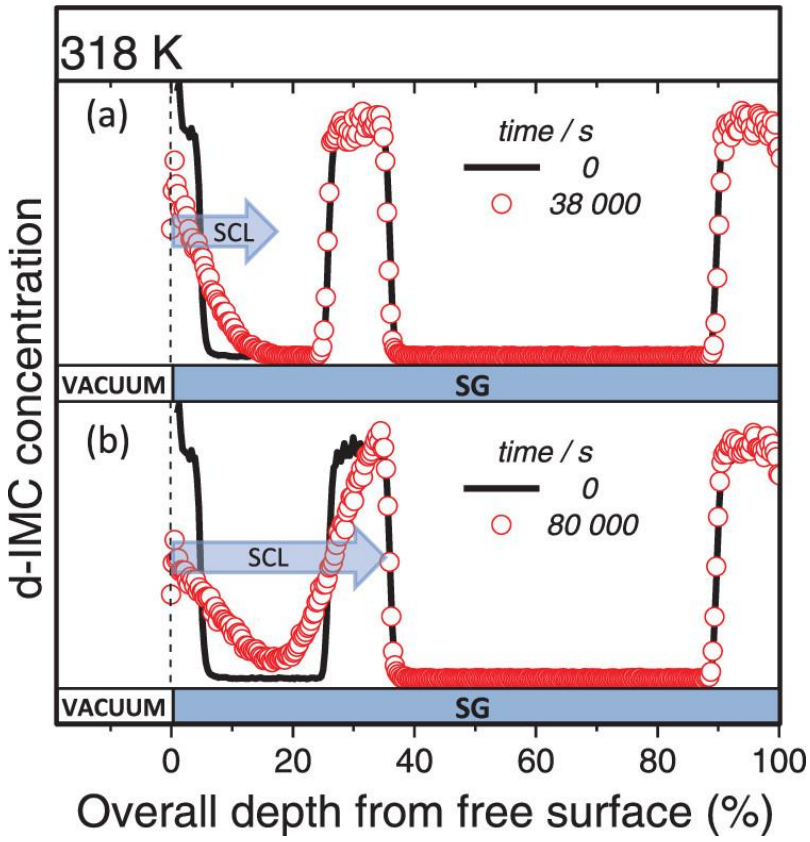

Figure 1.6. Secondary ion mass spectroscopy (SIMS) of a vapor-deposited indomethacin (IMC) film. Alternating layers of deuterated and protonated IMC were deposited with a substrate temperature of 265 K (0.85 T_g) to prepare a highly stable glass. Samples were annealed at 318 K (T_g + 3 K) for (a) 38,000 s and (b) 80,000 s. Black lines indicate the initial profile of the film, red circles indicated the measured d-IMC concentration after annealing. Used with permission from reference 48. Copyright 2013 American Institute of Physics.

film. Introducing a material with higher mobility to the bulk, such as a layer of liquid-cooled glass, creates additional interfaces with high mobility that facilitates a transformation front.[48] Similarly, capping the film with a highly stable glass eliminated the high mobility interface and hindered the ability for a front to occur.[48] The substrate sometimes initiates fronts, and this behavior may depend on the stability of the underlying glass. [21,45,48]

Transformation fronts in vapor-deposited glasses can be indirectly measured using nanocalorimetry. While nanocalorimetry is a bulk technique, Bhattacharya, et. al. and Rodríguez-Tinoco, et. al. found that the transformation times of thin films increased linearly with thickness.[47,49] By correcting for the different mass of each sample, they were able to measure the relative heat capacity of the films and, assuming a single transformation front initiated from the free surface, extract a front velocity time. While nanocalorimetry cannot directly observe the front propagate, this technique has fast scanning rates and allows for the front velocity to be measured over a wider range of annealing temperatures. Accessing higher annealing temperatures allowed Rodriguez-Viejo and coworkers to measure the activation barrier for the transformation front and show that it depends in part on the mobility of the supercooled liquid bordering the transforming glass.[50] This finding is consistent with the mechanism for transformation: a higher mobility liquid can better enhance mobility in the neighboring glass. Other techniques have also been used to measure transformation front velocities indirectly, such as inert gas permeation.[51]

Spectroscopic ellipsometry is an advantageous technique for studying transformation front behavior because it is able to directly track the progression of a front through a film, like SIMS,

but it is highly accessible and does not require any unique sample preparation, like nanocalorimetry. Ellipsometry is sensitive to changes in the refractive index and density of thin films. A vapor-deposited glass and a supercooled liquid have different densities and optical properties, and a two-layer ellipsometry model can track the location of this interface and measure the front velocity.[21,52] Ellipsometry was utilized to measure front velocity in vapor-deposited glass of indomethacin, a model glassformer.[21] A graded model where optical properties smoothly varied from isotropic near the surface to anisotropic in the bulk has also been used to fit ellipsometric data of a vapor deposited glass and is consistent with a front transformation mechanism.[53] In Chapter 3 of this thesis, I observe transformation fronts in vapor-deposited glasses of an organic semiconductor via ellipsometry and develop a high-throughput annealing protocol to understand the influence of the mobility of the supercooled liquid on front velocity.

While transformation front behavior has been characterized in a few model systems, the generality of this mechanism and the influence of glass properties on front behavior have not been well established. In particular, vapor deposited films serve as active layers in organic electronic devices, and understanding their transformation behavior could lead to increased device performance and lifetimes. In Chapter 3, I observe transformation fronts in vapor-deposited glasses of an organic semiconductor, suggesting this transformation behavior applies to this class of molecule.

Additionally, the influence of the glass structure on transformation front velocity is not well understood. It has been observed that transformation velocity is partially correlated with

density,[21] and it has been suggested that anisotropic molecular orientation in a glass may influence front velocity.[54] In Chapter 3, I develop a high-throughput annealing protocols that allow me to measure the front velocity for glasses prepared with a wide range of substrate temperatures that are annealed at many different temperatures. This allows me to illustrate that the influence of the mobility of the supercooled liquid and the structure of the glass are independent in controlling the front velocity.

1.3.2. Models of Transformation Fronts

Model systems of highly stable glasses transform via fronts initiated at the free surface. This is a natural consequence of a bulk material with low mobility that borders a highly mobile interface. Molecules are freer to rearrange when they are near a free surface or other interface with enhanced mobility. When heated above T_g, molecules near the interface can transform to the supercooled liquid. Then, the liquid has enhanced mobility, allowing neighboring molecules to have additional freedom and transform to the supercooled liquid as well. The liquid thus propagates linearly from the interface through the bulk of the film.

Harrowell and coworkers have used a facilitated kinetic Ising model to simulate vapor deposition of a two-dimension, two-state glass and reproduce transformation behavior in the experiments.[55,56] In this model, illustrated in Figure 1.7, a glass is treated as a collection of cells on a 2D lattice. Each cell can have two states: spin-up, indicating high mobility, and spin-down, indicating low mobility. The substrate is modeled as a fixed row of spin-down states, and the free surface is modeled as a fixed row of spin-up states. A deposited glass is prepared layer by

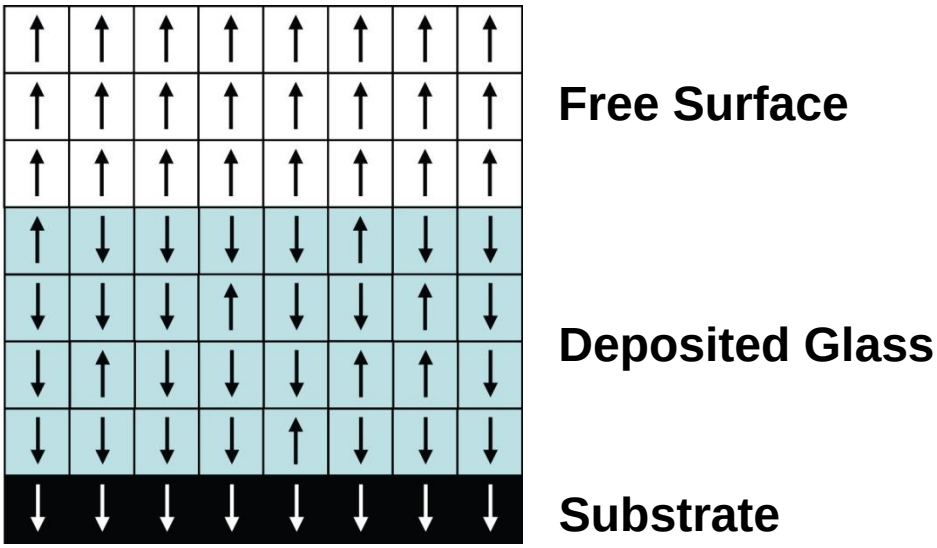

Figure 1.7. Illustration of the facilitated kinetic Ising model of a deposited glass. The glass is modeled as a series of cells of a two-dimensional lattice. Each cell can be spin-up, modeling high mobility, or spin-down, modeling low mobility. The cell spin is fixed at the substrate as spin-down and at the free surface as spin-up. Adapted with permission from reference 55.

layer, and the ratio of spin-up to spin-down states is influenced by the relaxation time and the temperature. A cell can only flip to spin-up if a sufficient number of its neighbors are spin-up.

The facilitated kinetic Ising model exhibits many of the features of vapor-deposited glasses. It is able to produce glasses with low fictive temperature, as has been seen in the experiments. Furthermore, on heating cells flip to spin-up near the surface and the spin-up states propagate linearly through the bulk. This indicates a transformation front and reproduces the transformation behavior seen in the experiments. Front velocity and fictive temperature vary with the temperature used to prepare the film. Glasses with low stability can have cells flip to spin-up within the bulk of the glass and spin-up states can propagate from these regions, simulating a bulk transformation mechanism. Tito et. al. studied a lattice model with more types of cell states and swapping conditions and also observes transformation fronts.[57] Additionally, the facilitated kinetic Ising model predicts a competition between homogenous bulk mechanism and transformation front mechanism under different conditions. This is discussed in further detail in the following section.

Random first order transition (RFOT) theory offers another model for understanding the transformation behavior of glasses and has demonstrated transformations fronts and reproduced experimental results.[58,59] In this theory, mobility can be transported from regions of high mobility to regions of low mobility. The RFOT calculations find that on annealing, high mobility initially found at the glass surface can be transferred to areas of low mobility in the bulk. This results in a transformation front, and they find that the front velocities agree with those measured experimentally for vapor-deposited, highly stable glasses. [59] The success of

RFOT in describing transformation front behavior further emphasizes the importance of facilitated mobility in this mechanism.

1.3.3. Bulk Transformation Mechanism

Thick films of vapor-deposited glasses can transform via both the heterogeneous front mechanism and the homogenous bulk transformation mechanism. A vapor-deposited film initially transforms by the front transformation mechanism. If the film is sufficiently thick, the bulk transformation mechanism is observed and the transformation to the supercooled liquid is then dominated by this mechanism.[28] This is illustrated for a vapor-deposited film of indomethacin in Figure 1.8. The transformation time for films less than 1 μm in thickness increases linearly, suggesting a propagating front with a constant velocity controls the transformation in this regime. For films thicker than 1 μm, all the films have similar transformation times. This suggests the transformation is dominated by bulk transformation mechanism and, once initiated, acts quickly regardless of the thickness of the film. The crossover thickness from which the front mechanism and the bulk mechanism dominates varies widely depending on the molecule studied. For instance, the crossover length is 5 μm for methyl-m-toluate,[60] but it is only 400 nm for toluene.[61]

The molecular interpretation of the bulk mechanism is unclear, but the leading view is that bubbles of the supercooled liquid are nucleated in the bulk. This mechanism is illustrated in the inset to Figure 1.8. The bubbles offer regions of high mobility throughout the glass, so mobility rapidly propagates from each of these nucleation points and the bulk quickly transforms. On average, nucleation points are believed to be far apart in the vapor-deposited glass. The

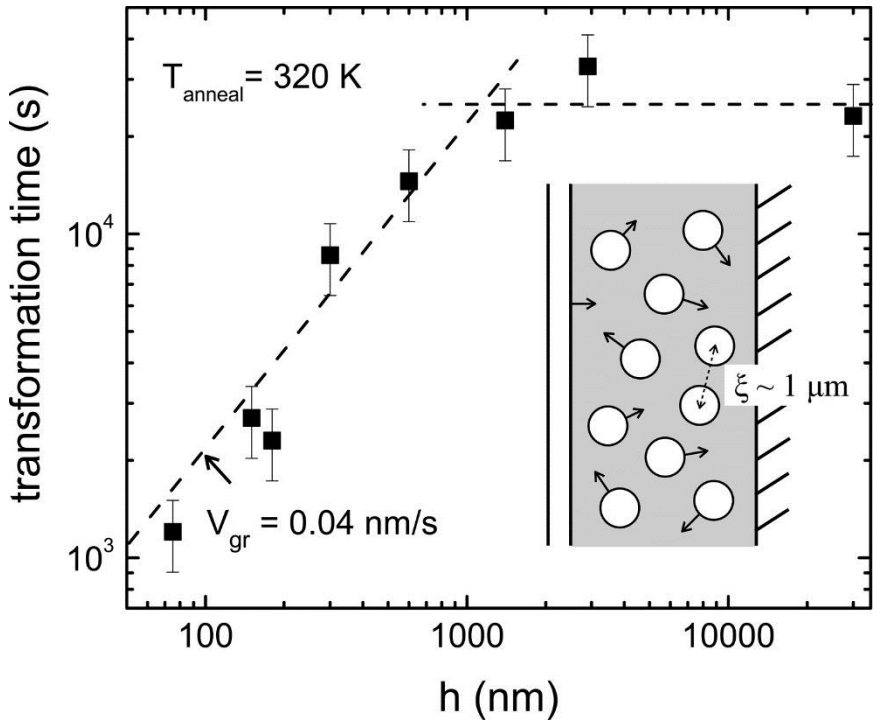

Figure 1.8. Transformation time for vapor-deposited films of indomethacin with a wide range of thicknesses. Films were annealed at 320 K, T_g + 5 K. Inset: Illustration of the bulk transformation mechanism. Used with permission from reference 28. Copyright 2010 American Institute of Physics.

crossover length is suggested to be the distance between nucleation points; films thinner than the crossover length are unlikely to have the bulk mechanism nucleate.[28] This bulk transformation mechanism is visualized in simulations using the facilitated kinetic Ising model, as discussed above.[55,56] For low stability glasses, there can exist regions with higher concentrations of up-spins. This can facilitate a spin flip in a neighboring glass and create a high mobility nucleation point in the bulk of the glass which facilitates further transformation. Simulations of glasses of moderate stability exhibit both a front and bulk transformation mechanism, showing how these can simultaneously exist in the same material and compete in controlling the transformation behavior. Both mechanisms rely on facilitated mobility and are fundamentally connected. However, the bulk mechanism is difficult to observe directly experimentally and fundamental questions about the mechanism remain unanswered.

1.4. Anisotropic Molecular Orientation in Organic Glasses

Vapor-deposited glasses can be highly anisotropic. This is surprising, because typically small molecule glasses are isotropic when they are prepared by more traditional methods such as cooling a liquid.[25] Anisotropic molecular orientation and packing is useful for applications in organic electronics. For instance, Yokoyama and coworkers reported that a film with horizontal molecular orientation had three times higher electron mobility than an isotropic glass.[8] Other remarkable properties of vapor-deposited glasses, such as high thermal stability and low enthalpy, are explained by enhanced equilibration at the liquid surface.[13] However, before the work presented in this thesis, it was unclear how equilibration at the surface could lead to anisotropic molecular orientation.

In this section, I will give a brief overview on general approaches for controlling the molecular structure of organic solids for applications in organic electronics. I will then describe past studies of anisotropic molecular orientation in vapor-deposited glasses and describe the two leading ideas for what controls molecular orientation in vapor-deposited glasses: molecular shape and surface mobility. My work was inspired by these views, and in Chapters 2 and 4 I propose a general mechanism for molecular orientation in vapor-deposited glasses.

1.4.1. Controlling Molecular Orientation and Packing in Organic Solids

Crystals have highly ordered and controlled packing and molecular orientation, and one avenue for controlling the molecular structure in organic solids is to generating different crystal polymorphs with different, more desirable types of packing. Recently, Loo and coworkers have shown that a vapor-deposited amorphous film of hexabenzocoronene can be crystallized to different polymorphs by change the processing conditions, such as thermal heating, exposure to hexane vapor, or contact with a PDMS stamp.[62–64] Hexabenzocoronene can be used as a hole transport material in organic electronics, and crystal polymorphs with more favorable molecular orientation showed a two orders of magnitude increase in hole mobility.[62] Controlled crystallization is a promising avenue for engineering molecular structure in organic solids.

However, engineering crystalline polymorphs may not be the best avenue for designing materials for use in organic electronics. Crystals can have grain boundaries, reducing charge mobility in organic electronic applications.[65–68] Additionally, a typical molecule only has a few stable polymorphs, limiting the range of crystalline structures that can be engineered.[69] Finally, recent work has drawn into question whether crystallinity is even needed for improved device

performance, such as enhanced charge mobility. A study aligned poly(3-hexylthiophene) (P3HT) films showed that charge mobility was primarily controlled by the hopping down the polymer backbone.[68] The strain-aligned film had an order of magnitude higher charge mobility than the crystalline film, likely due to polymer chains extending through grain boundaries. This work and other studies[70] suggest that crystallinity may not be necessary to enhance charge transport properties.

Amorphous systems are advantageous because they are easy to process, lack grain boundaries and can be prepared over large areas, and can have a wide range of molecular orientations and packings.[25,71,72] Anisotropic packing been studied in spin-coated polymer films for applications in organic electronics. The centrifugal force during spin-coating can align the backbone of polymer films, leading to anisotropic molecular orientation. Techniques like off-axis spin-coating show creative ways this process can be applied to change the molecular orientation.[73] However, spin-coating fails to align small molecules. Additionally, spin-coating is a solvent based technique, and the solvent can dissolve underlying layers during the spin-coating process.[9] For organic electronics, stacks of insulating, hole and electron transport, and emitting layers are used. Requiring that the spin-coating not disrupt underlying layers severely limits the applications of spin-coating for preparing active layers. Instead, vapor-deposition can be used to prepare layers without the use of solvent.[74] Molecular orientation in vapor-deposited films is discussed in-depth in the section below.

1.4.2. Anisotropic Vapor-Deposited Glasses

Vapor deposition can prepare amorphous films that are highly anisotropic. As discussed above, amorphous films are advantageous because they lack grain boundaries and can have a wide range of molecular orientations and packing structures. Vapor deposition is advantageous because it prepares systems without solvents that disrupt underlying layers. As described in Section 1.2, small molecules with high vapor pressures are needed for vapor-deposition. Oligomers mimicking the polymers used in spin-coated films were initially vapor-deposited.[75–77] Surprisingly, it was observed that vapor-deposited films could have highly anisotropic molecular orientation. In contrast, spin-coating or cooling a liquid small molecules result in an isotropic glass.[74] Understanding the origin of the anisotropic molecular orientation and controlling it is key for improving vapor-deposited active layers in organic electronics.

Yokoyama and coworkers were the first to systematically study the molecular orientation of a wide range of vapor-deposited glasses used in organic electronics, and they proposed that anisotropic molecular orientation was primarily controlled by molecular shape.[25] In particular, they proposed that more anisotropic molecular shapes resulted in more anisotropic vapor-deposited glasses. Linear molecules with a high aspect ratio had preferential horizontal molecular orientation in a vapor-deposited glass.[8,78] Horizontal molecular orientation was even seen for rod-shaped molecules in an isotropic host, suggesting intermolecular orientations were not important in controlling the molecular orientation.[78] In contrast, molecules with a spherical, compact structure produced nearly isotropic glasses by vapor deposition.[79] Most of their experiments were done on room temperature substrates, but they found that depositing on

heated substrates resulted in glasses with isotropic molecular orientation.[80] To explain these observations, Yokoyama and coworkers proposed a mechanism for molecular orientation in vapor-deposited glasses described below.

Yokoyama and coworkers proposed that anisotropy in vapor-deposited glasses was due to molecules preferring horizontal molecular orientation on the surface of a glass. [25] As illustrated in Figure 1.9, they believed molecules preferentially lie down on the surface of a glass to minimize their exposure to the vacuum and reduce their free energy during vapor deposition. There is a larger driving force for bigger, more anisotropic molecules to lie down, resulting in greater alignment of more anisotropic molecules. Alignment occurs for each layer, resulting in a bulk anisotropic glass. In contrast, at high temperatures molecules on the surface are able to move and randomize during the vapor-deposition process, resulting in an isotropic glass. This mechanism laid a foundation for understanding molecular orientation in vapor-deposited glasses, but could not account for all future findings.

Ediger and coworkers systematically studied the effect of substrate temperature on vapor-deposited glasses and found that a single molecule could have a wide range of molecular orientations depending on the deposition conditions. For example, the birefringence of vapor-deposited glasses of indomethacin changed from zero to positive values to negative values with decreasing substrate temperature,[29] as illustrated in the right panel of Figure 1.4. This suggested vapor deposition of a single molecule could produce glasses with molecular orientations that varied from isotropic to vertical to horizontal. Understanding this behavior could enable controlled molecular orientation in vapor-deposited active layers.

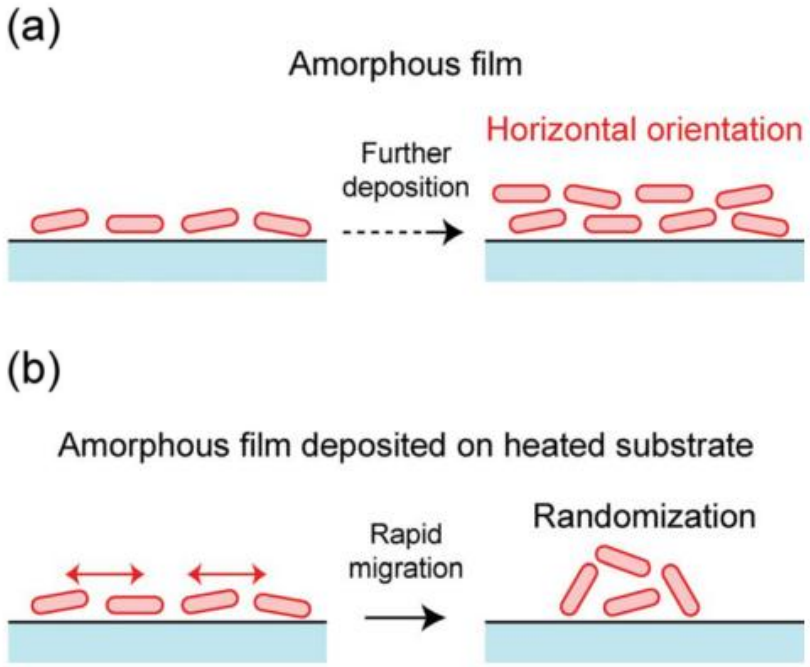

Figure 1.9. Schematic illustration of a mechanism for molecular orientation in vapor-deposited glasses. (a) When deposited at a low temperature, molecules preferentially adopt a horizontal orientation that is captured in the bulk film. (b) When deposited at a high temperature, molecular motion on the surface of the substrates randomizes the initial molecular orientation, resulting in an isotropic bulk glass. Adapted with permission from reference 25. Copyright 2011 The Royal Society of Chemistry.

The extraordinary properties of vapor-deposited glasses have been explained by enhanced equilibration at the surface of the vapor-deposited glass, but this mechanism alone cannot account for anisotropic molecular orientation. As was described in Section 1.2, anisotropic indomethacin glasses also exhibited enhanced thermal stability and high density, and these properties could be explained by enhanced surface equilibration.[29] However, it is unclear why molecules would equilibrate to different molecular orientations, although the dependence on substrate temperature suggests surface mobility is still an important factor in controlling the molecular orientation. Additionally, the orientation mechanism proposed by Yokoyama and coworkers cannot explain vertical molecular orientation. Better understanding of the molecular orientation mechanism is needed to explain all of the observed behavior.

Understanding the mechanism for molecular orientation in vapor-deposited glasses has been one of the main focuses of my dissertation. Inspired by the above studies illustrating the importance of molecular shape and substrate temperature, I investigate the molecular orientation of vapor-deposited glass of rod- and disk-shaped molecule prepared over a wide range of substrate temperatures. I propose a mechanism for molecular orientation that depends on enhanced equilibration at the glass surface and on the anisotropic surface structure of the equilibrium liquid. I suggest this mechanism is general for a wide variety of organic systems, proposing an avenue for controlling molecular orientation in vapor-deposited glasses.

1.5. Characterization of thin glass films – Spectroscopic ellipsometry

Glasses prepared by vapor deposition can be challenging to characterize. First, amorphous materials lack long-range order and characterizing them can involve differentiating a wide

range of structures.[4,29] Additionally, vapor-deposited films are challenging to characterize because they are quite thin. Generally vapor-deposited films are under 1 μm in thickness, and films used in applications such as organic electronics are typically 20-100 nm thick.[25] Characterizing this little material is difficult, and bulk techniques can be ineffective.

Spectroscopic ellipsometry is well suited for characterizing vapor-deposited glasses. Vapor-deposition prepares thin, homogenous glass films with smooth surfaces and substrates, which are ideal samples for characterizing with ellipsometry.[25] Ellipsometry detects subtle changes in the polarization state of light after interacting with a film, making it highly sensitive to the film thickness, refractive index, and extinction coefficient of the film.[81] This allows it to characterize a wide variety of amorphous states. Ellipsometry is the primary technique used in this thesis to study vapor-deposited glasses. This section will provide an overview on how an ellipsometer operates, how film properties are calculated from ellipsometric data, and how ellipsometry complements other characterization techniques.

1.5.1. Operation and Data Modeling

Spectroscopic ellipsometry measures the polarization state of light after interacting with a thin film. The initial polarization state of the light is controlled by passing the light through a linear polarizer and, frequently, a quarter-wave plate.[82] Rotating the quarter wave plate during the measurement changes the polarization of the incident light and allows for the impact of light with a wide variety of different initial polarization states can be surveyed.

The polarization state of the light will change depending on the optical properties of the material. Once the light encounters the sample, light will be reflected and refracted from each

interface, as illustrated in Figure 1.10. Light will propagate at a different rate and angle if there is a change in the refractive index, and light of certain polarization states may be absorbed if the material is dichroic. The interference of all these light rays results in a new polarization state being detected. The extent of these perturbations depends on the path length of the light. The path length depends on the incident angle and the thickness of the film. Frequently, ellipsometry measurements are made at multiple angles to probe how the polarization state changes with different path lengths and better understand the optical properties of the film.[25,81,82] Similarly, ellipsometry can be performed with a wide range of wavelengths. Light with different wavelengths has different periods when propagating through the glass resulting in a different final polarization states. After interacting with a sample, light is typically elliptically polarized, giving ellipsometry its name.

After an ellipsometry measurement is performed, a model is needed to calculate the sample thickness and optical properties from the measured polarization state. As illustrated in Figure 1.10, samples are modeled as a stack of discrete layers. The thickness and optical properties of each layer are fit so that the predicted polarization state for the sample best matches the experimental measurement. Models are as simple and use as few variables as possible in describing the thickness and optical properties in order to find a more unique fit. In this thesis, vapor-deposited samples consist of a silicon substrate, a thin layer silicon oxide naturally occurring on the surface of the silicon, and the vapor-deposited glass. The properties of the silicon substrate and native oxide layer are well characterized, leaving just the glass layer to be determined.

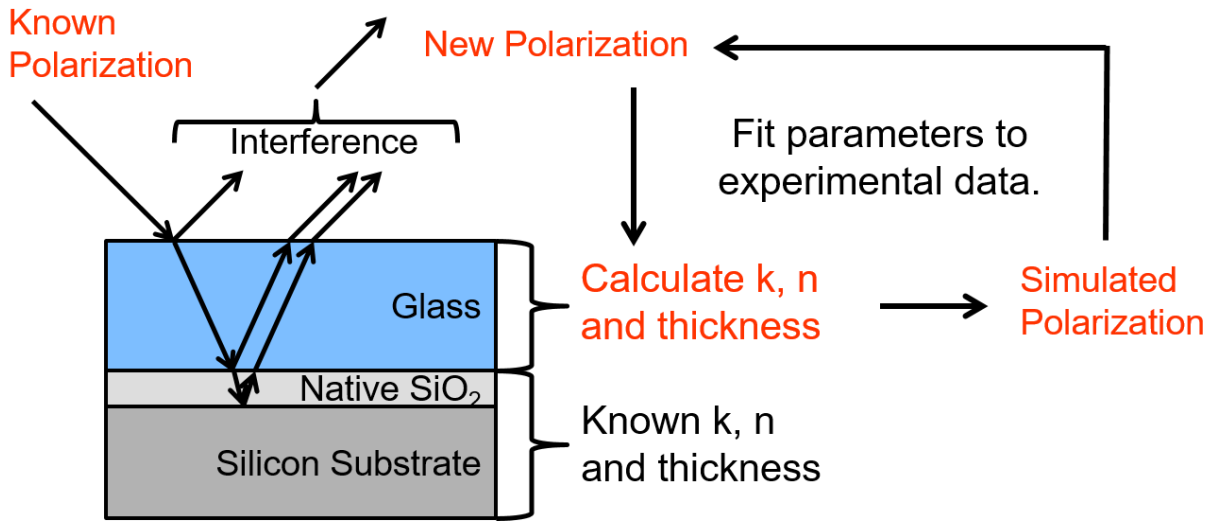

Figure 1.10. A schematic illustrate of an ellipsometry measurement and data modeling. Light with a known polarization state and incident angle encounters a sample. Light reflects and refracts from each interface, and the interference of all these light rays results in a new polarization state being detected by the ellipsometer. The thickness, refractive index, n, and extinction coefficient, k, are determined by fitting a model to the experimental data.

In this thesis, the vapor-deposited glass layer is described using either a simple, Cauchy model or a complex, oscillator model. The Cauchy model is a simple, three-variable equation that can accurately describe the refractive index of a wide range of organic and inorganic materials.[82] It can describe anisotropic materials with the addition of just a single variable.[17,26] The Cauchy model's simplicity makes it ideal for obtaining unique fits for ellipsometric data, but it can only be used in the wavelength range in which a film is transparent. To model absorptions, an oscillator model is constructed. This model uses Gaussian and Lorentzian oscillators to model the absorptions in the film and calculate the extinction coefficient.[25] Oscillator models are advantageous because only three or four variables are needed to describe each oscillator, so a complex absorption spectrum can be described with just a dozen variables. Developing oscillator models that can describe the absorptions for a wide range of anisotropic glasses was a key advance made in this dissertation. This is described in detail in Chapter 2.

1.5.2. Comparison with Other Techniques

In addition to ellipsometry, other techniques can overcome the challenges involved in characterizing thin, amorphous films and are used to study vapor-deposited glasses. These techniques can complement and expand on the work done by ellipsometry. A few examples are given below.

X-ray scattering can characterize molecular packing in vapor-deposited glasses. Typically, small molecule glasses lack long-range periodic order, resulting in only a broad amorphous halo in an x-ray scattering pattern. However, vapor-deposited glass can have anisotropic molecular packing that is observed as broad peaks. For instance, vapor-deposited glasses of indomethacin

exhibit layering.[15] Vapor deposition of a rod-shaped semiconductor can produce glasses with tunable packing, varying from edge-on to face-on depending on the substrate temperature.[83] In Chapter 2 of this thesis, ellipsometry shows this same material has anisotropic molecular orientation. These two techniques combined provide a more detailed molecular picture of the glass structure. They show that, when prepared at low substrate temperatures, molecules are preferentially packed edge-on with horizontal orientation, while at moderate substrate temperatures molecules are packed edge-on with preferential vertical orientation.

Nanocalorimetry requires only a few nanograms of material to characterize a sample and has widely been used to characterize vapor-deposited glasses. In addition to requiring very little material, the small size of a nanocalorimeter is advantageous because it can access high heating and cooling rates and characterize vapor-deposited glasses and higher temperatures than would otherwise be possible. As described in Section 3, Rodríguez- Viejo and coworkers used nanocalorimetry to measure transformation fronts velocities in vapor-deposited glasses at higher annealing temperatures than previously accessible.[47] However, transformation fronts have only been directly observed by ellipsometry and secondary ion mass spectroscopy.[21,45] Nanocalorimetry users use these observations to bolster their claim that films in their experiments also transform via fronts they cannot directly observe, illustrating how different characterization techniques complement each other.

Other absorption- and emission-based techniques can be used to characterize vapor-deposited glasses, such as infrared (IR) spectroscopy, and UV-vis absorption, and fluorescence. Like ellipsometry, these methods determine the average molecular orientation of a glass by

measuring the absorptions or emissions of the organic molecules and then connecting those features to the underlying glass structure. However, ellipsometry requires a model to calculate the absorbance while techniques like UV-vis measure it directly. Additionally, ellipsometry requires a much more complicated experimental set-up, since for the most reliable models data needs to be collected over a wide spectral range and several incident angles. On the hand, the set-up for IR, UV-vis, and fluorescence experiments is much simpler, but calculating the molecular orientation requires simplifying assumptions. Ellipsometry has validated the assumptions for these techniques and shown excellent agreement in the calculated molecular orientation.[84–86] For instance, I use both ellipsometry and UV-vis to characterize vapor-deposited glasses in Chapter 4 and see similar results for both techniques. I expect that techniques like UV-vis, IR, and fluorescence will be used more in the future. This will make studies of molecular orientation in amorphous films more accessible and hopefully expand the work done in this area.

1.6. Contributions of This Work

In the work presented in this thesis, I investigate the thermal stability and anisotropic molecular orientation of vapor-deposited glasses. For the first time, I show that vapor-deposited organic semiconductors can have tunable anisotropic molecular orientation and enhanced thermal stability. I propose a new mechanism that explains both of these features in terms of partial equilibration at the glass surface during the deposition process.

In Chapter 2, I show that a series of rod-shaped semiconductors can have tunable anisotropic molecular orientation and enhanced thermal stability when prepared by vapor-deposition. Prior to this work, it was believed that more anisotropic molecules made more

anisotropic glasses. My work showed that the mobility at the surface, which could be modulated by changing the substrate temperature, and the anisotropic surface structure of the equilibrium liquid that determined the molecular orientation. Rod-shaped molecules with a wide range of aspect ratios were all governed by this mechanism and had similar trends in molecular orientation and stability.

In Chapter3, I study the thermal stability and transformation behavior of one of the rod-shaped semiconductors discussed in Chapter 2. For the first time, I show that highly stable, vapor-deposited semiconductors transform by fronts initiated from the free surface. By developing a new high-throughput annealing protocol, I analyze the front velocities over a wide range of annealing temperature for many different glasses prepared at different substrate temperatures. This huge data set revealed that the front velocity was independently controlled by the mobility of the supercooled liquid after transformation and the properties of the vapor-deposited glass.

In Chapter 4, I prepare vapor-deposited glasses of disk-shaped organic semiconductors. I find they have tunable anisotropic molecular orientation and enhanced thermal stability. Compared to the rod-shaped molecules studied in Chapter 2, they have a similar trend in stability but a different trend in molecular orientation. Both of these features can be explained by partial equilibration at the glass surface during the deposition. Simulations of the equilibrium liquid reveal the surface has different molecular orientation for disk-shaped molecules and rod-shaped molecules that is consistent with the anisotropic molecular orientation of the vapor-deposited glass. This work suggests that surface equilibration can explain the behavior of a

wide variety of vapor-deposited glasses, including organic semiconductors of many different molecular shapes.

I hope my work bridges the divide between fundamental research on model glassformers and research targeted at developing materials for organic electronic devices. By understanding the mechanism underlying the formation of stable glasses with anisotropic orientation, this work could aid the choice of material and deposition conditions for active layers with improved properties, such as enhanced light outcoupling, charge mobility, and lifetimes.

1.7. References

(1) Ediger, M. D.; Nagel, S. R. Supercooled Liquids and Glasses. *J. Phys. Chem.* **1996**, *100* (31), 13200–13212.

(2) Angell, C. A.; Ngai, K. L.; McKenna, G. B.; McMillan, P. F.; Martin, S. W. Relaxation in Glassforming Liquids and Amorphous Solids. *J. Appl. Phys.* **2000**, *88* (6), 3113.

(3) Lubchenko, V.; Wolynes, P. G. Theory of Structural Glasses and Supercooled Liquids. *Annu. Rev. Phys. Chem.* **2007**, *58*, 235–266.

(4) Debenedetti, P. G.; Stillinger, F. H. Supercooled Liquids and the Glass Transition. *Nature* **2001**, *410* (March), 259–267.

(5) Cicerone, M. T.; Blackburn, F. R.; Ediger, M. D. How Do Molecules Move near Tg? Molecular Rotation of Six Probes in O-Terphenyl across 14 Decades in Time. *J. Chem. Phys.* **1995**, *102* (1), 471.

(6) Ediger, M. D. Spatially Heterogeneous Dynamics in Supercooled Liquids. *Annu. Rev. Phys. Chem.* **2000**, *51*, 99–128.

(7) Struik, L. C. E. Physical Aging in Amorphous Polymers and Other Materials Door. **1977**.

(8) Yokoyama, D.; Setoguchi, Y.; Sakaguchi, A.; Suzuki, M.; Adachi, C. Orientation Control of Linear-Shaped Molecules in Vacuum-Deposited Organic Amorphous Films and Its Effect on Carrier Mobilities. *Adv. Funct. Mater.* **2010**, *20* (3), 386–391.

(9) Forrest, S. R. The Path to Ubiquitous and Low-Cost Organic Electronic Appliances on Plastic. *Nature* **2004**, *428*, 911–918.

(10) Jiang, W. H.; Liu, F. X.; Wang, Y. D.; Zhang, H. F.; Choo, H.; Liaw, P. K. Comparison of

Mechanical Behavior between Bulk and Ribbon Cu-Based Metallic Glasses. *Mater. Sci. Eng. A* **2006**, *430* (1–2), 350–354.

(11) Ro, H. W.; Downing, J. M.; Engmann, S.; Herzing, A. A.; DeLongchamp, D. M.; Richter, L. J.; Mukherjee, S.; Ade, H.; Abdelsamie, M.; Jagadamma, L. K.; et al. Morphology Changes upon Scaling a High-Efficiency, Solution-Processed Solar Cell. *Energy Environ. Sci.* **2016**, *9* (9), 2835–2846.

(12) Semenza, P. OLEDs in Transition. *Inf. Disp. (1975).* **2011**, *27* (10), 14–16.

(13) Swallen, S. F.; Kearns, K. L.; Mapes, M. K.; Kim, Y. S.; McMahon, R. J.; Ediger, M. D.; Wu, T.; Yu, L.; Satija, S. Organic Glasses with Exceptional Thermodynamic and Kinetic Stability. *Science* **2007**, *315* (5810), 353–356.

(14) Zhu, L.; Yu, L. Generality of Forming Stable Organic Glasses by Vapor Deposition. *Chem. Phys. Lett.* **2010**, *499*, 62–65.

(15) Dawson, K. J.; Zhu, L.; Yu, L.; Ediger, M. D. Anisotropic Structure and Transformation Kinetics of Vapor-Deposited Indomethacin Glasses. *J. Phys. Chem. B* **2011**, *115* (3), 455–463.

(16) Guo, Y.; Morozov, A.; Schneider, D.; Chung, J. W.; Zhang, C.; Waldmann, M.; Yao, N.; Fytas, G.; Arnold, C. B.; Priestley, R. D. Ultrastable Nanostructured Polymer Glasses. *Nat. Mater.* **2012**, *11* (4), 337–343.

(17) Dalal, S. S.; Sepúlveda, A.; Pribil, G. K.; Fakhraai, Z.; Ediger, M. D. Density and Birefringence of a Highly Stable A,α,β-Trisnaphthylbenzene Glass. *J. Chem. Phys.* **2012**, *136* (20), 204501.

(18) Nakayama, H.; Omori, K.; Ino-u-e, K.; Ishii, K. Molar Volumes of Ethylcyclohexane and Butyronitrile Glasses Resulting from Vapor Deposition: Dependence on Deposition Temperature and Comparison to Alkylbenzenes. *J. Phys. Chem. B* **2013**, *117* (35), 10311–10319.

(19) Leon-Gutierrez, E.; Sepúlveda, A.; Garcia, G.; Clavaguera-Mora, M. T.; Rodríguez-Viejo, J. Stability of Thin Film Glasses of Toluene and Ethylbenzene Formed by Vapor Deposition: An in Situ Nanocalorimetric Study. *Phys. Chem. Chem. Phys.* **2010**, *12* (44), 14693–14698.

(20) Ramos, S. L. L. M.; Oguni, M.; Ishii, K.; Nakayama, H. Character of Devitrification, Viewed from Enthalpic Paths, of the Vapor-Deposited Ethylbenzene Glasses. *J. Phys. Chem. B* **2011**, *115* (49), 14327–14332.

(21) Dalal, S. S.; Ediger, M. D. Influence of Substrate Temperature on the Transformation Front Velocities That Determine Thermal Stability of Vapor-Deposited Glasses. *J. Phys. Chem. B* **2015**, *119* (9), 3875–3882.

(22) Yu, H.-B.; Luo, Y.; Samwer, K. Ultrastable Metallic Glass. *Adv. Mater.* **2013**, *25* (41), 5904–5908.

(23) Qiu, Y.; Antony, L. W.; De Pablo, J. J.; Ediger, M. D. Photostability Can Be Significantly Modulated by Molecular Packing in Glasses. *J. Am. Chem. Soc.* **2016**, *138* (35), 11282–11289.

(24) Fakhraai, Z.; Still, T.; Fytas, G.; Ediger, M. D. Structural Variations of an Organic Glassformer Vapor-Deposited onto a Temperature Gradient Stage. *J. Phys. Chem. Lett.* **2011**, *2* (5), 423–427.

(25) Yokoyama, D. Molecular Orientation in Small-Molecule Organic Light-Emitting Diodes. *J. Mater. Chem.* **2011**, *21* (48), 19187.

(26) Dalal, S. S.; Ediger, M. D. Molecular Orientation in Stable Glasses of Indomethacin. *J. Phys. Chem. Lett.* **2012**, *3* (10), 1229–1233.

(27) Kearns, K. L.; Swallen, S. F.; Ediger, M. D.; Wu, T.; Sun, Y.; Yu, L. Hiking down the Energy Landscape: Progress toward the Kauzmann Temperature via Vapor Deposition. *J. Phys. Chem. B* **2008**, *112* (16), 4934–4942.

(28) Kearns, K. L.; Ediger, M. D.; Huth, H.; Schick, C. One Micrometer Length Scale Controls Kinetic Stability of Low-Energy Glasses. *J. Phys. Chem. Lett.* **2010**, *1* (1), 388–392.

(29) Dalal, S. S.; Fakhraai, Z.; Ediger, M. D. High-Throughput Ellipsometric Characterization of Vapor-Deposited Indomethacin Glasses. *J. Phys. Chem. B* **2013**, *117* (49), 15415–15425.

(30) Whitaker, K. R.; Tylinski, M.; Ahrenberg, M.; Schick, C.; Ediger, M. D. Kinetic Stability and Heat Capacity of Vapor-Deposited Glasses of O-Terphenyl. *J. Chem. Phys.* **2015**, *143*, 84511.

(31) Liu, M.; Cao, C. R.; Lu, Y. M.; Wang, W. H.; Bai, H. Y. Flexible Amorphous Metal Films with High Stability. *Appl. Phys. Lett.* **2017**, *110* (3), 31901.

(32) Zhu, L.; Brian, C. W.; Swallen, S. F.; Straus, P. T.; Ediger, M. D.; Yu, L. Surface Self-Diffusion of an Organic Glass. *Phys. Rev. Lett.* **2011**, *106* (25), 256103.

(33) Chen, Y.; Zhang, W.; Yu, L. Hydrogen Bonding Slows Down Surface Diffusion of Molecular Glasses. *J. Phys. Chem. B* **2016**, *120* (32), 8007–8015.

(34) Zhang, W.; Yu, L. Surface Diffusion of Polymer Glasses. *Macromolecules* **2016**, *49* (2), 731–735.

(35) Brian, C.; Yu, L. Surface Self-Diffusion of Organic Glasses. *J. Phys. Chem. A* **2013**, *117* (50), 13303–13309.

(36) Zhang, Y.; Fakhraai, Z. Invariant Fast Surface Diffusion on the Surfaces of Ultra-Stable and Aged Molecular Glasses. *Phys. Rev. Lett.* **2017**, *118*, 66101.

(37) Dalal, S. S.; Walters, D. M.; Lyubimov, I.; de Pablo, J. J.; Ediger, M. D. Tunable Molecular Orientation and Elevated Thermal Stability of Vapor-Deposited Organic Semiconductors.

Proc. Natl. Acad. Sci. **2015**, *112* (14), 4227–4232.

(38) Lyubimov, I.; Antony, L.; Walters, D. M.; Rodney, D.; Ediger, M. D.; de Pablo, J. J. Orientational Anisotropy in Simulated Vapor-Deposited Molecular Glasses. *J. Chem. Phys.* **2015**, *143* (9), 94502.

(39) Reid, D.; Lyubimov, I.; Ediger, M.; de Pablo, J. Age and Structure of a Model Vapor-Deposited Glass. *Nat. Commun.* **2016**, *7*, 1–19.

(40) Laventure, A.; Gujral, A.; Lebel, O.; Pellerin, C.; Ediger, M. D. Influence of Hydrogen Bonding on the Kinetic Stability of Vapor-Deposited Glasses of Triazine Derivatives. *J. Phys. Chem. B* **2017**, *121*, 2350–2358.

(41) Tylinski, M.; Chua, Y. Z.; Beasley, M. S.; Schick, C.; Ediger, M. D. Vapor-Deposited Alcohol Glasses Reveal a Wide Range of Kinetic Stability. *J. Chem. Phys.* **2016**, *145*, 174506.

(42) Aziz, H.; Popovic, Z. D. Degradation Phenomena in Small-Molecule Organic Light-Emitting Devices. *Chem. Mater.* **2004**, *16* (23), 4522–4532.

(43) Lee, T. Y.-H.; Wang, Q.; Wallace, J. U.; Chen, S. H. Temporal Stability of Blue Phosphorescent Organic Light-Emitting Diodes Affected by Thermal Annealing of Emitting Layers. *J. Mater. Chem.* **2012**, *22* (43), 23175.

(44) Nenna, G.; Barra, M.; Cassinese, a.; Miscioscia, R.; Fasolino, T.; Tassini, P.; Minarini, C.; della Sala, D. Insights into Thermal Degradation of Organic Light Emitting Diodes Induced by Glass Transition through Impedance Spectroscopy. *J. Appl. Phys.* **2009**, *105* (12), 123511.

(45) Sepúlveda, A.; Swallen, S. F.; Kopff, L. a; McMahon, R. J.; Ediger, M. D. Stable Glasses of Indomethacin and A,α,β-Tris-Naphthylbenzene Transform into Ordinary Supercooled Liquids. *J. Chem. Phys.* **2012**, *137* (20), 204508.

(46) Bhattacharya, D.; Sadtchenko, V. Vapor-Deposited Non-Crystalline Phase vs Ordinary Glasses and Supercooled Liquids: Subtle Thermodynamic and Kinetic Differences. *J. Chem. Phys.* **2015**, *142* (16), 164510.

(47) Rodriguez-Tinoco, C.; Gonzalez-silveira, M.; Ra, J.; Lopeand, A. F.; Clavaguera-mora, M. T.; Rodríguez-Viejo, J. Evaluation of Growth Front Velocity in Ultrastable Glasses of Indomethacin over a Wide Temperature Interval. *J. Phys. Chem. B* **2014**, *118*, 10795–10801.

(48) Sepúlveda, A.; Swallen, S. F.; Ediger, M. D. Manipulating the Properties of Stable Organic Glasses Using Kinetic Facilitation. *J. Chem. Phys.* **2013**, *138* (12), 12A517.

(49) Bhattacharya, D.; Sadtchenko, V. Enthalpy and High Temperature Relaxation Kinetics of Stable Vapor-Deposited Glasses of Toluene. *J. Chem. Phys.* **2014**, *141* (9), 94502.

(50) Rodríguez-Tinoco, C.; Ràfols-Ribé, J.; González-Silveira, M.; Rodríguez-Viejo, J. Relaxation

Dynamics of Glasses along a Wide Stability and Temperature Range. *Sci. Rep.* **2016**, *6*, 35607.

(51) Smith, R. S.; May, R. A.; Kay, B. D. Probing Toluene and Ethylbenzene Stable Glass Formation Using Inert Gas Permeation. *J. Phys. Chem. Lett.* **2015**, *6*, 3639–3644.

(52) Walters, D. M.; Richert, R.; Ediger, M. D. Thermal Stability of Vapor-Deposited Stable Glasses of an Organic Semiconductor. *J. Chem. Phys.* **2015**, *142* (13), 134504.

(53) Komino, T.; Nomura, H.; Yahiro, M.; Adachi, C. Real-Time Measurement of Molecular Orientational Randomization Dynamics during Annealing Treatments by In-Situ Ellipsometry. *J. Phys. Chem. C* **2012**, *116* (21), 11584–11588.

(54) Rodríguez-Tinoco, C.; Gonzalez-Silveira, M.; Ràfols-Ribé, J.; Lopeandia, A.; Rodriguez-Viejo, J. Transformation Kinetics of Vapor-Deposited Thin Film Organic Glasses: Role of Stability and Molecular Packing Anisotropy. *Phys. Chem. Chem. Phys.* **2015**, *17*, 31195–31201.

(55) Léonard, S.; Harrowell, P. Macroscopic Facilitation of Glassy Relaxation Kinetics: Ultrastable Glass Films with Frontlike Thermal Response. *J. Chem. Phys.* **2010**, *133* (24), 244502.

(56) Douglass, I.; Harrowell, P. Can a Stable Glass Be Superheated? Modelling the Kinetic Stability of Coated Glassy Films. *J. Chem. Phys.* **2013**, *138*, 12A516.

(57) Tito, N. B.; Milner, S. T.; Lipson, J. E. G. Enhanced Diffusion and Mobile Fronts in a Simple Lattice Model of Glass-Forming Liquids. *Soft Matter* **2015**, *11* (39), 7792–7801.

(58) Wolynes, P. G. Spatiotemporal Structures in Aging and Rejuvenating Glasses. *Proc. Natl. Acad. Sci.* **2009**, *106* (5), 1353–1358.

(59) Wisitsorasak, A.; Wolynes, P. G. Fluctuating Mobility Generation and Transport in Glasses. *Phys. Rev. E* **2013**, *88* (2), 22308.

(60) Sepúlveda, A.; Tylinski, M.; Guiseppi-Elie, A.; Richert, R.; Ediger, M. D. Role of Fragility in the Formation of Highly Stable Organic Glasses. *Phys. Rev. Lett.* **2014**, *113* (4), 45901.

(61) Ahrenberg, M.; Chua, Y. Z.; Whitaker, K. R.; Huth, H.; Ediger, M. D.; Schick, C. In Situ Investigation of Vapor-Deposited Glasses of Toluene and Ethylbenzene via Alternating Current Chip-Nanocalorimetry. *J. Chem. Phys.* **2013**, *138* (2), 24501.

(62) Hiszpanski, A. M.; Lee, S. S.; Wang, H.; Woll, A. R.; Nuckolls, C.; Loo, Y. Post-Deposition Processing Methods To Induce Preferential Orientation in Contorted Hexabenzocoronene Thin Films. *ACS Nano* **2013**, *7* (1), 294–300.

(63) Hiszpanski, A. M.; Baur, R. M.; Kim, B.; Tremblay, N. J.; Nuckolls, C.; Woll, A. R.; Loo, Y. L. Tuning Polymorphism and Orientation in Organic Semiconductor Thin Films via Post-Deposition Processing. *J. Am. Chem. Soc.* **2014**, *136* (44), 15749–15756.

(64) Hiszpanski, A. M.; Loo, Y.-L. Directing the Film Structure of Organic Semiconductors via Post-Deposition Processing for Transistor and Solar Cell Applications. *Energy Environ. Sci.* **2014**, *7* (2), 592.

(65) Wo, S.; Headrick, R. L.; Anthony, J. E. Fabrication and Characterization of Controllable Grain Boundary Arrays in Solution-Processed Small Molecule Organic Semiconductor Films. *J. Appl. Phys.* **2012**, *111* (7).

(66) Murti, R.; Reddy, K. V. Grain Boundary Effects on the Carrier Mobility of Polysilicon. *Phys. Stat. Sol.* **1990**, *119* (237), 237–240.

(67) Wallace, S. K.; McKenna, K. P. Grain Boundary Controlled Electron Mobility in Polycrystalline Titanium Dioxide. *Adv. Mater. Interfaces* **2014**, *1* (5), 1–5.

(68) O'Connor, B. T.; Reid, O. G.; Zhang, X.; Kline, R. J.; Richter, L. J.; Gundlach, D. J.; Delongchamp, D. M.; Toney, M. F.; Kopidakis, N.; Rumbles, G. Morphological Origin of Charge Transport Anisotropy in Aligned Polythiophene Thin Films. *Adv. Funct. Mater.* **2014**, *24* (22), 3422–3431.

(69) Yu, L. Amorphous Pharmaceutical Solids: Preparation, Characterization and Stabilization. *Adv. Drug Deliv. Rev.* **2001**, *48* (1), 27–42.

(70) Zhang, X.; Bronstein, H.; Kronemeijer, A. J.; Smith, J.; Kim, Y.; Kline, R. J.; Richter, L. J.; Anthopoulos, T. D.; Sirringhaus, H.; Song, K.; et al. Molecular Origin of High Field-Effect Mobility in an Indacenodithiophene-Benzothiadiazole Copolymer. *Nat. Commun.* **2013**, *4*, 2238.

(71) Shirota, Y. Organic Materials for Electronic and Optoelectronic Devices. *J. Mater. Chem.* **2000**, *10*, 1–25.

(72) Kageyama, H.; Ohishi, H.; Tanaka, M.; Ohmori, Y.; Shirota, Y. High Performance Organic Photovoltaic Devices Using Amorphous Molecular Materials with High Charge-Carrier Drift Mobilities. *Appl. Phys. Lett.* **2009**, *94* (6), 1–4.

(73) Yuan, Y.; Giri, G.; Ayzner, A. L.; Zoombelt, A. P.; Mannsfeld, S. C. B.; Chen, J.; Nordlund, D.; Toney, M. F.; Huang, J.; Bao, Z. Ultra-High Mobility Transparent Organic Thin Film Transistors Grown by an off-Centre Spin-Coating Method. *Nat. Commun.* **2014**, *5*, 1–9.

(74) Shibata, M.; Sakai, Y.; Yokoyama, D. Advantages and Disadvantages of Vacuum-Deposited and Spin-Coated Amorphous Organic Semiconductor Films for Organic Light-Emitting Diodes. *J. Mater. Chem. C* **2015**, *3*, 11178–11191.

(75) Oelkrug, D.; Haiber, J. Electronic Spectra of Self-Organized Oligothiophene Films With "standing" and "lying" molecular Units. *Thin Solid Films* **1996**, *284–285*, 267–270.

(76) Lin, H. W.; Lin, C. L.; Chang, H. H.; Lin, Y. T.; Wu, C. C.; Chen, Y. M.; Chen, R. T.; Chien, Y. Y.; Wong, K. T. Anisotropic Optical Properties and Molecular Orientation in Vacuum-Deposited ter(9,9-Diarylfluorene)s Thin Films Using Spectroscopic Ellipsometry. *J. Appl.*

Phys. **2004**, *95* (3), 881–886.

(77) Lin, H. W.; Lin, C. L.; Wu, C. C.; Chao, T. C.; Wong, K. T. Influences of Molecular Orientations on Stimulated Emission Characteristics of Oligofluorene Films. *Org. Electron. physics, Mater. Appl.* **2007**, *8*, 189–197.

(78) Yokoyama, D.; Sakaguchi, A.; Suzuki, M.; Adachi, C. Horizontal Orientation of Linear-Shaped Organic Molecules Having Bulky Substituents in Neat and Doped Vacuum-Deposited Amorphous Films. *Org. Electron.* **2009**, *10* (1), 127–137.

(79) Yokoyama, D.; Sakaguchi, A.; Suzuki, M.; Adachi, C. Horizontal Molecular Orientation in Vacuum-Deposited Organic Amorphous Films of Hole and Electron Transport Materials. *Appl. Phys. Lett.* **2008**, *93* (17), 173302.

(80) Yokoyama, D.; Adachi, C. In Situ Real-Time Spectroscopic Ellipsometry Measurement for the Investigation of Molecular Orientation in Organic Amorphous Multilayer Structures. *J. Appl. Phys.* **2010**, *107* (12), 123512.

(81) N. Hilfiker, J.; Bungay, C. L.; Synowicki, R. a.; Tiwald, T. E.; Herzinger, C. M.; Johs, B.; Pribil, G. K.; Woollam, J. a. Progress in Spectroscopic Ellipsometry: Applications from Vacuum Ultraviolet to Infrared. *J. Vac. Sci. Technol. A Vacuum, Surfaces, Film.* **2003**, *21* (4), 1103.

(82) Fujiwara, H. *Spectroscopic Ellipsometry Principles and Applications*; John Wiley & Sons Ltd: Chichester, England, 2007.

(83) Gujral, A.; O'Hara, K. a.; Toney, M. F.; Chabinyc, M. L.; Ediger, M. D. Structural Characterization of Vapor-Deposited Glasses of an Organic Hole Transport Material with X-Ray Scattering. *Chem. Mater.* **2015**, *27* (9), 3341–3348.

(84) Jiang, J.; Walters, D. M.; Zhou, D.; Ediger, M. Substrate Temperature Controls Molecular Orientation in Two-Component Vapor-Deposited Glasses. *Soft Matter* **2016**, *12*, 3265–3270.

(85) Sakai, Y.; Shibata, M.; Yokoyama, D. Simple Model-Free Estimation of Orientation Order Parameters of Vacuum-Deposited and Spin-Coated Amorphous Films Used in Organic Light-Emitting Diodes. *Appl. Phys. Express* **2015**, *8*, 96601.

(86) Gómez, J.; Jiang, J.; Gujral, A.; Huang, C.; Yu, L.; Ediger, M. D. Vapor Deposition of a Smectic Liquid Crystal: Highly Anisotropic, Homogeneous Glasses with Tunable Molecular Orientation. *Soft Matter* **2016**, *12* (11), 2942–2947.

Chapter 2

Tunable molecular orientation and elevated thermal stability of vapor-deposited organic semiconductors

Diane M. Walters, Shakeel S. Dalal, M. D. Ediger

Department of Chemistry, University of Wisconsin-Madison, Madison, Wisconsin 53706

Ivan Lyubimov, Juan J. de Pablo

Institute for Molecular Engineering, University of Chicago, Chicago, IL 60637

Reprinted with permission from Proceedings of the National Academy of Sciences, Volume 112, Issue 14, 4227 – 4232, 2015.

2.1. Significance

Glasses are solids that lack the regular order of crystals. Organic glasses, when produced by deposition from the vapor, can exhibit high levels of molecular orientation that improve performance of devices such as organic light-emitting diodes. We show here that molecular orientation in such glasses is primarily controlled by the substrate temperature during deposition, suggesting that the performance of almost any device based upon amorphous organic materials might be systematically optimized by this route. We explain molecular orientation in the glass in terms of the orientation present near the surface of the corresponding liquid. The highly oriented glasses formed here also exhibit high density and improved thermal stability. These features will likely further enhance the performance of organic electronics devices.

2.2. Abstract

Physical vapor deposition is commonly used to prepare organic glasses that serve as the active layers in light-emitting diodes, photovoltaics, and other devices. Recent work has shown that orienting the molecules in such organic semiconductors can significantly enhance device performance. We apply a high-throughput characterization scheme to investigate the effect of the substrate temperature ($T_{substrate}$) on glasses of three organic molecules used as semiconductors. The optical and material properties are evaluated with spectroscopic ellipsometry. We find that molecular orientation in these glasses is continuously tunable and controlled by $T_{substrate}/T_g$, where T_g is the glass transition temperature. All three molecules can produce highly anisotropic glasses; the dependence of molecular orientation upon substrate

temperature is remarkably similar and nearly independent of molecular length. All three compounds form “stable glasses” with high density and thermal stability, and have properties similar to stable glasses prepared from model glass formers. Simulations reproduce the experimental trends and explain molecular orientation in the deposited glasses in terms of the surface properties of the equilibrium liquid. By showing that organic semiconductors form stable glasses, these results provide an avenue for systematic performance optimization of active layers in organic electronics.

2.3. Introduction

Glasses (or amorphous solids) of low molecular weight organic compounds exhibit desirable properties for organic electronics. Because these materials are made from organic molecules, properties that depend on chemical identity such as optical absorptions, bandgap, and glass transition temperature can be tuned via chemical synthesis. These glasses have solid-like mechanical properties similar to those of crystalline materials, but offer morphological homogeneity, greater ease of processing, and nearly unlimited compositional tunability. An underappreciated feature of these materials, a result of their nonequilibrium nature, is that many different glasses can be prepared with the same chemical composition.

There has been considerable recent interest in controlling molecular orientation in organic semiconducting glasses (1–7). Whereas one might expect all glasses to be isotropic because of their structural disorder, Yokoyama et al. and other groups have shown that molecular orientation in vapor-deposited glasses can be quite anisotropic (3, 4, 8, 9) and depend upon deposition conditions (3). It has recently been suggested that orientation resulting from

deposition could be used as a figure of merit to identify promising compounds for these applications (10). Oriented materials can increase light outcoupling by a factor of 1.5 by directing emission out of the plane of the device (10–14). It has also been shown that oriented layers can improve device lifetime (15) and charge mobility (16–18). Given the potential utility of controlling molecular orientation in device layers (4, 5, 7), it is desirable to understand the extent to which molecular orientation can be tuned in glasses made from a particular compound and the mechanistic origins of this effect. Anisotropic glassy solids are also of interest for applications in optics and optoelectronics (19).

Concurrently, other investigators have shown that vapor-deposited glasses can have desirable physical properties unobtainable by any other means, when the substrate temperature during deposition ($T_{substrate}$) is held somewhat below the glass transition temperature (T_g). Discovered using model glass formers and labeled “stable glasses,” these glasses have lower enthalpies (20), higher densities (21), and resist structural reorganization to higher temperatures than is possible with any other preparation route (22–24). The properties of stable glasses are explained by the high mobility of the free surface during the vapor deposition process[20, 25]. Because of lowered constraints to motion (26), molecules near the free surface can adopt near-equilibrium packing arrangements during deposition even at temperatures where the bulk structural relaxation time is thousands of years (21, 27). Subsequent deposition traps this efficient packing into the bulk solid. Like organic semiconductors, stable glasses can be birefringent[21] and also anisotropic in wideangle X-ray scattering (28, 29).

Here we show that organic semiconductors form stable glasses, and that surface mobility during vapor deposition governs bulk molecular orientation in these materials. Using a high-throughput experimental scheme, we are able to efficiently characterize the effect of Tsubstrate on three organic compounds used in semiconducting devices: TPD, NPB, and DSA-Ph [Fig. 1E; N,N'-Bis(3-methylphenyl)-N,N'-diphenylbenzidine, N,N'-Di(1-napthyl)-N,N'-diphenyl-(1,1'-biphenyl)-4,4'-diamine, and 1–4-Di-[4-(N,Ndiphenyl)amino]styryl-benzene, respectively]. We find that these compounds form stable glasses, and we show that the orientation of the vapor-deposited molecules is controlled by $T_{substrate}/T_g$ and is nearly independent of the molecular aspect ratio. Using simulations, we show that anisotropic molecular orientation in the glass can be understood in terms of molecular orientation and mobility near the free surface of the equilibrium liquid. By connecting two apparently disparate bodies of work, we develop avenues for research on organic devices and the physics of glasses, and further the development of "designer" anisotropic solids.

2.4. Results

Fig. 1 illustrates our experimental procedure. Molecules are vapor-deposited in a vacuum chamber with base pressure near 10^{-7} torr onto a substrate with a controlled gradient of temperatures using a previously described apparatus (21). On a single substrate, this produces many glasses with identical chemical composition but different physical properties (*Materials and Methods*). The different glasses are characterized using spectroscopic ellipsometry with Kramers–Kronig consistent models (3). (*SI Text, Ellipsometry Measurements; Model Construction.*)

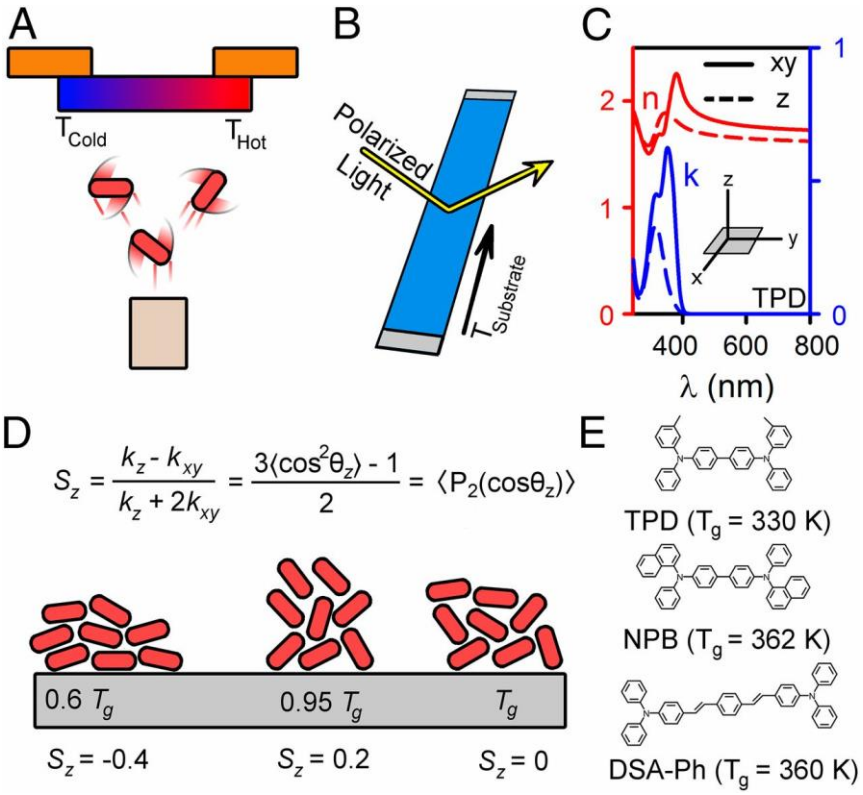

Fig. 1. Schematic illustration of the experimental procedure. (A) Organic molecules are vapor-deposited in a vacuum chamber. A silicon substrate with a controlled range of temperatures allows simultaneous deposition of many glasses with different properties but identical chemical composition. (B) After vapor deposition, each glass is independently interrogated using spectroscopic ellipsometry with a focused beam. (C) Example optical constants for TPD at $T_{substrate}$ = 215 K. The optical constants for light polarized normal to (z) and in the plane of the substrate (xy) can be independently determined (49). (D) Using the optical constants, the orientation order parameter, S_z, can be computed at each $T_{substrate}$. θ_z is the angle of the long molecular axis relative to the substrate normal and P_2 is the second Legendre polynomial. (E) Structures and glass transition temperatures for the three compounds studied.

Fig. 2A illustrates the determination of key material properties of a vapor-deposited glass using spectroscopic ellipsometry. When the “as-deposited” glass is initially heated, it expands as a solid while maintaining its as-deposited molecular orientation. At T_{onset}, which is greater than T_g for all of the materials reported here, the glass begins to transform into supercooled liquid (SCL). This results in an abrupt change in the film thickness. After the entire sample has become the SCL, it is cooled at a controlled rate. The thickness decreases linearly until the glass transition temperature, T_g, after which the material falls out of equilibrium and becomes the ordinary, liquid-cooled glass. By comparing the film thickness before and after temperature cycling, we are able to determine the density of the as-deposited glass relative to the ordinary glass (Δρ). For temperature gradient samples, Tonset is determined for many glasses during a single heating experiment, whereas Δρ is determined by mapping the sample thickness before and after heating (21).

The three semiconducting compounds investigated here (TPD, NPB, and DSA-Ph) all form stable glasses via vapor deposition. This is illustrated in Fig. 2B by the high onset temperatures and in Fig. 2C by the high densities . The elevated thermal stability of these materials may provide an avenue to increase device lifetime by imparting greater stability to the useful structures formed by vapor deposition (see *Discussion*). The results in Fig. 2 B and C are in good agreement with previously reported results for indomethacin (IMC) (21), the most extensively studied stable glass former, and can be interpreted as follows. At $T_{substrate}/T_g \geq 1$, surface and bulk mobility are high enough to allow total equilibration at the deposition temperature; when the sample is cooled to 293 K for measurement, it becomes the ordinary glass and has the expected values of T_{onset}/T_g and Δρ. At lower values of $T_{substrate}/T_g$, there is a thermodynamic

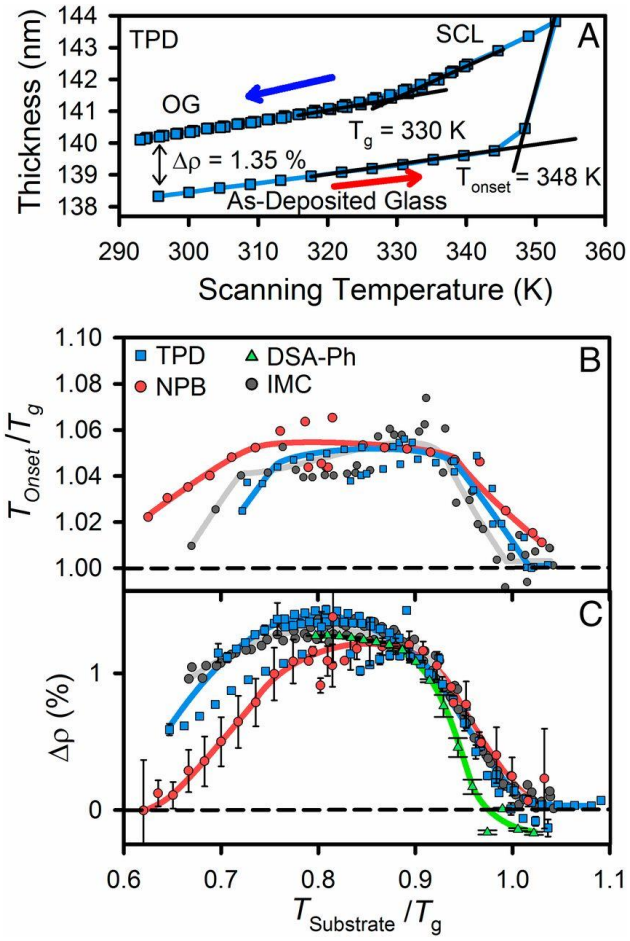

Fig. 2. Properties of as-deposited glasses measured with spectroscopic ellipsometry. (A) Sample thickness during heating and cooling for a vapor-deposited glass of TPD ($T_{substrate}$ = 289 K). We compute a relative density, Δρ, between the as-deposited glass and the ordinary glass from the change in film thickness. T_{onset}, a measure of structural stability against heating, is the temperature at which the sample begins to transform into the liquid. Each data point represents an independent fit of the optical constants and film thickness at the measurement temperature. (B) T_{onset}/T_g for three molecules used as organic semiconductors and one model glass former (21). T_{onset} is greater than T_g for these materials, indicating that more thermal energy is required to dislodge the molecules from their solid-state packing, relative to the liquid-cooled glass. Each data point represents a single, independently characterized material.

(C) The dependence of Δρ upon $T_{substrate}/T_g$ for glasses made of four compounds. Competition between kinetics and thermodynamics produces materials with many different densities. The T_{onset}/T_g and Δρ data for TPD, NPB, and DSA-Ph are consistent with previous data for IMC (21), a model glass former. The data shown are from 1,064 independently characterized materials (475 are IMC). For only DSA-Ph, Δρ is determined using the Lorentz–Lorenz equation *(SI Text, Density Determination for DSA-Ph)* (50–52). Error bars represent 90% confidence intervals (n = 3–6) and are independently calculated for each $T_{substrate}/T_g$ on each sample, and are smaller than the symbol size for most measurements.

driving force to form the equilibrium SCL at that temperature resulting in higher stability, higher density materials. The mobility of the surface enables molecules to find these tight packing arrangements (20, 25, 27), even though this would require a prohibitively long time for a bulk material. T_{onset}/T_g and $\Delta\rho$ are maximized when high surface mobility is paired with a large thermodynamic driving force. At the lowest $T_{substrate}/T_g$ the surface is so immobile that only marginally stable glasses are formed despite the presence of the largest driving force for densification. Our results are in good agreement with a recent report that NPB forms a stable glass when deposited onto a room-temperature substrate (15).

Using spectroscopic ellipsometry, we find that vapor-deposited glasses of the three compounds are anisotropic, each with continuously tunable average molecular orientation that is well-correlated with $T_{substrate}/T_g$. Fig. 3 shows the order parameter, S_z, and the birefringence as a function of $T_{substrate}/T_g$. Using films 70–150 nm thick, S_z is computed from the dichroism of the absorption associated with the long axis of each molecul*e (SI Text, Computing the Orientation Order Parameter)*. As shown in Fig. 1D, S_z is a measure of the average orientation of the long axis relative to the surface normal. At the lowest temperatures, S_z closely approaches the limit ($S_z = -0.5$) where the long axes of all molecules lie in the plane of the substrate. Such horizontal alignment may be useful in increasing the light outcoupling efficiency of emitting molecules (2), or the absorption of light in the photoactive layer of a solar cell. Using films 70–900 nm thick, the birefringence, $\Delta n = n_z - n_{xy}$, is calculated at 632.8 nm; Δn results from molecular orientation and the anisotropic polarizability tensors of these molecules. By comparing different samples and models, we estimate that the S_z and Δn values reported in Fig. 3 are accurate to ± 0.05 and ±0.01, respectively.

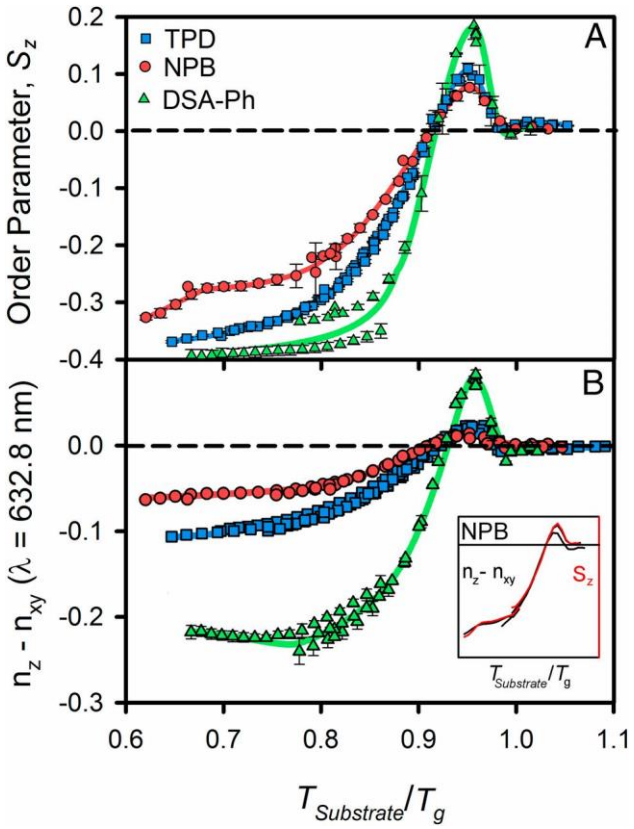

Fig. 3. Measures of molecular orientation as a function of $T_{substrate}/T_g$ for vapor-deposited glasses of three molecules used in organic semiconductors. (A) The order parameter Sz reporting the average orientation of molecules in the glass. Fig. 1D schematically interprets these results. A wide range of S_z values is accessed and a generic trend is observed for these three linear molecules with different aspect ratios. The data shown are from 612 independently characterized materials. (B) The birefringence, which for these materials is also sensitive to the average orientation of the long molecular axis relative to the substrate. The birefringence and S_z show good correspondence, as shown in the inset for NPB. The data shown are from 828 independently characterized materials. Error bars represent 90% confidence intervals (n = 3–6).

Our high-throughput methodology allows us to differentiate between the effect of molecular shape and $T_{substrate}/T_g$ for the first time, to our knowledge. The influence of these two variables on molecular orientation has been studied by Yokoyama (3) and our results are broadly consistent with this previous work. Whereas Yokoyama concluded that molecules with more anisotropic shapes produce more anisotropic materials (30, 31), our extended data show in addition that even relatively short molecules like TPD and NPB can be significantly oriented, as long as $T_{substrate}$ is correctly chosen. Given the similar trend observed for the three different compounds studied here, we propose that the parameter which primarily controls the orientation of linear molecules is $T_{substrate}/T_g$ rather than molecular aspect ratio. This is a significant change in perspective, as it suggests that a wide range of molecular orientations might be achieved with almost any organic compound.

To understand the origin of molecular orientation in vapor-deposited glasses, we simulated the vapor deposition of a coarse-grained representation of TPD composed of six Lennard-Jones spheres connected by harmonic springs (Fig. 4, *Inset*). We used a previously described algorithm that mimics the essential features of the deposition process (*Materials and Methods*) (32). A small number of molecules is introduced to the simulation box in the gas phase and allowed to condense at the free surface of a growing film. The just-deposited molecules are maintained at an elevated temperature to mimic the effect of enhanced surface mobility; these molecules are then gradually cooled to the substrate temperature. After an energy minimization step, the next group of molecules is introduced. The process is continued until a vapor-deposited film with a thickness of roughly 15 molecular diameters is obtained. These simulations were performed over a range of substrate temperatures. Fig. 4 shows that the molecular orientation

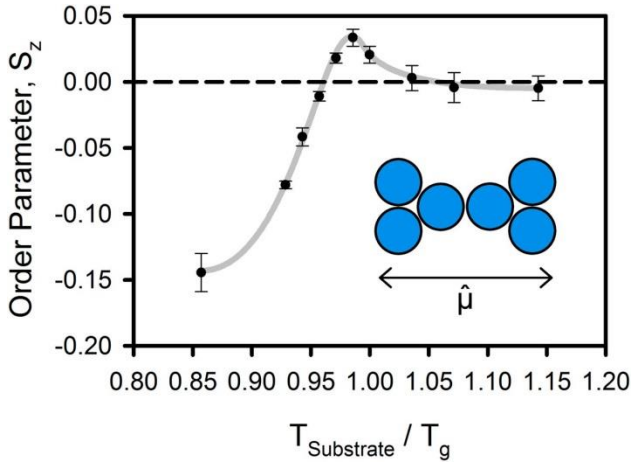

Fig. 4. Order parameter S_z as a function of $T_{substrate}/T_g$ from simulations of vapor-deposited glasses of the inset molecule. These simulations qualitatively reproduce the experimental results shown in Fig. 3A. The orientation of the deposited material is defined by comparing the long axis of the molecule to the substrate normal, $S_z = \langle P_2(\hat{u}\cdot\hat{z})\rangle$. The T_g obtained by cooling a liquid of these molecules at the lowest accessible rate is 0.70. The error bars represent the standard error of five independently prepared samples.

in these simulated vapor-deposited films has the same dependence upon substrate temperature as observed in the experiments shown in Fig. 3A. In particular, near T_g, the simulated glasses display a weak tendency to orient molecules normal to the substrate, and at lower temperatures a stronger tendency to orient molecules in the plane of the substrate. The simulated glasses exhibit high density and high onset temperatures, in analogy to Fig. 2 (*SI Text, Simulations*). Note that this model was designed to explore the generic features of the experiments and has not been parameterized against atomistic simulations, ab initio calculations, or the experimental results.

Molecular orientation in vapor-deposited glasses can be understood to be a remnant of the molecular orientation present near the surface of the equilibrium liquid. We performed additional simulations, using conventional molecular dynamics, to investigate the order parameter and density for thin films of the equilibrium liquid above Tg; these results are shown in Fig. 5 A and B. Molecules nearest the free surface ($0 < z < 1.5$, in bead diameter units) have a propensity to lie in the plane of the surface. Further from the surface as the liquid reaches the bulk density ($1.5 < z < 3.5$), molecules have a tendency to orient vertically, and this tendency becomes stronger at lower temperatures. Beyond $z = 3.5$, orientation in the liquid is isotropic, as expected for a bulk liquid. At a given deposition rate, there will be some substrate temperature at which surface mobility is just sufficient to equilibrate the surface to a depth of $z = 2.5$ but no further. Molecules at this depth show a tendency toward vertical orientation and will become locked into this orientation when further deposition takes place.

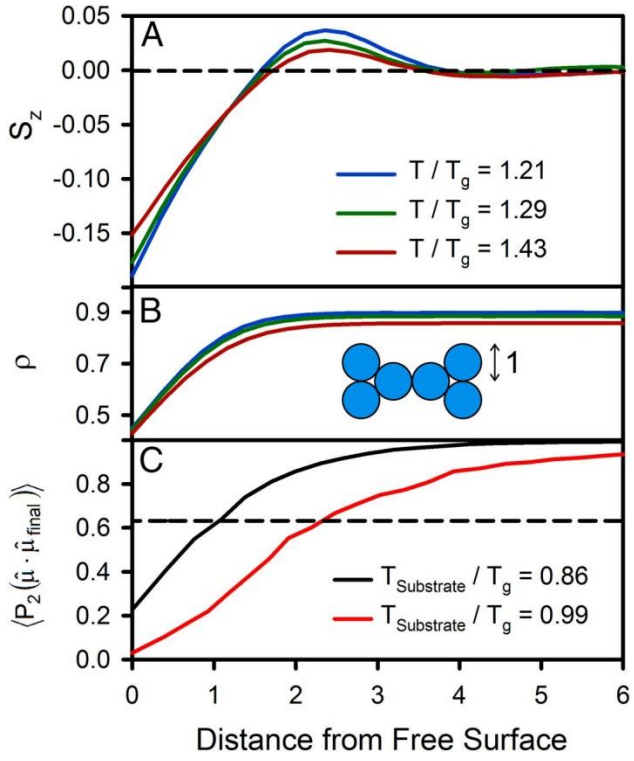

Fig. 5. Simulation results for the equilibrium liquid and the vapor-deposition process reveal the origin of molecular orientation in the glass. (A) The order parameter S_z for the equilibrium liquid at three temperatures above T_g. Molecules at the free surface (z = 0) tend to lie parallel to the surface. Just below the free surface (z ~ 2.5, in units of the bead diameter), molecules adopt a slight vertical orientation, and this tendency becomes stronger as the temperature decreases. (B) The number density (ρ) of the equilibrium liquid at three temperatures. The free surface (z = 0) is defined as the position where the density drops to half of the bulk value. (C) The immobilization of molecular orientation during deposition at two substrate temperatures. The y axis displays a local order parameter defined by the orientation of individual molecules relative to their final orientation. Molecular orientation becomes fixed closer to the free surface at lower substrate temperatures. The data in A and B were acquired using conventional molecular dynamics to equilibrate the liquid at the simulation temperature and is the average of 5,000 configurations. The x axis of all panels is provided in units of the bead diameter.

Within the context of the simulations of the deposition process, we can test this hypothesis for the origin of molecular orientation in the glass. We quantify the depth at which molecular orientation becomes fixed during deposition by calculating $\langle P_2(\hat{u}\cdot\hat{u}_{final})\rangle$, where $\hat{u}_{final}$ is the orientation of the long axis of the molecule after the deposition is complete. This function, shown in Fig. 5C, approaches unity as each molecule attains its final orientation in the glass and we use the 1/e point of this approach to define the thickness of the equilibrated layer at the free surface during deposition. We observe that equilibration to $z \sim 2.5$ occurs near $T_{substrate}/T_g = 0.99$, and Fig. 4 shows that this indeed is the vapor-deposited glass with the maximum value of S_z. At $T_{substrate}/T_g = 0.86$, the surface will only be equilibrated to a depth of $z \sim 1$. At this depth, molecules tend to be oriented parallel to the surface and this orientation becomes locked into the glass. When $T_{substrate}/T_g$ is above 1.02, mobility extends far enough into the film to ensure that an isotropic set of orientations are trapped in the vapor-deposited glass. We note that this explanation accounts for the qualitatively different dependences of S_z and $\Delta\rho$ upon the substrate temperature, as shown in Figs. 2 and 3.

The simulations suggest that orientation in vapor-deposited organic glasses is explained by two factors: (*i*) molecular orientation near the free surface of the equilibrium liquid at $T_{substrate}$, and (*ii*) mobility near the surface of the glass. The first factor might be investigated in greater detail with atomistic simulations and surface sensitive spectroscopy (33), whereas a number of new experimental methods are available to probe dynamics at the surface of glasses (25, 34). Structure at liquid surfaces is an active area of study (35, 36), and our results indicate that physical vapor deposition might be a useful tool in this endeavor.

2.5. Discussion

We anticipate that these results can influence work in organic electronics and related fields in several ways. Molecular orientation is already recognized as a key factor influencing device performance (1, 2, 4, 5, 10–15, 37, 38) and our results provide a predictive tool for choosing the deposition temperature needed to produce the desired orientation, effectively adding a dimension to device design. The ability to predictably tune refractive indices across a wide range is analogously useful in applications that rely on redirection of light, such as waveguides or antireflective coatings (39). Although the results shown in Fig. 3 are only known to apply to molecules of roughly linear shape, they suggest that a more general understanding of molecular orientation in vapor-deposited glasses may be attainable with high-throughput characterization and simulations. It is possible that liquid-crystal–forming molecules or systems with specific intermolecular interactions will exhibit orientation trends distinct from those found here, and this would be a further route toward control of molecular anisotropy in glassy solids. High-throughput experiments that directly measure charge mobility (16–18) would complement the results presented here.

Because the three systems investigated here show the density and onset temperatures expected for stable glasses, we anticipate that organic semiconductors will generally have other stable glass properties that should provide control over some known failure modes (40–42). For example, high glass density reduces uptake of atmospheric gases which can cause chemical degradation (43). Also, it is likely that stable semiconducting glasses will transform via a

surface-initiated mobility front (26, 44, 45), allowing the possibility of further enhancing thermal stability by engineering device interfaces.

These results also open avenues for increasing our fundamental understanding of glasses. At present, it is hard to discern what features of local packing provide the structural basis for high stability glasses. The anisotropic packing of these organic semiconductors provides additional experimental observables related to local structure [e.g., molecular orientation and anisotropic charge mobility (7)], thus providing the opportunity for a comprehensive understanding of structural stability in amorphous packing. One could ask whether it is possible to prepare stable glasses that do not have substantial anisotropy. Such systems would be ideal for understanding how the Kauzmann entropy crisis is resolved for very deeply supercooled liquids (46). Finally, anisotropy can be viewed as a type of ordering that drives a glass toward crystalline or liquid crystalline states. The existence of highly anisotropic glasses raises the question whether there is a level of anisotropy that cannot be surpassed while maintaining the macroscopic homogeneity associated with amorphous packing.

2.6. Materials and Methods

2.6.1. Experimental Methods

Our procedure for preparation and measurement of samples has previously been discussed (21). Physical vapor deposition of samples takes place inside a vacuum chamber with base pressure near 10^{-7} torr. After evacuating the chamber with a turbomolecular pump (occasionally in concert with cryopumping to lower the partial pressure of water) a copper cold cup is cooled via liquid-nitrogen–cooled gas. This copper cup is mechanically coupled to two

fingers supporting a single substrate that are independently temperature controlled using a Lakeshore 336 (Lakeshore Cryotronics), resistive heater cartridges (Southwest Heater Corporation), and 100-Ω platinum resistive temperature detectors (Omega). To produce a library of glasses of a single compound, the two fingers are set to different temperatures. After the gradient of temperatures in the substrate is established, it is held constant until the end of the deposition.

TPD and NPB were purchased from Sigma-Aldrich. DSA-Ph, 99% HPLC grade, was purchased from Luminescence Technology Corporation. All compounds were used without further purification. The compound for deposition is placed inside an alumina crucible that is heated by flow of current through resistive wire. The crucible is ∼18 cm away from the substrate. The deposition rate is controlled to be constant using a quartz crystal microbalance, and the true deposition rate is determined by the mean sample thickness divided by the duration of the deposition. The true deposition rate for TPD is 0.24 ± 0.03, NPB is 0.23 ± 0.03, and DSA-Ph is 0.27 ± 0.03, all in nm/s. Substrate temperatures are confirmed by comparison of temperature gradient samples to single-temperature substrates. The glass transition temperature, T_g, for TPD and NPB is determined by heating and cooling at 1 K/min while measuring with spectroscopic ellipsometry. T_g for DSA-Ph is determined by differential scanning calorimetry at 10 K/min.

Once the deposition is complete, the entire sample is brought to 293 K. The vacuum chamber is vented with nitrogen and the samples are either measured immediately or stored at

253 K before measurement. A temperature gradient sample of TPD was measured before and after storage at 253 K for 6 mo with no detectable evolution of its optical constants.

2.6.2. Simulation Methods

The coarse-grained TPD molecule considered here (Fig. 4, *Inset*) consists of six spherical beads representing the aromatic rings of the actual molecule (Fig. 1E). Each sphere interacts through a Lennard-Jones (LJ) potential energy function with parameters $\sigma_{bb} = 1.0$, $\varepsilon_{bb} = 1.0$. The cutoff distance for the potential is rc = 2.5 with a smooth decay starting at r = 2.4. To maintain the intramolecular structure, the six LJ particles of one molecule are connected by seven stiff bonds ($l_b = 1.0$, $k_b = 1{,}000$). Angle potentials are applied to four groups of three particles that include two interior beads and one of the exterior beads ($\theta = 150°$, $k_{angle} = 1{,}000$). No additional restrictions are applied on the relative rotation of the two halves of the molecule about the longitudinal ($\hat{u}$) axis.

The simulation box size is $20\ \sigma_{bb} \times 20\ \sigma_{bb}$ in the plane of the substrate ($\hat{x}$–$\hat{y}$), and at least $10\ \sigma_{bb}$ larger than the deposited film thickness normal to the substrate ($\hat{z}$). Periodic boundary conditions are applied in the $\hat{x}$–$\hat{y}$ plane. The substrate is generated from 1,000 randomly placed smaller LJ particles. The LJ potential parameters for the substrate are chosen in such a way as to minimize their effect on deposited molecules and prevent undesirable ordering (47). The parameters for the interaction with other substrate atoms are $\sigma_{ss} = 0.6$, $\varepsilon_{ss} = 0.1$, and with beads representing benzene rings $\sigma_{sb} = 1.0$ and $\varepsilon_{sb} = 1.0$, with a cutoff distance of $2.5\sigma_{\alpha\beta}$, where $\alpha,\beta \in s,b$. All substrate atoms are fixed to their random initial position with harmonic springs.

The simulated vapor deposition process is analogous to that reported earlier (9, 32). Iterative cycles are repeated until a film with thickness of ~35 σ_{bb} is grown. Each cycle consists of (*i*) introduction of four randomly oriented molecules in proximity of the film surface, (*ii*) equilibration of newly introduced molecules at high temperature (T=1.0), (*iii*) linear cooling of these molecules to the substrate temperature in 7 × 105 time steps, and (*iv*) energy minimization of the entire system. The previously deposited molecules and the substrate particles are maintained at a constant temperature throughout the process using a separate thermostat. For the results shown in Fig. 4, the order parameter is calculated from the middle layer of the films to reduce the effect of the substrate and free surface.

The equilibrium liquid profiles in Fig. 5 A and B were obtained by conventional molecular dynamics simulations and represent time averages over simulation runs comprising 108 time steps. All simulations were performed using the Large-Scale Atomic/Molecular Massively Parallel Simulator package (48) in the canonical ensemble with simulation time step of 0.001.

2.7. Acknowledgements

We thank Daisuke Yokoyama and Ken Kearns for helpful discussions. The experimental work was supported by the US Department of Energy, Office of Basic Energy Sciences, Division of Materials Sciences and Engineering, Award DE-SC0002161 (to S.S.D., D.M.W., and M.D.E.). The simulations were supported by National Science Foundation DMR-1234320 (to I.L. and J.J.d.P.).

Author contributions: S.S.D., I.L., J.J.d.P., and M.D.E. designed research; S.S.D., D.M.W., and I.L. performed research; S.S.D., D.M.W., I.L., J.J.d.P., and M.D.E. analyzed data; and S.S.D. and M.D.E. wrote the paper.

2.8. References

(1) Yokoyama D, Setoguchi Y, Sakaguchi A, Suzuki M, Adachi C (2010) Orientation control of linear-shaped molecules in vacuum-deposited organic amorphous films and its effect on carrier mobilities. Adv Funct Mater 20(3):386–391.

(2) Frischeisen J, Yokoyama D, Endo A, Adachi C, Brütting W (2011) Increased light outcoupling efficiency in dye-doped small molecule organic light-emitting diodes with horizontally oriented emitters. Org Electron 12(5):809–817.

(3) Yokoyama D (2011) Molecular orientation in small-molecule organic light-emitting diodes. J Mater Chem 21(48):19187–19202.

(4) Oh-e M, Ogata H, Fujita Y, Koden M (2013) Anisotropy in amorphous films of cross-shaped molecules with an accompanying effect on carrier mobility: Ellipsometric and sum-frequency vibrational spectroscopic studies. Appl Phys Lett 102(10):101905.

(5) Tumbleston JR, et al. (2014) The influence of molecular orientation on organic bulk heterojunction solar cells. Nat Photonics 8(5):385–391.

(6) Marchetti AP, Haskins TL, Young RH, Rothberg LJ (2014) Permanent polarization and charge distribution in organic light-emitting diodes (OLEDs): Insights from near-infrared charge-modulation spectroscopy of an operating OLED. J Appl Phys 115(11):114506.

(7) Wakamiya A, et al. (2014) On-top π-stacking of quasiplanar molecules in hole-transporting materials: Inducing anisotropic carrier mobility in amorphous films. Angew Chem Int Ed Engl 53(23):5800–5804.

(8) Lin HW, et al. (2004) Anisotropic optical properties and molecular orientation in vacuum-deposited ter(9,9-diarylfluorene)s thin films using spectroscopic ellipsometry. J Appl Phys 95(3):881–886.

(9) Lin P-H, Lyubimov I, Yu L, Ediger MD, de Pablo JJ (2014) Molecular modeling of vapor-deposited polymer glasses. J Chem Phys 140(20):204504.

(10) Mayr C, Taneda M, Adachi C, Brütting W (2014) Different orientation of the transition dipole moments of two similar Pt(II) complexes and their potential for high efficiency organic light-emitting diodes. Org Electron 15(11):3031–3037.

(11) Komino T, Tanaka H, Adachi C (2014) Selectively controlled orientational order in linear-shaped thermally activated delayed fluorescent dopants. Chem Mater 26(12):3665–3671.

(12) Kuma H, Hosokawa C (2014) Blue fluorescent OLED materials and their application for high-performance devices. Sci Technol Adv Mater 15(3):034201.

(13) Ogiwara T, et al. (2014) Efficiency improvement of fluorescent blue device by molecular orientation of blue dopant. J Soc Inf Disp 22(1):76–82.

(14) Kim B, et al. (2013) Synthesis and elecpagetroluminescence properties of highly efficient blue fluorescence emitters using dual core chromophores. J Mater Chem C 1(3):432–440.

(15) Kearns KL, et al. (2014) in SPIE Organic Photonics + Electronics, eds So F, Adachi C (International Society for Optics and Photonics, Bellingham, WA), Vol 9183, p 91830F.

(16) Yokoyama D, Sasabe H, Furukawa Y, Adachi C, Kido J (2011) Molecular stacking induced by intermolecular C–H···N hydrogen bonds leading to high carrier mobility in vacuum-deposited organic films. Adv Funct Mater 21(8):1375–1382.

(17) Chen W-C, et al. (2014) Staggered face-to-face molecular stacking as a strategy for designing deep-blue electroluminescent materials with high carrier mobility. Adv Opt Mater 2(7):626–631.

(18) Hiszpanski AM, Loo Y-L (2014) Directing the film structure of organic semiconductors via post-deposition processing for transistor and solar cell applications. Energy Environ Sci 7(2):592–608.

(19) Kim C, Marshall KL, Wallace JU, Chen SH (2008) Photochromic glassy liquid crystals comprising mesogenic pendants to dithienylethene cores. J Mater Chem 18(46):5592–5598.

(20) Swallen SF, et al. (2007) Organic glasses with exceptional thermodynamic and kinetic stability. Science 315(5810):353–356.

(21) Dalal SS, Fakhraai Z, Ediger MD (2013) High-throughput ellipsometric characterization of vapor-deposited indomethacin glasses. J Phys Chem B 117(49):15415–15425.

(22) Leon-Gutierrez E, Garcia G, Lopeandia AF, Clavaguera-Mora MT, Rodríguez-Viejo J (2010) Size effects and extraordinary stability of ultrathin vapor deposited glassy films of toluene. J Phys Chem Lett 1(1):341–345.

(23) Leon-Gutierrez E, Sepúlveda A, Garcia G, Clavaguera-Mora MT, Rodríguez-Viejo J (2010) Stability of thin film glasses of toluene and ethylbenzene formed by vapor deposition: An in situ nanocalorimetric study. Phys Chem Chem Phys 12(44):14693–14698.

(24) Ahrenberg M, et al. (2013) In situ investigation of vapor-deposited glasses of toluene and ethylbenzene via alternating current chip-nanocalorimetry. J Chem Phys 138(2):024501.

(25) Zhu L, et al. (2011) Surface self-diffusion of an organic glass. Phys Rev Lett 106(25):256103.

(26) Léonard S, Harrowell P (2010) Macroscopic facilitation of glassy relaxation kinetics: Ultrastable glass films with frontlike thermal response. J Chem Phys 133(24):244502.

(27) Brian CW, Yu L (2013) Surface self-diffusion of organic glasses. J Phys Chem A 117(50):13303–13309.

(28) Dawson KJ, Zhu L, Yu L, Ediger MD (2011) Anisotropic structure and transformation kinetics of vapor-deposited indomethacin glasses. J Phys Chem B 115(3):455–463.

(29) Singh S, de Pablo JJ (2011) A molecular view of vapor deposited glasses. J Chem Phys 134(19):194903.

(30) Yokoyama D, Sakaguchi A, Suzuki M, Adachi C (2008) Horizontal molecular orientation in vacuum-deposited organic amorphous films of hole and electron transport materials. Appl Phys Lett 93(17):173302.

(31) Yokoyama D, Sakaguchi A, Suzuki M, Adachi C (2009) Horizontal orientation of linear-shaped organic molecules having bulky substituents in neat and doped vacuum-deposited amorphous films. Org Electron 10(1):127–137.

(32) Lyubimov I, Ediger MD, de Pablo JJ (2013) Model vapor-deposited glasses: Growth front and composition effects. J Chem Phys 139(14):144505.

(33) Hommel EL, Allen HC (2003) 1-methyl naphthalene reorientation at the air−liquid interface upon water saturation studied by vibrational broad bandwidth sum frequency generation spectroscopy. J Phys Chem B 107(39):10823–10828.

(34) Chai Y, et al. (2014) A direct quantitative measure of surface mobility in a glassy polymer. Science 343(6174):994–999.

(35) Waring C, Bagot PAJ, Costen ML, McKendrick KG (2011) Reactive scattering as a chemically specific analytical probe of liquid surfaces. J Phys Chem Lett 2(1):12–18.

(36) Andersson G, Ridings C (2014) Ion scattering studies of molecular structure at liquid surfaces with applications in industrial and biological systems. Chem Rev 114(17):8361–8387.

(37) Lee SS, Loo Y-L (2010) Structural complexities in the active layers of organic electronics. Annu Rev Chem Biomol Eng 1(1):59–78.

(38) Noguchi Y, et al. (2013) Influence of the direction of spontaneous orientation polarization on the charge injection properties of organic light-emitting diodes. Appl Phys Lett 102(20):203306.

(39) Yokoyama D, Nakayama K, Otani T, Kido J (2012) Wide-range refractive index control of organic semiconductor films toward advanced optical design of organic optoelectronic devices. Adv Mater 24(47):6368–6373.

(40) Jørgensen M, Norrman K, Krebs FC (2008) Stability/degradation of polymer solar cells. Sol Energy Mater Sol Cells 92(7):686–714.

(41) Krebs FC, Norrman K (2007) Analysis of the failure mechanism for a stable organic photovoltaic during 10 000 h of testing. Prog Photovolt Res Appl 15(8):697–712.

(42) Grossiord N, Kroon JM, Andriessen R, Blom PWM (2012) Degradation mechanisms in organic photovoltaic devices. Org Electron 13(3):432–456.

(43) Dawson KJ, Kearns KL, Ediger MD, Sacchetti MJ, Zografi GD (2009) Highly stable indomethacin glasses resist uptake of water vapor. J Phys Chem B 113(8):2422–2427.

(44) Sepúlveda A, Leon-Gutierrez E, Gonzalez-Silveira M, Clavaguera-Mora MT, Rodríguez-Viejo J (2012) Anomalous transformation of vapor-deposited highly stable glasses of toluene into mixed glassy states by annealing above Tg. J Phys Chem Lett 3(7):919–923.

(45) Wolynes PG (2009) Spatiotemporal structures in aging and rejuvenating glasses. Proc Natl Acad Sci USA 106(5):1353–1358.

(46) Kauzmann W (1948) The nature of the glassy state and the behavior of liquids at low temperatures. Chem Rev 43(2):219–256.

(47) Haji-Akbari A, Debenedetti PG (2014) The effect of substrate on thermodynamic and kinetic anisotropies in atomic thin films. J Chem Phys 141:024506.

(48) Plimpton S (1995) Fast parallel algorithms for short-range molecular dynamics. J Comput Phys 117(1):1–19.

(49) Woollam JA, et al. (1999) Overview of variable angle spectroscopic ellipsometry (VASE), Part I: Basic theory of typical applications. SPIE Proc CR72:3–28.

(50) Dalal SS, Ediger MD (2012) Molecular orientation in stable glasses of indomethacin. J Phys Chem Lett 3:1229–1233.

(51) Vuks MF (1966) Determination of the optical anisotropy of aromatic molecules from the double refraction of crystals. Opt Spectrosc 20:361–364.

(52) Vuks MF (1966) On the theory of double refraction of liquids and solution in an electric field. Opt Spectrosc 21:383–388.

2.9. Supplemental Information

2.9.1. Ellipsometry Measurements

Samples are measured using a custom-built temperature control and translation stage mounted to a spectroscopic ellipsometer (J.A. Woollam M-2000U). Measurements proceed by characterizing the as-deposited properties of the material, heating and cooling the material to prepare a known reference state for comparison, and then measuring the final state of the sample.

Because the beam footprint is small (1.5mm × 0.6 mm) relative to our sample (1 cm × 3.2 cm) we are able to independently characterize different locations, and thus different substrate temperatures. To characterize the as-deposited materials, we typically perform measurements in 16 rows (each row is perpendicular to the temperature gradient) and 5 columns (each column is parallel to the gradient), for a total of 80 independently characterized glasses per sample.

After the initial mapping, the entire sample is heated at 1 K/min to measure T_{onset} (Fig. 2 A and B). Twelve different substrate temperatures are measured periodically during this heating ramp. An example of one of these measurements is shown in Fig. 2A. Once the entire sample has become the supercooled liquid, it is cooled at 1 K/min to form the ordinary glass. The data acquired during heating and cooling are only used to determine T_{onset} as they are taken at only a single angle and are thus not as reliable as the data acquired before and after heating.

Once the sample has returned to 293 K, the same locations that were measured before transformation are remeasured. The change in the thickness between the initial and this final measurement is used to determine Δρ as shown in Fig. 2C for TPD and NPB. (Density and thickness are inversely related because the sample dimensions are fixed in the plane of the substrate.) Complete transformation of all locations on the temperature gradient sample was verified by observing that the entire sample had identical optical constants in the final mapping. Minimal physical aging was observed during the course of the final measurement and no correction was made for this effect. A different procedure was used to obtain Δρ for DSA-Ph as described below in Density Determination of DSA-Ph.

The initial and final measurements are performed at seven incident angles evenly spaced between 45° and 75° from the normal, or at three incident angles, 50°, 60°, and 70° from the normal, over the wavelength range of 245–1,000 nm. This allows us to determine the optical properties as a function of substrate temperature (from the data along each column) and calculate the precision of our characterization for each substrate temperature independently (from the data along each row). Data from rows are averaged and presented in Figs. 2 and 3 as a single point, with error bars indicating a 90% confidence interval. For most points, the error bars are smaller than the symbol size. In total, 828 glasses (111 DSA-Ph, 115 NPB, 602 TPD) were characterized for this study. We have excluded data on 36 glasses (18 DSA-Ph, 8 NPB, 10 TPD) due to the presence of imperfections on the substrate before or after characterization. Without the high-throughput techniques we use here, systematic examination of this many samples would have been nearly impossible.

2.9.1.1. Model Construction

To determine the orientation order parameter, S_z, we treat the organic films using Kramers–Kronig consistent absorptive models in CompleteEase (J.A. Woollam Company). Our procedures are similar to those used by Yokoyama (1) and are described below for completeness. Because we produce many glasses of the same compound we are able to perform a global analysis that requires any given model to fit all of the glasses of a given compound (see Reliability of Models below).The Kramers–Kronig equation exactly specifies the relationship between the real (n) and imaginary (k) components of the complex index of refraction ($\tilde{n} = n + ik$) as a function of wavelength. Our models use parameters to specify $k(\lambda)$ and calculate $n(\lambda)$. We initially design

our models on ordinary glasses of the organic compound we are interested in, which are optically isotropic. An approximate determination of k(λ) is made using a model with unconstrained absorption properties. Once the approximate curve shapes are established, k(λ) is reparameterized as the sum of oscillators.

The positions, breadths, and amplitudes of the oscillators are determined by fitting to the data collected on an ordinary glass of each compound. The fitting process simulates ñ(λ) from seed values, compares the simulation to the data, and alters the model parameters to minimize the root-mean-squared error (MSE) between the simulation and the data. Representative optical constants determined from these isotropic oscillator models for ordinary glasses are shown in Fig. S1 and model parameters are given in Table S1. Whereas each oscillator in a given model might represent an electronic state of the molecule, our data cannot make such assignments conclusively. We are able to construct models with similarly shaped k(λ) that fit our data on anisotropic materials equally well, despite having different numbers of oscillators or different types of oscillators. We selected as the best models those with the smallest number of oscillators that were able to adequately describe isotropic samples.

2.9.1.2. Adapting Models for Dichroic Glasses and Ensuring Their Accuracy

To account for the dichroism of the as-deposited glasses, we use anisotropic optical models (2). Optical constants for light polarized perpendicular to the substrate are denoted n_z and k_z; for light polarized in the plane of the substrate they are denoted n_{xy} and k_{xy}. We assume that the anisotropic packing of the different glasses does not perturb the electronic structure of the molecules, and that the electronic structure determines the breadth and position of peaks in

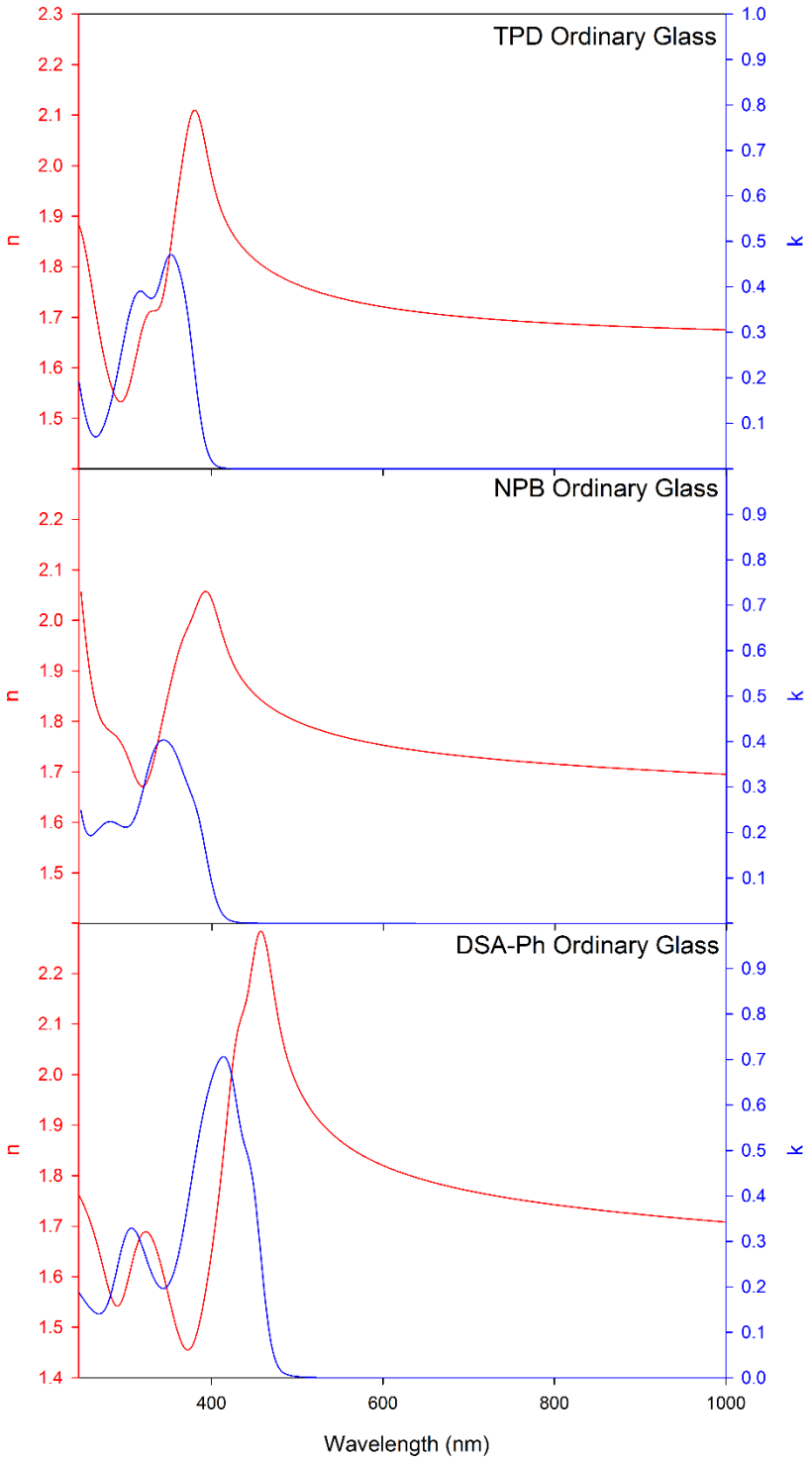

Fig. S1. Optical constants for ordinary glasses of TPD, NPB, and DSA-Ph thin films are shown. These optical constants are determined from isotropic models.

Table S1. Oscillator model parameters for ordinary glasses of organic semiconducting compounds measured at 293 K.

Compound	Oscillator Type[a]	Amplitude (unitless)	Breadth (eV)	Energy (eV)	λ (nm)	Gap Energy (E_g, eV)
TPD	Gaussian	0.613	0.213	3.313	374.2	
	Gaussian	1.247	0.309	3.478	356.5	
	Gaussian	1.250	0.611	3.870	320.4	
	Gaussian	0.274	0.576	4.340	285.7	
	Gaussian	1.400	0.840	5.461	227.0	
NPB	Gaussian	0.660	0.269	3.254	381.0	
	Tauc-Lorentz	26.058	0.570	3.471	357.2	2.879
	Gaussian	0.363	0.565	4.517	274.5	
	Gaussian	4.583	0.949	5.793	214.0	
DSA-Ph	Gaussian	1.166	0.151	2.759	449.4	
	Tauc-Lorentz	39.023	0.299	2.884	430.0	2.549
	Gaussian	0.898	0.475	3.077	402.9	
	Gaussian	0.732	0.539	4.021	308.3	
	Gaussian	0.757	1.688	5.664	218.9	

[a] Detailed explanation of oscillator models, including the mathematical form of the oscillators, can be found in Chapter 5 of *Spectroscopic Ellipsometry: Principles and Applications* by Hiroyuki Fujiwara (John Wiley & Sons Ltd).

k(λ). Therefore, we fix the type, position, and breadth of each oscillator as determined for the ordinary glass, while allowing the amplitude of each oscillator to differ between k_z and k_{xy}.

The data in Fig. 3 use anisotropic models for all materials. When ordinary glasses were fit with anisotropic models, the quality of fit was not improved and the optical constants produced were consistent with isotropy within ± 0.05 for S_z and within ±0.003 for Δn. In contrast, anisotropic materials fit with isotropic models produced poor fits (Fig. S2). The quality of fit was determined by the MSE between the model and data. For TPD and NPB, both the as-deposited and ordinary glasses had MSEs near 5. DSA-Ph had MSEs near 9. [The MSE is a unitless quantity that sums the squares of the experimental residuals, and then divides by the number of degrees of freedom (3).]

For DSA-Ph it was necessary to further constrain the anisotropic model used to fit the vapor-deposited glasses. The oscillator centered at 2.759 eV was allowed to vary its amplitude, but the amplitude was constrained to be the same in and out of the plane of the substrate. The oscillator centered at 4.021 eV was allowed to vary its breadth in the as-deposited glasses, but was also coupled to be the same in and out of the plane of the substrate. These couplings are likely related to model complexity and limitations of the fit algorithms used in this work and not the behavior of the material. Comparing coupled and uncoupled models produces only small changes in S_z and Δn. Coupled models of DSA-Ph are significantly more computationally tractable, however.

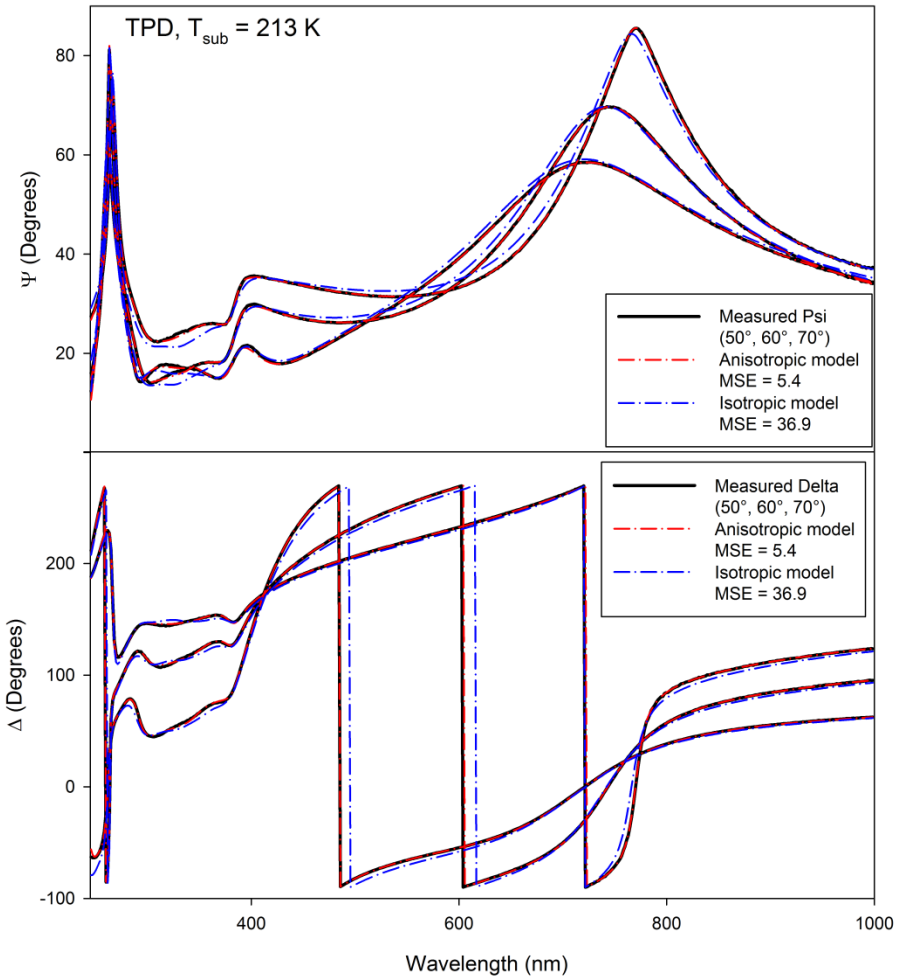

Fig. S2. Measured ellipsometric parameters are compared with isotropic and anisotropic models for TPD; see text for model descriptions. Ψ and Δ together can be expressed as the complex Fresnel reflection coefficient. They depend on ñ(λ) for silicon, the native oxide of silicon, and the organic film. They also depend on the thickness of the native oxide and the organic film. Only the properties of the organic film are optimized in these fits.

2.9.1.3. Reliability of Models

One aspect of our modeling procedure which is novel is the consistent application of a single model to many glasses of the same compound, spanning a wide range of molecular orientations. Because we are able to assume that the ordinary glass is optically isotropic, we are able to define the structure of our models on materials with known properties ($S_z = 0$, $\Delta n = 0$). We expect that models that are sufficiently robust to accurately fit the entire range of glasses produce results that are more realistic. Another indication of the robustness of the models used here is the smooth, systematic changes in n_{xy}, n_z, k_{xy}, and k_z as a function of $T_{substrate}$. Fig. S3 shows optical constants of TPD at many $T_{substrate}$, all treated with a single model. The only values allowed to vary from glass-to-glass are the amplitude of the oscillators underlying k(λ) and the film thickness.

During model development, we generate models which fit the ellipsometry data almost as well as our best model for each compound (described in Table S1). These models can have different numbers, types, widths, positions, and amplitudes of oscillators and do not necessarily have quantitatively identical shapes for k(λ). Nonetheless, when these models are applied to the full range of glasses for a given compound, the values of S_z and Δn reported in the main text are generally reproduced within our stated errors. This provides evidence that the reported values are accurate.

As an additional check on our modeling, we also performed ellipsometry experiments on films 400–900 nm thick for all three compounds. We fit these data only for wavelengths at which the material does not absorb light using a previously described anisotropic Cauchy

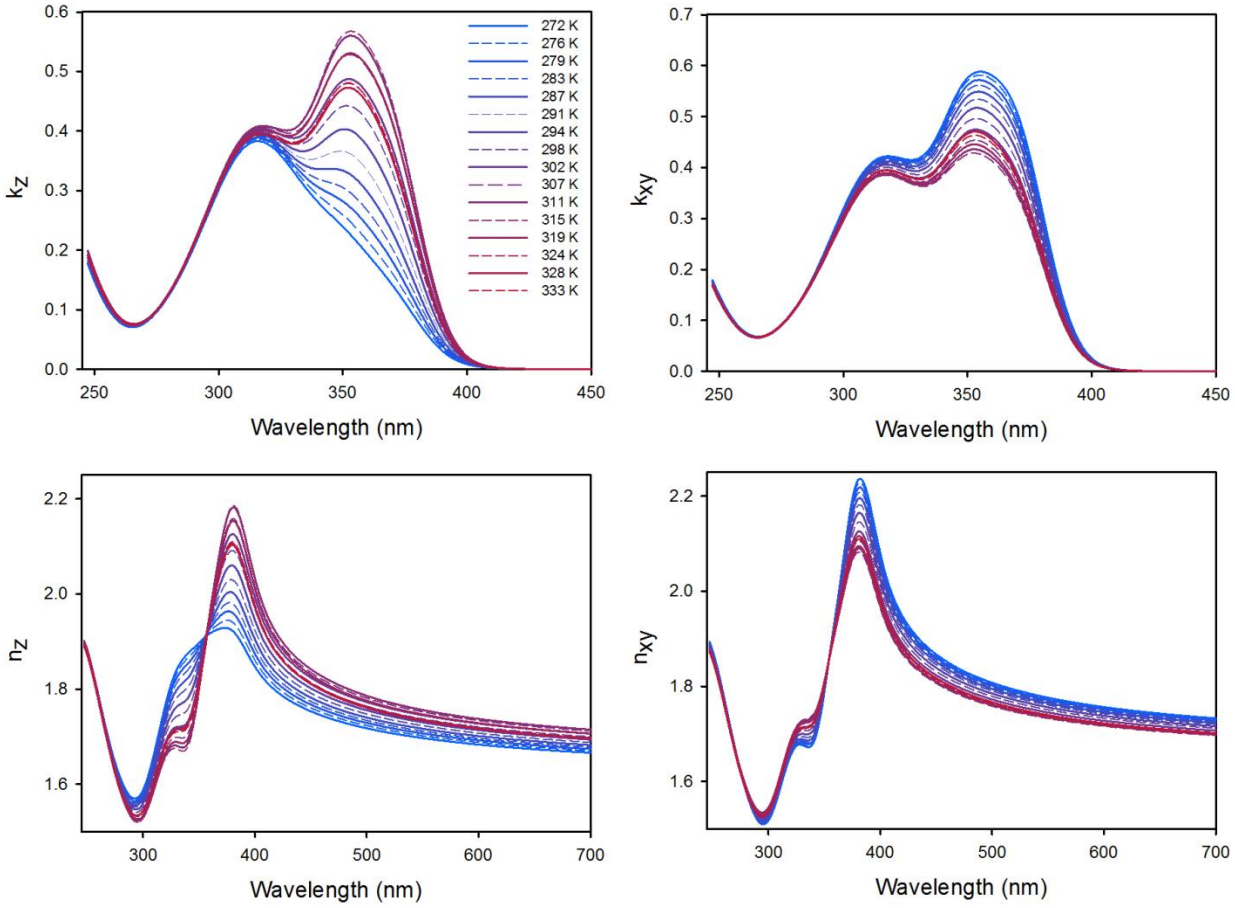

Fig. S3. Optical constants for TPD at many different substrate temperatures. All glasses made from TPD are treated with a single optical model which allowed only the strength of absorption (oscillator amplitude) for each polarization to vary, in addition to the film thickness.

model (4) to determine the birefringence; MSEs for Cauchy-based models were near 5 for all compounds. Yokoyama has previously established that the optical constants for vapor-deposited films do not depend upon film thickness (5). Data on thick films are presented in Figs. 2 B and C and 3B but are not distinguished because of the good agreement between thin films and thick films. Obtaining the same birefringence from two independent routes is a strong argument that the oscillator models are accurately describing the ellipsometry data. (The order parameter S_z could not be determined for thick films, because of the high absorptivity of the compounds in the UV. Applying Cauchy models to films thin enough to use absorptive models resulted in nonunique fits and were not used for this reason.)

2.9.2. Simulations

Using conventional molecular dynamics, we performed temperature ramping simulations comparable to the ellipsometric experiments shown in Fig. 2A. Fig. S4 shows the potential energy of simulated glasses prepared by vapor deposition or cooling the liquid. The potential energy is determined by the sum of the energy of all interactions in the system. Symbols represent vapor-deposited films where the substrate temperature was in the range $0.6 \leq T_{substrate} \leq 0.8$. For comparison, we display the potential energy of the equilibrium liquid cooled at four different cooling rates ranging from $q_c = 10^{-3}$ to $q_c = 10^{-6}$ (temperature/time, in LJ units). The fictive temperatures, T_f, for each cooling rate were found as the intersection of two slopes representing the equilibrium liquid line and the extrapolated line from the glassy region. The cooling-rate dependence of the fictive temperature is linear and the temperature shift is equal to approximately $\Delta T_f = 0.02$ per decade of cooling rate.

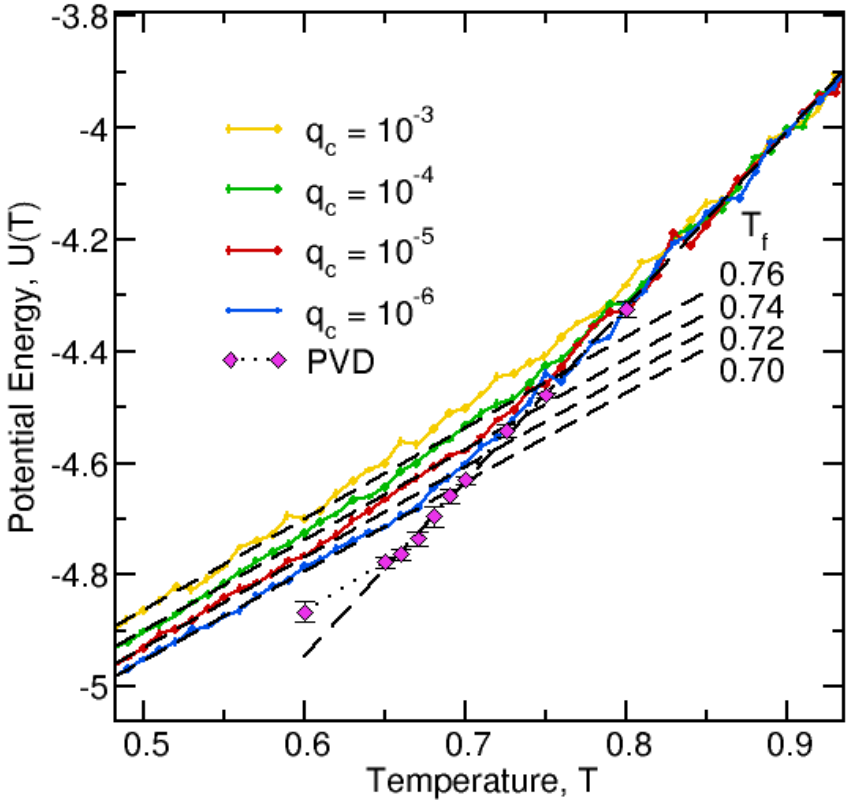

Fig. S4. Potential energy as a function of temperature. Symbols represent the films deposited on the substrate at temperatures in the range $0.6 \leq T_{substrate} \leq 0.8$. Colored lines show the temperature dependence of the potential energy while cooling from the equilibrium liquid at four cooling rates ranging from $q_c = 10^{-3}$ to $q_c = 10^{-6}$.

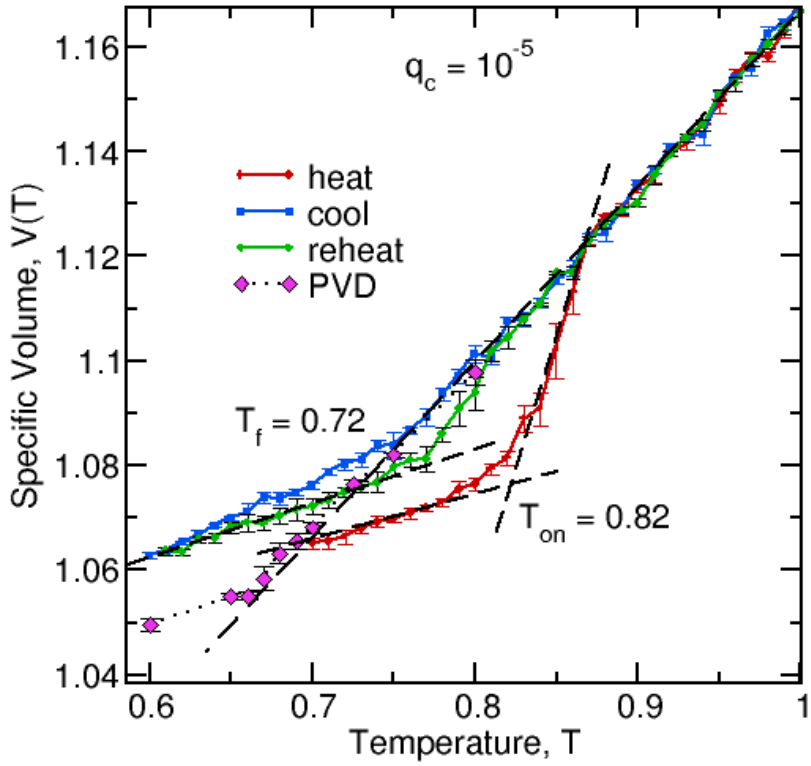

Fig. S5. Specific volume as a function of temperature. Symbols represent films deposited on substrates with temperatures in the range $0.6 \leq T_{substrate} \leq 0.8$. The red, blue, and green lines correspond to heating, cooling, and reheating curves starting from a film deposited at $T_{substrate} = 0.69$. At this substrate temperature the largest value of S_z is observed (most vertical orientation of the molecules). The heating–cooling rate was $q_c = 10^{-5}$.

Fig. S5 shows the temperature dependence of the specific volume during temperature cycling for the film deposited at the substrate temperature $T_{substrate}$ = 0.69; this is the substrate temperature with the largest order parameter (most vertically oriented molecules). During the first heat, T_{onset} = 0.82, indicating substantial kinetic stability relative to that observed during reheating. For all simulation results except Fig. 5 we report values measured from the middle layer of the film to reduce the effect of the substrate and the free surface (6).

The simulation results shown in Figs. S4 and S5 indicate that the coarse-grained model of TPD is a good glass former and resistant to crystallization. This model has not been parameterized against atomistic simulations, ab initio calculations, or the experimental results. The model was designed as a generic model for the linear molecules used in the experiments. Despite its simplicity, the favorable comparison with the experimental results (Figs. 3A and 4) shows that the simulation model captures the essential features of the physical system which result in molecular orientation in vapor-deposited glasses. The amplitude of the ordering effect observed in Fig. 4 is about three times weaker than in the experimental measurements shown in Fig. 3A. We attribute this to the simplicity of the model, including the lack of dipole interactions. Nevertheless, the qualitative correspondence between the simulations and experiments indicates that the model does allow an exploration of important generic features of the deposition process.

Fig. 5 provides the simulation results that explain the mechanism of molecular orientation in as-deposited glasses. For Fig. 5C only and for Fig. S6 below, we make use of the simulations that mimic the deposition process. Fig. 5 A and B uses conventional molecular dynamics. For

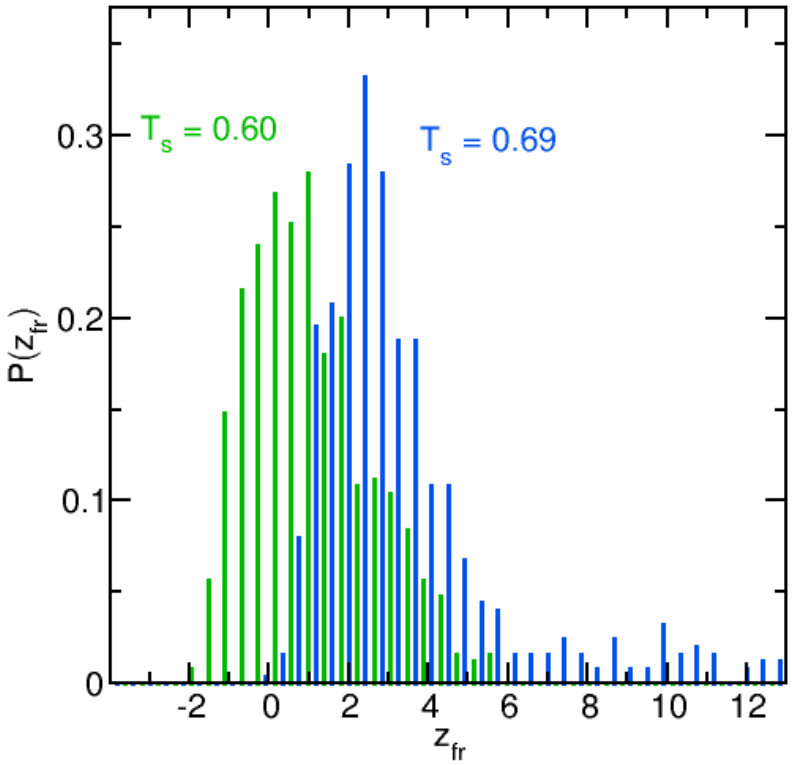

Fig. S6. Distribution function of the freezing distances z_{fr} calculated from $\langle P_2(\hat{\mu} \cdot \hat{\mu}_{final})\rangle$ for individual molecules. The blue bars correspond to the molecules deposited at $T_{substrate}$ = 0.69 (most vertical molecular orientation) and the green bars correspond to $T_{substrate}$ = 0.60 (most horizontal molecular orientation).

convenience we define the free surface to be where the local density of the film is 50% of the bulk value. Fig. 5C illustrates how average molecular orientation changes starting from the time when a molecule first strikes the free surface until it is immobilized. On the y axis of Fig. 5C we plot the function that characterizes the molecular orientation relative to its frozen state:

$$\langle P_2\left(\hat{\mu}\cdot\hat{\mu}_{final}\right)\rangle = \frac{3}{2}\langle\left(\hat{\mu}\cdot\hat{\mu}_{final}\right)^2\rangle - \frac{1}{2}$$

where $\cos^{-1}\left(\hat{\mu}\cdot\hat{\mu}_{final}\right)$ is the angle between the long molecular axis ($\hat{\mu}$, Fig. 4) at a given moment during deposition and the final orientation. The angle brackets correspond to averaging over 500 molecules which were deposited near the middle of the film. The abscissa for Fig. 5C is average position of the molecules relative to the free surface; we have verified that the average position increases linearly in time. As $\langle P_2\left(\hat{\mu}\cdot\hat{\mu}_{final}\right)\rangle$ approaches unity, it indicates that the molecules are approaching their final orientation. With analogy to autocorrelation functions, we define a characteristic distance for orientation arrest as distance from the surface at which $1-\langle P_2\left(\hat{\mu}\cdot\hat{\mu}_{final}\right)\rangle = 1/e$ (dashed line in Fig. 5C). We refer to this distance as the average freezing distance, z_{fr}. Fig. 5C shows that the average freezing distance decreases with decreasing substrate temperature.

We have also calculated the distribution of freezing distances, z_{fr}, for these 500 molecules and these are displayed in Fig. S6; z_{fr} for an individual molecule is defined as the position of the molecule relative to the free surface at the largest z where $P_2\left(\hat{\mu}\cdot\hat{\mu}_{final}\right) \leq 1-(1/e)$. The blue bars correspond to the substrate temperature $T_{substrate}$ = 0.69 at which the most vertical orientation is observed and the green bars represent the result for $T_{substrate}$ = 0.60 at which the

molecules tend to orient parallel to the substrate. The average values for the distributions are consistent with Fig. 5C. The negative values of z_{fr} in Fig. S6 indicate molecules whose orientations became frozen at distances where the average film density has not yet reached half of the bulk value.

2.9.3. Computing the Orientation Order Parameter

Because the transition dipole moment of interest for each compound is the one associated with the long axis of the molecule, we calculated S_z at λ_{max} for the longest wavelength absorption peak which showed anisotropy. For TPD, λ_{max} = 353.0 nm, for NPB λ_{max} = 377.5 nm, and for DSA-Ph λ_{max} = 415.1 nm. Fig. S7 shows representative optical constants for the most positively and most negatively anisotropic glass of each compound. Fig. S8 shows representative optical constants for glasses deposited near room temperature for each compound.

2.9.4. Density Determination for DSA-PH

As described in the main text, Δρ for vapor-deposited TPD and NPB glasses was determined by mapping the sample thickness before and after heating a temperature gradient sample. This approach was not possible for DSA-Ph. On heating to the temperatures required to induce transformation into the supercooled liquid, DSA-Ph thermally desorbs from the substrate. Δρ for DSA-Ph was instead determined using the Lorentz–Lorenz equation as modified by Vuks (7, 8) and tested on vapor-deposited glasses previously by Dalal and Ediger (9). The density determined by the Lorentz–Lorenz equation is in good correspondence with the density of DSA-

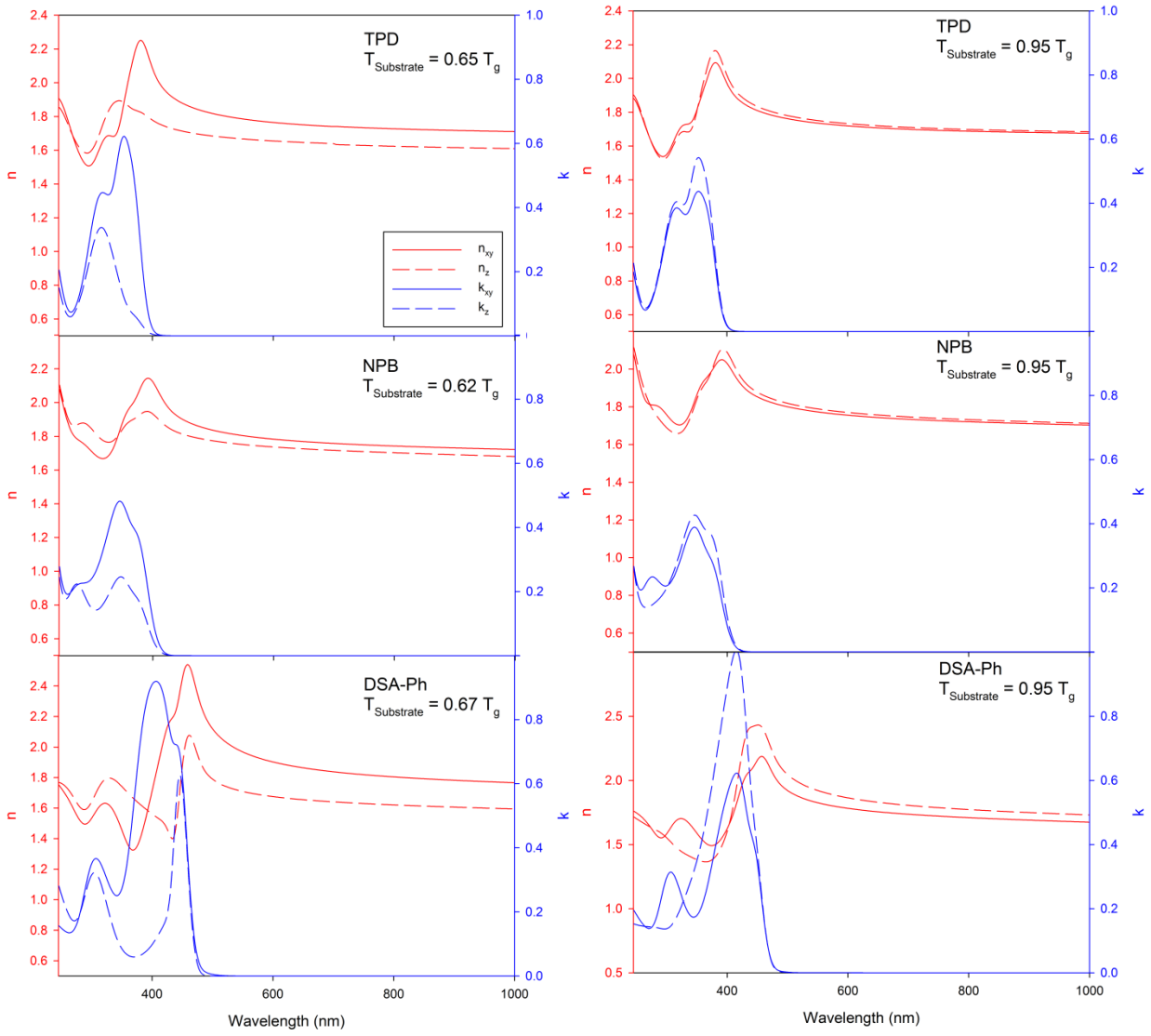

Fig. S7. Optical constants for the most anisotropic glasses of three compounds. (Left) Optical constants for each compound deposited at the lowest substrate temperatures reported in this work. (Right) Optical constants for each compound near 0.95 T_g, where S_z is maximized for each compound.

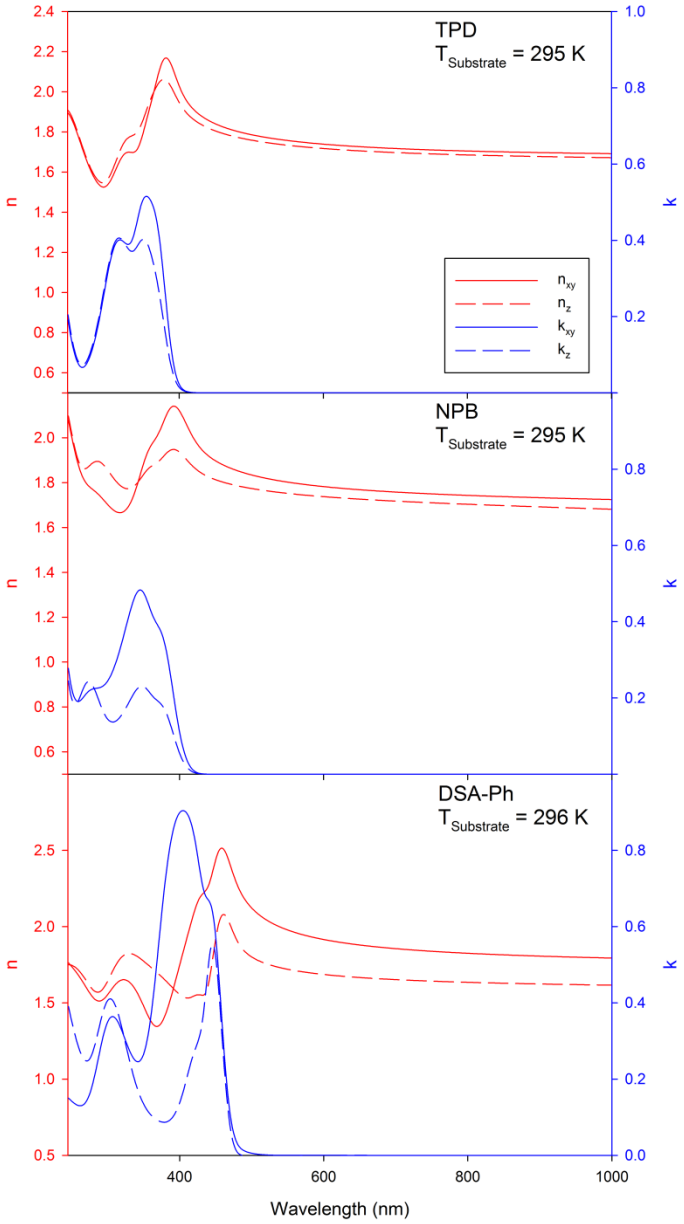

Fig. S8. Optical constants for vapor-deposited glasses with $T_{substrate}$ near room temperature for three compounds.

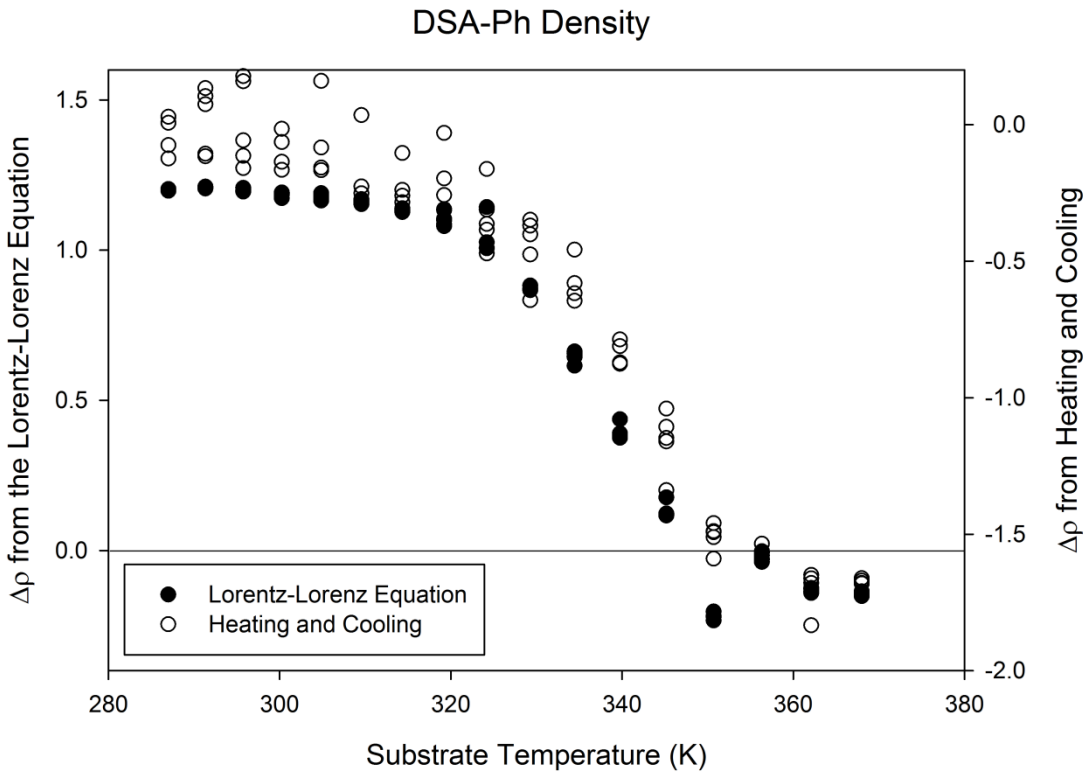

Fig. S9. Density of DSA-Ph determined using two methods. The Lorentz–Lorenz density depends only on comparing the index of refraction at λ = 632.8 nm at a particular $T_{substrate}$ to $T_{substrate}$ = 358 K. The trend in the density is quantitatively consistent with Δρ from heating and cooling, once the results from heating and cooling are vertically shifted to account for the evaporation of material during the transformation.

Ph determined by heating and cooling, except for a vertical shift required to account for thermal desorption. These two ways of determining Δρ for DSA-Ph are compared in Fig. S9.

2.9.5. References

1. Yokoyama D, Sakaguchi A, Suzuki M, Adachi C (2009) Horizontal orientation of linear-shaped organic molecules having bulky substituents in neat and doped vacuum-deposited amorphous films. Org Electron 10(1):127–137.

2. Fujiwara H (2007) Spectroscopic Ellipsometry: Principles and Applications (John Wiley &Sons, Ltd., Chichester, UK), pp 209–248.

3. Woollam JA, et al. (1999) Overview of variable angle spectroscopic ellipsometry (VASE), Part I: Basic theory of typical applications. SPIE Proc CR72:3–28.

4. Dalal SS, Fakhraai Z, Ediger MD (2013) High-throughput ellipsometric characterization of vapor-deposited indomethacin glasses. J Phys Chem B 117(49):15415–15425.

5. Yokoyama D, Adachi C (2010) In situ real-time spectroscopic ellipsometry measurement for the investigation of molecular orientation in organic amorphous multilayer structures. J Appl Phys 107(12):123512.

6. Lyubimov I, Ediger MD, de Pablo JJ (2013) Model vapor-deposited glasses: Growth front and composition effects. J Chem Phys 139(14):144505.

7. Vuks MF (1966) Determination of the optical anisotropy of aromatic molecules from the double refraction of crystals. Opt Spectrosc 20:361–364.

8. Vuks MF (1966) On the theory of double refraction of liquids and solution in an electric field. Opt Spectrosc 21:383–388.

9. Dalal SS, Ediger MD (2012) Molecular orientation in stable glasses of indomethacin. J Phys Chem Lett 3:1229–1233.

Chapter 3

Thermal Stability of Vapor-Deposited Stable Glasses of an Organic Semiconductor

Diane M. Walters, M. D. Ediger

Department of Chemistry, University of Wisconsin-Madison, Madison, Wisconsin 53706

Ranko Richert

Department of Chemistry and Biochemistry, Arizona State University, Tempe, Arizona 85287

Reprinted with permission from The Journal of Chemical Physics, Volume 142, 134504, 2015.

3.1. Abstract

Vapor-deposited organic glasses can show enhanced kinetic stability relative to liquid-cooled glasses. When such stable glasses of model glassformers are annealed above the glass transition temperature T_g, they lose their thermal stability and transform into the supercooled liquid via constant velocity propagating fronts. In this work, we show that vapor-deposited glasses of an organic semiconductor, N,N′-Bis(3-methylphenyl)-N,N′-diphenylbenzidine (TPD), also transform via propagating fronts. Using spectroscopic ellipsometry and a new high-throughput annealing protocol, we measure transformation front velocities for TPD glasses prepared with substrate temperatures ($T_{Substrate}$) from 0.63 to 0.96 T_g, at many different annealing temperatures. We observe that the front velocity varies by over an order of magnitude with $T_{Substrate}$, while the activation energy remains constant. Using dielectric spectroscopy, we measure the structural relaxation time of supercooled TPD. We find that the mobility of the liquid and the structure of the glass are independent factors in controlling the thermal stability of TPD films. In comparison to model glassformers, the transformation fronts of TPD have similar velocities and a similar dependence on $T_{Substrate}$, suggesting universal behavior. These results may aid in designing active layers in organic electronic devices with improved thermal stability.

3.2. Introduction

Organic glasses are widely studied and are used in a variety of applications. Glasses are advantageous in part because they are non-equilibrium materials and their properties can be tuned depending on the route of preparation.[1–3] In particular, physical vapor deposition can prepare organic glasses with exceptional thermal stability if the deposition conditions are

chosen appropriately;[4–6] transformation to the supercooled liquid has been observed to occur at temperatures up to 35 K higher than the glass transition temperature (T_g) of the liquid-cooled glass.[7] Stable glasses also have high density[6,8–11] and low enthalpy[5–7,12–15], and can exhibit useful anisotropic structures[16] as evidenced by birefringence[10,11,17], dichroism[17], and X-ray scattering.[14,15,18,19] These solid-state properties are lost on transformation to the equilibrium supercooled liquid, so high thermal stability is important for extending the range of applications for these materials.

A recent study has shown that several compounds used in vapor-deposited active layers in organic electronic devices can form glasses of high thermal stability[17], but there are unanswered questions about the mechanism by which these materials thermally degrade. The thermal stability of active layers in organic devices is important as demonstrated by observations that device performance degrades after annealing,[20–22] likely due to pinhole formation and loss of anisotropy. Adachi and coworkers have investigated the transformation mechanism of vapor-deposited active layers, and found that films transformed heterogeneously and were best fit by a model in which mobility is highest near the free surface.[23] Stable glass formation is quite general for vapor-deposited organic molecules and occurs over a wide range of substrate temperatures, so the active layers in many organic devices are likely stable glasses. Understanding the transformation mechanism for the glasses that form active layers could advance device design and improve thermal stability.

Work on model glassformers has established that the thermal stability of thin films of vapor-deposited stable glasses is controlled by a different mechanism than liquid-cooled,

ordinary glasses.[24–27] When an ordinary glass is annealed above T_g, it transforms to the supercooled liquid by a spatially homogenous process. In contrast, when stable glasses of model glassformers are heated, they transform via constant velocity propagating fronts initiated at a free surface or other interface. For thin stable glass films under about a micron in thickness, the front mechanism dominates and completely controls the thermal stability of the film. Transformation fronts have been directly detected or inferred using a wide variety of experimental techniques. Calorimetry,[25,28–30] dielectric,[26,31] and ellipsometric[27] experiments have observed that the transformation time depends linearly on film thickness for thin films, as is expected for constant velocity propagating fronts. Secondary ion mass spectrometry[24,32,33]and ellipsometry[27] experiments have directly observed the transformation fronts. Transformation fronts are believed to result from kinetic facilitation.[34–36] On annealing, molecules in the interior of a stable glass do not have sufficient mobility to rearrange on a reasonable timescale. However, heightened mobility at a free surface[37] or liquid[37] interface enables adjacent molecules otherwise trapped in the glass to join the liquid. Newly created liquid molecules facilitate motion in their neighbors, causing transformation to propagate from the initial interface into the bulk in the form of a front. Front behavior naturally arises in a kinetic Ising model[34] and in calculations using the random first order transition (RFOT) theory of glasses[36]. These calculations reproduce key experimental features, such as the existence of transformation fronts,[34,36] the competition between front and homogeneous transformation mechanisms under different conditions,[34] and front velocities over a range of annealing temperatures.[36]

In this work, we investigate the thermal stability of vapor-deposited stable glasses of an organic semiconductor, N,N'-Bis(3-methylphenyl)-N,N'-diphenylbenzidine (TPD), that has been widely studied as a hole transport layer.[3,17,20,22,38] We build upon a previously developed high-throughput sample preparation scheme in which deposition occurs onto a substrate with an imposed temperature gradient.[39] We demonstrate a new, high-throughput annealing protocol that uses ellipsometry to efficiently monitor the transformation of nearly fifty different stable glasses of TPD over a wide range of annealing temperatures. We perform dielectric spectroscopy to measure the mobility of supercooled TPD and compare the front velocities to those of other glassformers.

We find that the thermal stability of TPD glasses with high kinetic stability is determined by the velocity of propagating transformation fronts. We observe that the front velocity varies by over an order of magnitude for TPD glasses prepared at substrate temperatures between 0.63 and 0.96 T_g, and is imperfectly correlated with the density of glass, similar to results previously reported for indomethacin, a model glassformer. Using our new high-throughput annealing protocol, we calculate the activation energies of the transformation fronts for a wide variety of glasses. We show that the transformation front velocities for TPD glasses prepared at different substrate temperatures have the same activation energy. We find that the mobility of the supercooled liquid and the structure of the glass are independent factors in controlling the thermal stability of TPD films. These results may aid in designing organic electronic devices with improved lifetimes.

3.3. Experimental Methods

Glasses were prepared by physical vapor deposition as has been previously described.[39] TPD (N,N'-Bis(3-methylphenyl)-N,N'-diphenylbenzidine, 99% purity, T_g = 330 K), structure shown in the inset of Figure 2b, was purchased from Sigma-Aldrich and used without modification. Crystalline TPD was loaded into a crucible and placed in a vacuum chamber with a base pressure of 10^{-7} torr. The crucible was heated to evaporate TPD and maintain a constant deposition rate of 2.2 ± 0.1 Å/s as monitored by a quartz crystal microbalance next to the substrate. TPD vapor condensed on a temperature controlled silicon substrate 18 cm away from the crucible until the condensed film was about 100 nm thick. The precise thickness and deposition rate were subsequently determined from ellipsometric measurements.

Many glasses with the same chemical composition but different substrate temperatures during deposition ($T_{Substrate}$) were prepared on a single sample using a previously described high-throughput sample preparation scheme.[39] A silicon substrate was suspended between two copper fingers in a vacuum chamber. During vapor deposition, a temperature gradient was imposed on the substrate by heating or cooling each copper finger to a different temperature. A typical temperature gradient spanned 100 K over a 3.2 cm substrate. The substrate temperature during the deposition was determined to be accurate to ±2 K by comparing the birefringence and order parameter of the deposited glasses to previously published work.[17] Three different temperature gradient samples were utilized in this work.

Samples were annealed on the ellipsometer using a home-built temperature controlled translation stage.[10] Ellipsometric measurements were made before, during, and after annealing.

Measurements were made on a J.A. Woollam M-2000 spectroscopic ellipsometer at three angles (50°, 60°, 70°) over a 245-1000 nm spectroscopic range. The temperature of the stage was accurate to ±1 K over the temperature range used here based on the comparison to several melting point standards. Nitrogen gas was blown over the ellipsometry stage during measurements to control the environment around the sample. Samples were annealed using either an isothermal or a high-throughput annealing protocol. The annealing protocols are described below.

In the isothermal annealing protocol, samples were annealed at a single temperature for a long period of time. First, ellipsometry measurements were performed at room temperature. Then the sample was ramped at 50 K/min to the annealing temperature and held at that temperature for one hour. Ellipsometric measurements were made every 60 seconds during the annealing. Finally, the sample was returned to room temperature with a cooling rate of 50 K/min; this was maintained through 330 K, the T_g of the material. The sample was measured again at room temperature. This annealing protocol is illustrated in Figure 1a below. Only samples prepared with a single substrate temperature were annealed using the isothermal protocol and one location was measured on each sample.

In the high-throughput annealing protocol, samples were repeatedly annealed for two minutes at steadily increasing annealing temperatures and were measured at room temperature between each annealing step. This temperature protocol is illustrated in Figure 2a below. First, ellipsometry measurements were performed at room temperature. For temperature gradient samples, different locations on the sample were glasses prepared with

different substrate temperatures. To measure all these glasses, the sample was "mapped". During mapping, the entire sample was scanned using the translation stage to measure about 90 different glasses prepared at 18 different substrate temperatures; these measurements required about 80 minutes. No measureable aging effects were seen during mapping, as expected because the measurements were done far below T_g. After mapping, the sample was brought to the annealing temperature for two minutes before being cooled again to room temperature. The heating and cooling rates were 50 K/min for all but one of the samples analyzed, which was ramped at an uncontrolled, but similar, rate. At room temperature, one glass prepared with each substrate temperature was measured, so about 20 minutes were needed to acquire data. The sample was then annealed again for two minutes at an annealing temperature 2K higher than the previous annealing temperature and then measured again at room temperature. This process was repeated until the sample was fully transformed as confirmed by spectroscopic ellipsometry.

After the above annealing steps, samples were heated to T_g + 15 K at 1 K/min and immediately cooled at the same rate to room temperature. This prepared a 1 K/min liquid-cooled, ordinary glass which is a useful reference state for vapor-deposited organic glasses.[17,39] The entire sample (~ 90 spots) was then mapped again using spectroscopic ellipsometry. The densities of the vapor-deposited glasses were calculated relative to the ordinary glasses on a spot-to-spot basis as previously described.[17,39] Ellipsometric measurements of the as-deposited glass and the 1 K/min liquid-cooled glass were fit with a homogenous model, described below, to determine the film thicknesses. Changes in film thickness are inversely proportional to changes in film density because the film adheres to the substrate and does not flow. The

relative densities of the vapor-deposited glasses, combined with the data from reference 17, are shown in Figure 8 below. The T_g of TPD was determined by reheating the 1 K/min liquid-cooled glass at 1 K/min and ellispometrically measuring where the thermal expansion of the material changes from that of the glass to that of the supercooled liquid, as has previously been described for model glassformers.[10,39] The T_g for the model glassfomer indomethacin used for comparison was determined by the same method in Ref 39.

Ellipsometric data were fit with three different models similar to those used previously:[27] a homogenous model, a one front model, and a two front model. All models describe the TPD film on a silicon substrate with 2 nm of native silicon oxide. (1) The homogenous model for TPD is a previously described anisotropic absorptive oscillator model.[17] The TPD film is treated as a single layer and the optical constants and film thickness are fit independently for each measurement. (2) The one front model describes the vapor-deposited film as two layers where the optical constants of each layer are fixed and the layer thicknesses can vary. The bottom layer is the stable glass and the top layer is the ordinary glass (or the supercooled liquid if the measurements were made when annealing above T_g.) The optical constants of the stable glass were determined by fitting the homogenous model to the first measurement at the measurement temperature. The optical constants of the ordinary glass (or supercooled liquid) were determined by fitting the homogenous model to the final measurement at the measurement temperature after the sample was fully transformed. The location of the interface between the two layers was determined independently for each measurement. (3) The two front model, illustrated in Figure 1a below, describes the TPD film using three layers: the middle layer has the optical constants of the stable glass and the top and bottom layers

have the optical constants of the ordinary glass (or supercooled liquid depending on the temperature during the measurement.)

We note that the as-deposited TPD glasses are birefringent and dichroic, as established in recent work.[17] The birefringence and dichroism of the as-deposited samples produced for this work are highly consistent and consistent with the previously published results. See Figure S1 in Supplementary Materials for the refractive indexes and extinction coefficients of the as-deposited TPD glasses.[40]

As $T_{Substrate}$ approaches T_g from below, the kinetic stability of vapor-deposited glasses markedly decreases.[17,39,41] Both the one front and two front models failed to fit glasses prepared with substrate temperatures from 0.90 to 0.95 T_g and above 0.96 T_g and these data are not reported; this occurs either because fronts do not exist for these glasses or because there is not sufficient optical contrast between the vapor-deposited glass and the ordinary glass for the fronts to be detected with ellipsometry. Glasses prepared with substrate temperatures ranging from 0.63 to 0.90 T_g were best fit with the two front model, as indicated by monotonically changing front heights and the lowest MSE. Glasses prepared at 0.95 T_g and 0.96 T_g were also best fit using the two front model, as indicated by monotonically changing front heights and the lowest MSE (within a few percent.)

Dielectric measurements were performed as has previously been described for similar small organic molecules.[42] TPD crystals were melted and quenched to form a glass. The glass was heated above T_g and the frequency dependence of the dielectric response of the supercooled

liquid was measured over a range of temperatures. A dielectric relaxation time, τ_α, was calculated from the peak in the frequency response of ε".

3.4. Results

3.4.1. Detection of TPD Transformation Fronts with Ellipsometry

As shown in Figure 1, the thermal stability of TPD stable glasses annealed above T_g is determined by the velocity of transformation fronts. Figure 1a illustrates the isothermal annealing of a vapor-deposited stable glass of TPD. Between the vertical dashed lines, the sample was annealed for one hour at T_g + 10 K while being measured using spectroscopic ellipsometry. Each ellipsometric measurement was fit independently using the "two front" model described above. The two front model, shown schematically in Figure 1a, describes the vapor-deposited film using three layers with fixed optical constants but variable thickness: a top supercooled liquid layer, a middle stable glass layer, and a bottom supercooled liquid layer. Fitting the two front model to the experimental data finds the heights of the two interfaces between the layers. The interface heights during the annealing of this sample are plotted in Figure 1b and track the progression of the transformation fronts.

Figure 1b shows the presence of two propagating transformation fronts during the annealing of a vapor-deposited stable glass of TPD at 10 K above its T_g. One front originates at the free surface and the other front originates at the substrate. Both fronts progress monotonically with time. Since each ellipsometry measurement is fit independently, this is strong evidence that this film is transforming via a propagating front mechanism.

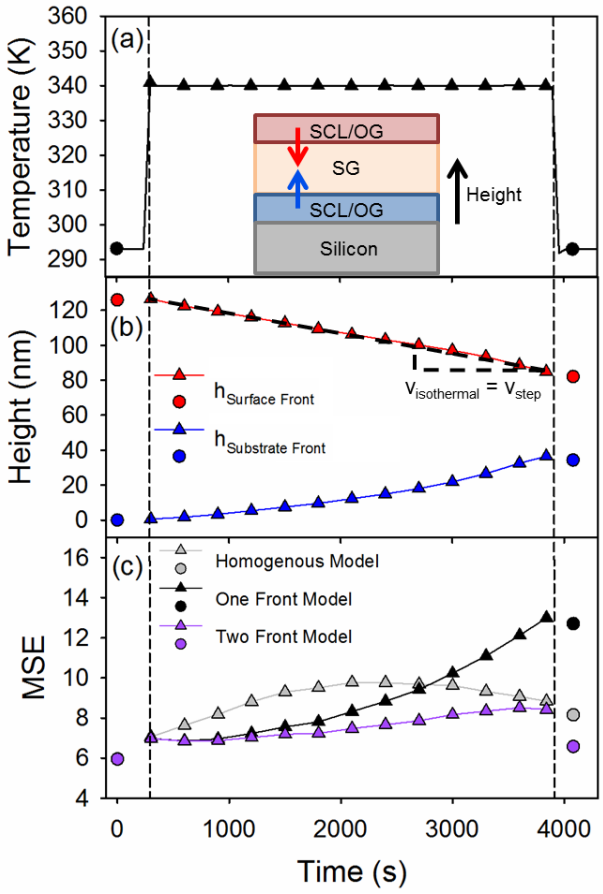

FIG. 1. Isothermal annealing at 340 K of a TPD glass vapor-deposited at $T_{Substrate}$ = 284 K. Vertical dashed lines mark the start and end of the annealing period. Circles denote measurements made at 293 K. Triangles denote measurements made at 340 K. Data density is reduced to 20% for clarity. (a) Temperature profile for the isothermal annealing protocol. Symbols denote ellipsometric measurements. Inset: A schematic illustration of the two front model used to fit ellipsometry measurements. (b) Height of the surface-initiated (red) and substrate-initiated (blue) transformation fronts, as determined by the two front model. (c) Comparison of the root mean square error (MSE) for three different models fit to the ellipsometric data. The two front model has the lowest MSE during the annealing.

Figure 1c compares the root mean square error (MSE), a measure for the goodness of the fit to the ellipsometric data, for three models used to fit the film. All the models described the as-deposited glass equally well and have the same MSE, but during annealing the two front model provided the best description of the data. This provides further evidence that the film transforms via surface- and substrate-induced fronts. The other models used to fit the data were a one front model and a homogenous model. The one front model described the organic film with just two layers with fixed optical constants: a supercooled liquid layer over a stable glass layer. The homogenous model describes the organic film as just one layer, but allows the optical constants as well as the thickness of that layer to vary. All samples were best fit using the two front model as indicated by monotonically changing front heights and the lowest MSE (within a few percent.)

The front velocity can be calculated from the ellipsometric measurements shown in Figure 1b. The slope of the triangles indicates the front velocity of the surface-initiated front at the annealing temperature. The same velocity is found by using the difference between the two room temperature measurements (circles) and dividing by the annealing time. Since the front velocities measured by these two methods are equivalent, we can develop a high-throughput annealing protocol in which front velocities are calculated using only measurements made at room temperature before and after annealing, as described in the next section.

3.4.2. High-Throughput Annealing

We used a high-throughput protocol to measure the thermal stability of vapor-deposited glasses at many different annealing temperatures in a single experiment, as illustrated in

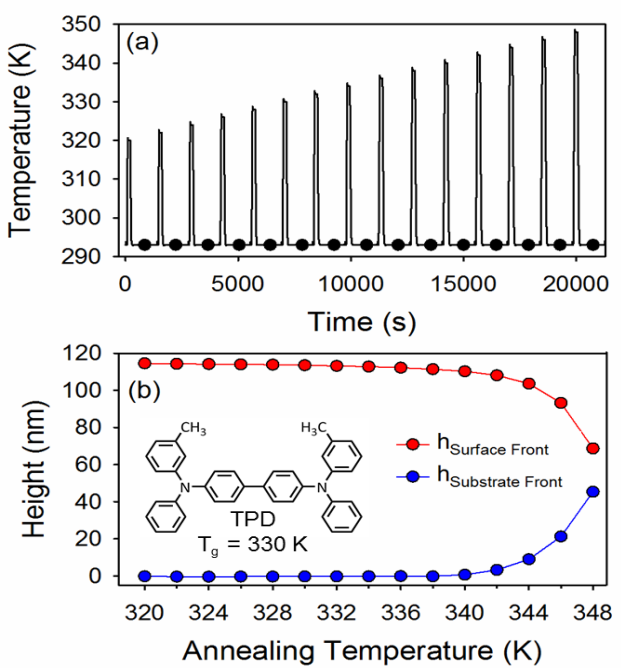

FIG. 2. High-throughput annealing of a TPD glass vapor-deposited at $T_{Substrate}$ = 283 K. (a) Temperature profile of the high-throughput annealing protocol. Ellipsometric measurements are made at 293 K and are denoted with circles. (b) Height of the surface-initiated (red) and substrate-initiated (blue) transformation fronts after each annealing step. Inset: The molecular structure of TPD and its glass transition temperature, T_g.

Figure 2. In this protocol, the sample is annealed for many short (two minute) intervals and is measured using ellipsometry at room temperature between each annealing step. Ellipsometric data were fit with three different models and all samples were best fit using a two front model, as described above; data after each annealing step were fit independently. The annealing temperature was increased by 2 K with each annealing step. By annealing the sample for two minutes with 2 K steps in annealing temperature, our step ramp protocol is similar to a continuous 1 K/min ramp.

Figure 2b illustrates the propagation of transformation fronts in a TPD stable glass annealed with our high-throughput protocol. Transformation fronts are initiated at the free surface and substrate and progress monotonically through the film with each annealing step. At low annealing temperatures, there is essentially no change in the heights of the fronts, while at higher annealing temperatures there are larger and larger changes in the front heights during each two minute annealing period. Front velocity is calculated by dividing the front progression during the annealing step by the annealing time, so front velocities at higher annealing temperatures are larger. This will be discussed further in the next section.

In a single experiment, we measured the thermal stability of many different glasses over a range of annealing temperatures using our high-throughput annealing protocol. Figure 2 illustrates the thermal stability of just one of eighteen different glasses prepared on a temperature gradient sample. Simultaneously measuring the thermal stability of many glasses over a range of annealing temperatures is possible in our protocol because the annealing times are short and the ellipsometry measurements are made at room temperature. By having short

annealing times, the sample can be annealed at many different annealing temperatures before it is fully transformed to the supercooled liquid; this allows an efficient survey of the effect of annealing temperature on thermal stability. By making measurements at room temperature after each annealing step, we decouple the measurement time from the annealing time. Long measurement times are needed to measure the many different glasses prepared at different substrate temperatures in order to determine how they changed during each annealing. Room temperature is far enough below T_g for TPD that there are no measureable changes in the properties of the sample over the course of the measurements.

3.4.3. Influence of Substrate Temperature on Thermal Stability

As illustrated in Figure 3, vapor-deposited glasses of TPD prepared at different substrate temperatures ($T_{Substrate}$) have different thermal stabilities. Figure 3a shows the propagation of transformation fronts initiated at the free surface for five TPD glasses prepared at different substrate temperatures on the same sample. For each glass, there are greater changes in front height at higher annealing temperatures. Glasses prepared with higher substrate temperatures, up to $T_{Substrate}$ = 283 K, resist transformation most effectively. These glasses have previously been reported to have higher onset temperatures for transformation into the supercooled liquid.[17]

Transformation front velocities for a range of annealing temperatures are plotted in Figure 3b for the five stable glasses of TPD. The front velocities for each glass were calculated by measuring how far the front progressed during an annealing step (shown in Figure 3a) and dividing by the annealing time. Glasses prepared at different substrate temperatures have very

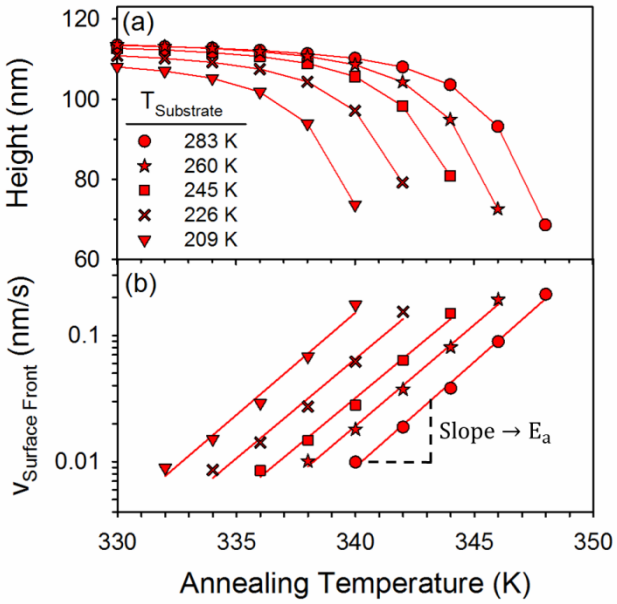

FIG. 3. (a) Height of the surface-initiated transformation fronts after each annealing step in the high-throughput annealing protocol. Different symbols denote glasses prepared at different substrate temperatures on the same sample. (b) Velocities of the surface-initiated transformation fronts in panel (a) during each annealing step. Log ($v_{Surface\ Front}$) increases linearly with the annealing temperature, indicating that the activation energy of the front velocities can be calculated using Equation 1 as described in the text.

different thermal stabilities. For example, when annealed at 340 K, a glass prepared at $T_{Substrate}$ = 209 K (Figure 3b, triangles) has a transformation front that moves nearly 18 time faster than a glass prepared at $T_{Substrate}$ = 283 K (Figure 3b, circles.) For the most kinetically stable glasses near $T_{Substrate}$ = 283 K, the front velocity was only calculated at high annealing temperatures because no measureable front progression was observed at low annealing temperatures. For the least kinetically stable glasses ($T_{Substrate}$ = 209 K), front velocity was only calculated for annealing temperatures just above T_g because the film fully transformed before annealing steps at the highest annealing temperatures were performed. The front velocities for each glass in Figure 3b have very similar temperature dependences, as indicated by the similar slopes. Thus transformation fronts for all of these glasses have the same activation energy, independent of substrate temperature, as will be discussed in more detail in the following section.

Figure 4 illustrates how the transformation front velocity for TPD glasses depends upon the substrate temperature during deposition. At two different annealing temperatures, the front velocity varies with substrate temperature by over an order of magnitude. This represents a very significant difference in the thermal stability of these TPD glasses. As shown in Figure 4, front velocities for TPD glasses are similar to those previously measured for indomethacin (IMC, a model glassformer) when comparing the annealing temperatures and the substrate temperatures relative to T_g of each system.[27] In both TPD and IMC, the lowest front velocities (the glasses with highest thermal stability) are produced when the substrate temperature is held near 0.87 T_g during deposition.

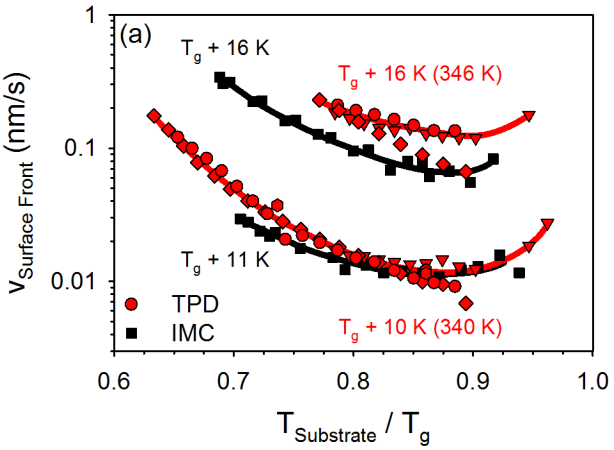

FIG. 4. TPD (red) and IMC (black) surface-initiated transformation front velocities over a range of substrate temperatures for selected annealing temperatures. IMC data are from reference 27. Different symbols represent different samples for TPD. Substrate and annealing temperatures are expressed relative to T_g to compare the two systems.

Transformation fronts initiated from the substrate have qualitatively the same behavior as fronts initiated from the free surface (substrate-initiated fronts had about 10% larger velocities on average at the annealing temperatures shown in Figure 4), with three important differences. First, as indicated in Figure 1b, the substrate-initiated front does not always propagate at constant velocity. Second, for some glasses on one sample, the substrate-initiated front appeared to show an induction time. Third, different samples showed up to factor of two variation in the velocity of the substrate-initiated front. We do not know to what extent the behavior exhibited at the substrate is an artifact of the fitting procedures. It is possible that modifying the substrate surface prior to deposition would result in more consistent observations. Further discussion will focus on the behavior of surface-initiated fronts.

3.4.4. Activation Energy of Transformation Fronts

As shown in Figure 3b, the temperature dependence of the transformation front velocity appears to be independent of substrate temperature. We can test this observation quantitatively by fitting each data set to the Arrhenius equation to extract the activation energy:

$$E_a = -R \frac{\partial \ln v_{Surface\ Front}}{\partial (1/T)} \quad (1)$$

Here R is the universal gas constant.

The activation energies for transformation front propagation into vapor-deposited TPD glasses prepared over a wide range of substrate temperature are plotted in Figure 5. The activation energies of the transformation front velocities have no dependence upon the

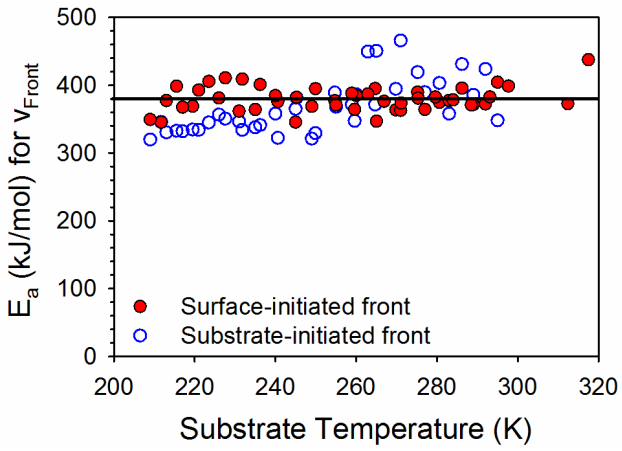

FIG. 5. Activation energies for the surface-initiated (red) and substrate-initiated (blue) transformation front velocities over a wide range of substrate temperatures. A line marks the average activation energy of the surface-initiated fronts, 380 ± 20 kJ/mol.

substrate temperature. The surface-initiated front velocity has an average activation energy of 380 ± 20 kJ/mol. Fronts initiated at the substrate had similar activation energies and an average value of 370 ± 30 kJ/mol.

3.4.5. Dielectric Spectroscopy

We used dielectric spectroscopy to measure the frequency-dependent dielectric response of the supercooled liquid of TPD over a wide range of temperature. Figure 6a shows the loss component of the dielectric response, $\varepsilon''(\omega)$, which can be represented by Havriliak-Negami fits with $\Delta\varepsilon$ = 0.25, α_{HN} = 0.92, and γ_{HN} = 0.29. A characteristic dielectric relaxation time, τ_α, can be calculated from the peak frequency (f_{max}) of the loss profile using the following equation:[42]

(2) $\tau_\alpha = 1/(2\pi f_{max})$

Figure 6b shows the calculated τ_α as a function of temperature. The temperature dependence of τ_α is well-described by the Vogel-Fulcher-Tammann (VFT) equation:[43–45]

(3) $\tau = \tau_0 e^{\left(\frac{B}{T-T_0}\right)}$

The fit parameters for the VFT equation are $\log(\tau_0/s)$ = -19.2, B = 1517.2 K, and T_0 = 258.9 K. The T_g calculated from the dielectric relaxation (based upon □□ = 100 s) was 330 K. This is in good agreement with the dilatometric T_g of 330 K obtained using ellipsometry and a cooling rate of 1 K/min.[17] The kinetic fragility parameter "m" has a value of 98 for TPD indicating that TPD is a fragile glassformer. We note that the τ_α values shown for the two lowest temperatures in Figure 6b were determined by an alternate procedure. At these temperatures, the peak of the dielectric loss does not occur in the observed frequency window. The values of τ_α at these

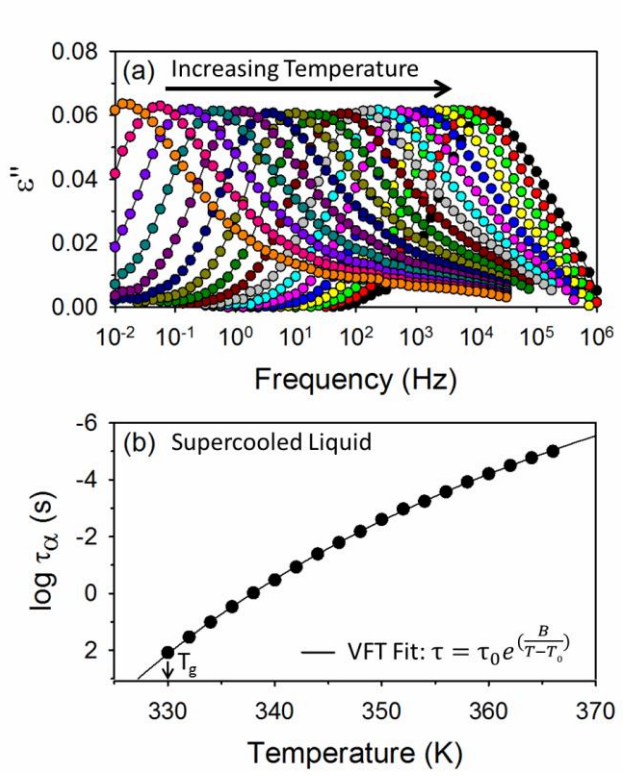

FIG. 6. (a) Dielectric loss spectra for the supercooled liquid of TPD at temperatures spanning 334 K to 366 K with 2 K intervals. The peak in the frequency response shifts to higher frequencies as the temperature increases. (b) Temperature dependence of the dielectric relaxation time τ_α. Data are fit with the Vogel-Fulcher-Tammann (VFT) equation shown.

temperatures were obtained by shifting the observed dielectric response to higher temperatures and assuming that the shape of the dielectric response is independent of temperature.

3.5. Discussion

3.5.1. Universality of Transformation Front Behavior for Glasses with High Kinetic Stability

Kinetic facilitation,[46–48] the idea that areas with high mobility can induce mobility in neighboring regions of low mobility, offers an explanation for why stable glasses transform into the supercooled liquid via a front mechanism. From this perspective, heightened mobility at a free surface[37] enhances motion in neighboring molecules in a glass. As molecules that border high mobility regions rearrange and equilibrate, they become highly mobile and facilitate further motion. This results in a mobility front that propagates through a glass at constant velocity. Within the framework of kinetic facilitation, propagating transformation fronts are expected to be important for every glass with high kinetic stability that has a high mobility surface or interface.

Our results show that vapor-deposited stable glasses of TPD transform to the supercooled liquid via propagating fronts when annealed above T_g. This is illustrated in Figures 1, 2, and 3 for a wide variety of TPD glasses annealed at many different temperatures. All TPD glasses deposited with substrate temperatures ($T_{Substrate}$) between 0.63 and 0.96 T_g transformed by fronts initiated at the free surface and the substrate. Stable glasses can also transform via a bulk mechanism, but the front mechanism dominates in thin films. The film thickness where the

front mechanism no longer describes the transformation has been measured for several systems and is on the order of microns.[25,26] The transformation front velocities are the relevant parameter for evaluating the stability of thin TPD films, such as the ~120 nm films in this work.

Transformation via a propagating front appears to be a universal feature in thin glassy films with high kinetic stability, as expected from kinetic facilitation. Figure 7 compares the transformation front velocity of TPD to two model glassformers, indomethacin and ααβ-trisnaphthylbenzene.[32] To fairly compare the different systems, all the glasses shown were vapor-deposited at 0.85 T_g. The front velocities in Figure 7 are plotted against the structural relaxation time τ_α for the supercooled liquid at the annealing temperature in order to account for the different T_g values of the different systems. Figure 7 shows that TPD exhibits transformation fronts similar to model stable glassformers. Among these systems, TPD forms the most stable glasses, as it has the lowest front velocity for a given mobility of the liquid. Figure 4 illustrates that stable glasses of TPD and indomethacin prepared with a wide range of substrate temperatures have similar front velocities when substrate and annealing temperatures are expressed relative to T_g.

The high-throughput annealing protocol used here is roughly equivalent to experiments in which temperature is increased at a constant rate and complements temperature-scanning calorimetry measurements by allowing for the direct detection of transformation fronts. Rodríguez-Tinoco et al.[30] and Bhattacharya et al.[29] have investigated stable glasses using calorimetric methods where temperature is rapidly scanned and the excess heat capacity of a stable glass is measured over a broad range of temperatures in a single experiment. Both of

these groups observe that the transformation rate is independent of film thickness, which is consistent with transformation via a propagating front mechanism. Rodríguez-Tinoco et al. studied indomethacin and supplemented the fast-scanning measurements with differential scanning calorimetry.[30] They calculated front velocities in quantitative agreement with previously published isothermal annealing experiments and extended the range of investigated annealing temperatures up to T_g + 75 K. Our high-throughput annealing protocol also allows us to access a range of annealing temperatures in a single experiment. Although this range is smaller than in the calorimetry measurements, we access lower annealing temperatures which are likely more relevant for evaluating the thermal stability of molecules used in organic electronics. In addition, ellipsometry experiments directly detect transformation fronts (rather than infer them) and can directly determine the behavior of multiple fronts if they are present.

3.5.2. What controls the transformation front velocity?

3.5.2.1. Influence of Annealing Temperature

Within the framework of kinetic facilitation, a propagating transformation front is expected to move more rapidly at higher annealing temperatures because of the higher mobility of the supercooled liquid. Figure 7 is consistent with this idea and further shows that front velocities for the three systems show a similar dependence upon the structural relaxation time τ_α of the liquid. Using temperature-ramping calorimetry experiments, Rodríguez-Tinoco et al.[30] have shown that the power law relationship between velocity and τ_α continues for indomethacin over a large temperature range up to T_g + 75 K. It is noteworthy that the front velocities have weaker temperature dependences than τ_α for all three systems. Front velocities have

temperature dependences more similar to that of the supercooled liquid diffusion coefficients for indomethacin and ααβ-trisnaphthylbenzene.[32]

Using a high-throughput annealing protocol, we find that the temperature dependence of the transformation front velocity is independent of substrate temperature and is the same for fronts initiated at the free surface and the substrate (Figure 5). A possible explanation for why all the transformation fronts for many different stable glasses have the same activation energy is that all the different glasses transform into the same supercooled liquid with the same mobility. This provides further evidence that the mobility of the supercooled liquid influences the front velocity.

3.5.2.2. Influence of Substrate Temperature

In Figure 8a, the transformation front velocities for TPD glasses are scaled to the mobility of the supercooled liquid at the annealing temperature and compared. In constructing the ordinate, we divide the front velocities by $\tau_\alpha^{-0.73}$, as suggested by Figure 7; this is approximately equivalent to an activation energy of 380 kJ/mol, in agreement with Figure 5. When this scaling is applied, the front velocities at many different annealing temperatures collapse onto a single curve to a good approximation. The successful data collapse shows that the influences of substrate temperature and annealing temperature on the propagation front velocity are independent. The curve shown in Figure 8a expresses the complete dependence of the front velocity on substrate temperature. In this section we consider why glasses deposited at different substrate temperatures transform at different rates.

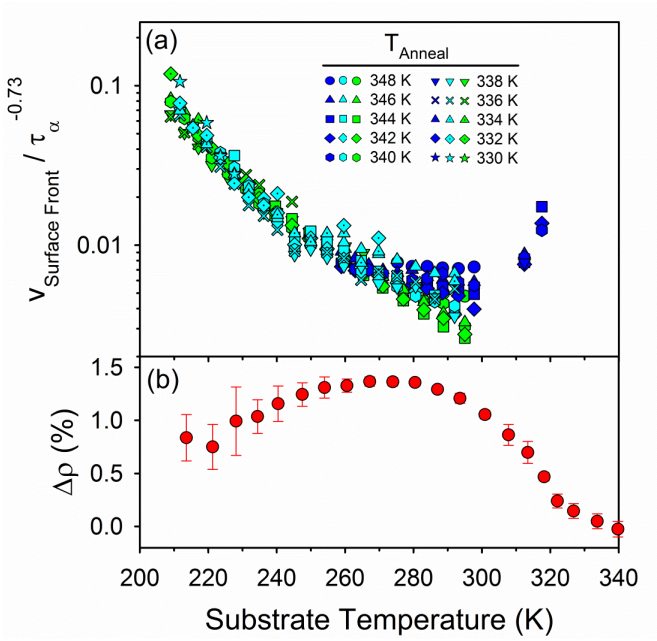

FIG. 8. (a) Surface-initiated transformation front velocities for annealing temperatures ranging from 332 to 348 K scaled by $\tau_\alpha^{-0.73}$ at the annealing temperature, for glasses prepared at a wide range of substrate temperatures. Scaled front velocities are approximately the same for all annealing temperatures and show the same substrate temperatures dependence. Different colors represent different samples, and individual symbols are used for each annealing temperature. (b) Density of the vapor-deposited glasses of TPD relative to the ordinary glass prepared by cooling the liquid at 1K/min, for glasses prepared at different substrate temperatures. Data are from this work and reference 17. Each data point is the average across multiple samples for 2 to 10 glasses with similar substrate temperatures, with the density difference measured at room temperature. Error bars give the 90% confidence interval.

Figure 8a shows that the substrate temperature during deposition has a large impact on the transformation front velocity for TPD glasses, independent of annealing temperature. The front velocity can vary by more than an order of magnitude with substrate temperature, similar to published results for the model glassformer indomethacin (Figure 4). This significant dependence of front velocity upon substrate temperature has not yet been captured by calculations using kinetic Ising models or RFOT theory.[34,36] A published calculation of front velocities for stable glasses of □□□-trisnaphthylbenzene showed no systematic dependence on the fictive temperature, which specifies the stability of the glass, over a 10 K range.[36] Based on aging experiments on ordinary glasses,[49] it would be reasonable if denser glasses exhibited lower molecular mobility and lower transformation front velocities. The densities of vapor-deposited TPD glasses are shown in Figure 8b. A comparison between the two panels of Figure 8 illustrates that the front velocities for TPD are partially correlated with density. TPD glasses with the greatest densities ($T_{Substrate}$ in the range 260 to 285 K) have the lowest front velocities. However, glasses of equivalent densities can show quite different front velocities. Glasses with $T_{Substrate}$ greater than 285 K transform more slowly than glasses of equivalent density when $T_{Substrate}$ is less than 285 K. A similar imperfect correlation between propagation front velocity and glass density has been reported for indomethacin.[27]

3.5.2.3. Stability in Organic Electronics

Thermal stability in vapor-deposited glasses is important for maintaining high performance in organic electronics. On annealing, vapor-deposited active layers can form pinholes, crystallize, lose mechanical integrity, and lose anisotropy. These changes in the properties of the organic layers can cause organic electronic devices to fail or reduce their efficiency.

Understanding how the properties of active layers evolve during annealing could aid in designing organic electronics with improved thermal stability and extended lifetimes.

The thermal stability of active layers in many organic electronics devices may be controlled by transformation front propagation. Many organic molecules have been shown to form stable glasses, including molecules used in organic devices[17], and stable glass formation occurs over a wide range of substrate temperatures; thus many active layers may be stable glasses. The front transformation mechanism would potentially be applicable to any active layer that forms a stable glass, and the front velocity allows for a rough estimate of the thermal stability for such an active layer. Front velocity can be estimated based on the annealing temperature and the substrate temperature of the glass, as shown in Figures 7 and 8. While this method may not be quantitatively accurate, particularly since it is unknown how many fronts will be initiated in an active layer, it still provides guidance for how deposition conditions might change the thermal stability of an active layer.

Adachi and coworkers have also used ellipsometry to investigate the transformation mechanism of glasses composed of molecules used in organic electronics.[23] Their data were better described with a graded mobility model rather than with a transformation front model like the one used here. Their graded model described the vapor-deposited films as three layers with variable thicknesses where each layer is some mixture of the pre- and post-transformation material. While they did not observe a sharp transformation front, they did find that the vapor-deposited glasses transformed first at the surface and later in the film interior. This feature

appears robust in the transformation of thin films of vapor-deposited stable glasses, although the generality of the graded transformation mechanism requires further investigation.

Understanding the mechanism of thin film transformation could aid in designing active layers in organic electronics with extended lifetimes and improved thermal stability. Replacing free surfaces with a "capping" layer, a vapor-deposited glassy film of a high T_g, low mobility material, can suppress transformation fronts at interfaces as recently demonstrated.[33] The capping layer eliminates the high mobility material that would otherwise initiate a front. Transformation may still eventually initiate from such an interface but it is possible that interface modification, perhaps by tailoring deposition to control the interface breadth between two adjacent layers, might provide further stability. Understanding the transformation mechanism offers ideas for suppressing transformation fronts and designing organic electronics with enhanced lifetimes.

3.6. Concluding Remarks

In this work, we show that vapor-deposited glasses of TPD with high thermal stability transform into the supercooled liquid via fronts propagating with constant velocity. This is the first illustration that a compound used as an active layer in organic electronics transforms via propagating fronts. Transformation fronts in TPD stable glasses have similar velocities and a similar dependence on $T_{Substrate}$ as previously studied model glass formers. Front velocity can vary by more than an order of magnitude for TPD glasses prepared with different substrate temperatures. By using a new high-throughput annealing protocol, the activation energies of the transformation fronts are measured and found to be independent of substrate

temperature. We find that the effect of annealing temperature and the substrate temperature on the front velocity are independent. Density is imperfectly correlated with front velocity but may be a useful proxy for front velocity since the densest glasses are the most stable and have the lowest front velocities.

An improved understanding of the thermal stability of an organic semiconductor could lead to better design of organic electronics. We expect that many of the amorphous active layers utilized in organic devices are stable glasses that transform via propagating fronts. For such systems, the results presented here provide a means of predicting which deposition conditions will result in devices with the highest thermal stability. The role of device interfaces in initiating front propagation deserves more study. It is possible that eliminating high mobility interfaces bordering an active layer may improve device lifetime.

3.7. Acknowledgements

We thank Shakeel Dalal for helpful discussions. The ellipsometry work (D.M.W., M.D.E.) was supported by the U.S. Department of Energy, Office of Basic Energy Sciences, Division of Materials Sciences and Engineering, award DE-SC0002161. The dielectric relaxation experiments (R.R.) were supported by NSF CHE-1265737.

3.8. References

(1) Angell, C. A. Formation of Glasses from Liquids and Biopolymers. *Science* **1995**, *267* (5206), 1924–1935.

(2) Angell, C. A.; Ngai, K. L.; McKenna, G. B.; McMillan, P. F.; Martin, S. W. Relaxation in Glassforming Liquids and Amorphous Solids. *J. Appl. Phys.* **2000**, *88* (6), 3113.

(3) Yokoyama, D. Molecular Orientation in Small-Molecule Organic Light-Emitting Diodes. *J. Mater. Chem.* **2011**, *21* (48), 19187.

(4) Ishii, K.; Nakayama, H. Structural Relaxation of Vapor-Deposited Molecular Glasses and Supercooled Liquids. *Phys. Chem. Chem. Phys.* **2014**, *16* (24), 12073–12092.

(5) Lyubimov, I.; Ediger, M. D.; de Pablo, J. J. Model Vapor-Deposited Glasses: Growth Front and Composition Effects. *J. Chem. Phys.* **2013**, *139* (14), 144505.

(6) Swallen, S. F.; Kearns, K. L.; Mapes, M. K.; Kim, Y. S.; McMahon, R. J.; Ediger, M. D.; Wu, T.; Yu, L.; Satija, S. Organic Glasses with Exceptional Thermodynamic and Kinetic Stability. *Science* **2007**, *315* (5810), 353–356.

(7) Dawson, K.; Zhu, L.; Kopff, L. a.; McMahon, R. J.; Yu, L.; Ediger, M. D. Highly Stable Vapor-Deposited Glasses of Four Tris-Naphthylbenzene Isomers. *J. Phys. Chem. Lett.* **2011**, *2* (21), 2683–2687.

(8) Ishii, K.; Nakayama, H.; Moriyama, R.; Yokoyama, Y. Behavior of Glass and Supercooled Liquid Alkylbenzenes Vapor-Deposited on Cold Substrates: Toward the Understanding of the Curious Light Scattering Observed in Some Supercooled Liquid States. *Bull. Chem. Soc. Jpn.* **2009**, *82* (10), 1240–1247.

(9) Nakayama, H.; Omori, K.; Ino-u-e, K.; Ishii, K. Molar Volumes of Ethylcyclohexane and Butyronitrile Glasses Resulting from Vapor Deposition: Dependence on Deposition Temperature and Comparison to Alkylbenzenes. *J. Phys. Chem. B* **2013**, *117* (35), 10311–10319.

(10) Dalal, S. S.; Sepúlveda, A.; Pribil, G. K.; Fakhraai, Z.; Ediger, M. D. Density and

Birefringence of a Highly Stable A,α,β-Trisnaphthylbenzene Glass. *J. Chem. Phys.* **2012**, *136* (20), 204501.

(11) Dalal, S. S.; Ediger, M. D. Molecular Orientation in Stable Glasses of Indomethacin. *J. Phys. Chem. Lett.* **2012**, *3* (10), 1229–1233.

(12) León-Gutierrez, E.; Garcia, G.; Clavaguera-Mora, M. T.; Rodríguez-Viejo, J. Glass Transition in Vapor Deposited Thin Films of Toluene. *Thermochim. Acta* **2009**, *492*, 51–54.

(13) Ramos, S. L. L. M.; Oguni, M.; Ishii, K.; Nakayama, H. Character of Devitrification, Viewed from Enthalpic Paths, of the Vapor-Deposited Ethylbenzene Glasses. *J. Phys. Chem. B* **2011**, *115* (49), 14327–14332.

(14) Rodríguez-Tinoco, C.; Gonzalez-Silveira, M.; Ràfols-Ribé, J.; Garcia, G.; Rodríguez-Viejo, J. Highly Stable Glasses of Celecoxib: Influence on Thermo-Kinetic Properties, Microstructure and Response towards Crystal Growth. *J. Non. Cryst. Solids* **2014**.

(15) Zhu, L.; Yu, L. Generality of Forming Stable Organic Glasses by Vapor Deposition. *Chem. Phys. Lett.* **2010**, *499*, 62–65.

(16) Lin, P.-H.; Lyubimov, I.; Yu, L.; Ediger, M. D.; de Pablo, J. J. Molecular Modeling of Vapor-Deposited Polymer Glasses. *J. Chem. Phys.* **2014**, *140* (20), 204504.

(17) Dalal, S. S.; Walters, D. M.; Lyubimov, I.; de Pablo, J. J.; Ediger, M. D. Tunable Molecular Orientation and Elevated Thermal Stability of Vapor-Deposited Organic Semiconductors. *Proc. Natl. Acad. Sci.* **2015**, *112* (14), 4227–4232.

(18) Dawson, K. J.; Zhu, L.; Yu, L.; Ediger, M. D. Anisotropic Structure and Transformation

Kinetics of Vapor-Deposited Indomethacin Glasses. *J. Phys. Chem. B* **2011**, *115* (3), 455–463.

(19) Dawson, K.; Kopff, L. a; Zhu, L.; McMahon, R. J.; Yu, L.; Richert, R.; Ediger, M. D. Molecular Packing in Highly Stable Glasses of Vapor-Deposited Tris-Naphthylbenzene Isomers. *J. Chem. Phys.* **2012**, *136* (9), 94505.

(20) Aziz, H.; Popovic, Z. D. Degradation Phenomena in Small-Molecule Organic Light-Emitting Devices. *Chem. Mater.* **2004**, *16* (23), 4522–4532.

(21) Lee, T. Y.-H.; Wang, Q.; Wallace, J. U.; Chen, S. H. Temporal Stability of Blue Phosphorescent Organic Light-Emitting Diodes Affected by Thermal Annealing of Emitting Layers. *J. Mater. Chem.* **2012**, *22* (43), 23175.

(22) Nenna, G.; Barra, M.; Cassinese, a.; Miscioscia, R.; Fasolino, T.; Tassini, P.; Minarini, C.; della Sala, D. Insights into Thermal Degradation of Organic Light Emitting Diodes Induced by Glass Transition through Impedance Spectroscopy. *J. Appl. Phys.* **2009**, *105* (12), 123511.

(23) Komino, T.; Nomura, H.; Yahiro, M.; Adachi, C. Real-Time Measurement of Molecular Orientational Randomization Dynamics during Annealing Treatments by In-Situ Ellipsometry. *J. Phys. Chem. C* **2012**, *116* (21), 11584–11588.

(24) Swallen, S. F.; Traynor, K.; McMahon, R. J.; Ediger, M. D. Stable Glass Transformation to Supercooled Liquid via Surface-Initiated Growth Front. *Phys. Rev. Lett.* **2009**, *102* (6), 65503.

(25) Kearns, K. L.; Ediger, M. D.; Huth, H.; Schick, C. One Micrometer Length Scale Controls

Kinetic Stability of Low-Energy Glasses. *J. Phys. Chem. Lett.* **2010**, *1* (1), 388–392.

(26) Sepúlveda, A.; Tylinski, M.; Guiseppi-Elie, A.; Richert, R.; Ediger, M. D. Role of Fragility in the Formation of Highly Stable Organic Glasses. *Phys. Rev. Lett.* **2014**, *113* (4), 45901.

(27) Dalal, S. S.; Ediger, M. D. Influence of Substrate Temperature on the Transformation Front Velocities That Determine Thermal Stability of Vapor-Deposited Glasses. *J. Phys. Chem. B* **2015**, *119* (9), 3875–3882.

(28) Ahrenberg, M.; Chua, Y. Z.; Whitaker, K. R.; Huth, H.; Ediger, M. D.; Schick, C. In Situ Investigation of Vapor-Deposited Glasses of Toluene and Ethylbenzene via Alternating Current Chip-Nanocalorimetry. *J. Chem. Phys.* **2013**, *138* (2), 24501.

(29) Bhattacharya, D.; Sadtchenko, V. Enthalpy and High Temperature Relaxation Kinetics of Stable Vapor-Deposited Glasses of Toluene. *J. Chem. Phys.* **2014**, *141* (9), 94502.

(30) Rodriguez-Tinoco, C.; Gonzalez-silveira, M.; Ra, J.; Lopeand, A. F.; Clavaguera-mora, M. T.; Rodríguez-Viejo, J. Evaluation of Growth Front Velocity in Ultrastable Glasses of Indomethacin over a Wide Temperature Interval. *J. Phys. Chem. B* **2014**, *118*, 10795–10801.

(31) Chen, Z.; Sepúlveda, a; Ediger, M. D.; Richert, R. Dynamics of Glass-Forming Liquids. XVI. Observation of Ultrastable Glass Transformation via Dielectric Spectroscopy. *J. Chem. Phys.* **2013**, *138* (12), 12A519.

(32) Sepúlveda, A.; Swallen, S. F.; Kopff, L. a; McMahon, R. J.; Ediger, M. D. Stable Glasses of Indomethacin and A,α,β-Tris-Naphthylbenzene Transform into Ordinary Supercooled Liquids. *J. Chem. Phys.* **2012**, *137* (20), 204508.

(33) Sepúlveda, A.; Swallen, S. F.; Ediger, M. D. Manipulating the Properties of Stable Organic Glasses Using Kinetic Facilitation. *J. Chem. Phys.* **2013**, *138* (12), 12A517.

(34) Léonard, S.; Harrowell, P. Macroscopic Facilitation of Glassy Relaxation Kinetics: Ultrastable Glass Films with Frontlike Thermal Response. *J. Chem. Phys.* **2010**, *133* (24), 244502.

(35) Wolynes, P. G. Spatiotemporal Structures in Aging and Rejuvenating Glasses. *Proc. Natl. Acad. Sci.* **2009**, *106* (5), 1353–1358.

(36) Wisitsorasak, A.; Wolynes, P. G. Fluctuating Mobility Generation and Transport in Glasses. *Phys. Rev. E* **2013**, *88* (2), 22308.

(37) Brian, C. W.; Yu, L. Surface Self-Diffusion of Organic Glasses. *J. Phys. Chem. A* **2013**, *117* (50), 13303–13309.

(38) Adachi, C.; Tsutsui, T.; Saito, S. Organic Electroluminescent Device Having a Hole Conductor as an Emitting Layer. *Appl. Phys. Lett.* **1989**, *55* (15), 1489.

(39) Dalal, S. S.; Fakhraai, Z.; Ediger, M. D. High-Throughput Ellipsometric Characterization of Vapor-Deposited Indomethacin Glasses. *J. Phys. Chem. B* **2013**, *117* (49), 15415–15425.

(40) MATERIAL), (SPACE FOR SUPPLEMENTAL. (SPACE FOR SUPPLEMENTAL MATERIAL). **2015**.

(41) Kearns, K. L.; Swallen, S. F.; Ediger, M. D.; Wu, T.; Yu, L. Influence of Substrate Temperature on the Stability of Glasses Prepared by Vapor Deposition. *J. Chem. Phys.* **2007**, *127* (15), 154702.

(42) Richert, R.; Duvvuri, K.; Duong, L.-T. Dynamics of Glass-Forming Liquids. VII. Dielectric Relaxation of Supercooled Tris-Naphthylbenzene, Squalane, and Decahydroisoquinoline.

J. Chem. Phys. **2003**, *118* (4), 1828.

(43) Vogel, H. VFT Equation.pdf. *Phys. Z.* **1921**, *22*, 645.

(44) Fulcher, G. S. Analysis of Recent Measurements of the Viscosity of Glasses. *J. Am. Ceram. Soc.* **1925**, *8* (6), 339–355.

(45) Tammann, G.; Hesse, W. Die Abhangigkeit Der Viscositat von Der Temperatur Bei Unterkuhlten Fltissigkeiten. *Z. Anorg. Allg. Chem.* **1924**, *156*, 245.

(46) Fredrickson, G.; Andersen, H. Kinetic Ising Model of the Glass Transition. *Phys. Rev. Lett.* **1984**, *53* (13), 1244–1247.

(47) Chandler, D.; Garrahan, J. P. Dynamics on the Way to Forming Glass: Bubbles in Space-Time. *Annu. Rev. Phys. Chem.* **2010**, *61*, 191–217.

(48) Keys, A. S.; Hedges, L. O.; Garrahan, J. P.; Glotzer, S. C.; Chandler, D. Excitations Are Localized and Relaxation Is Hierarchical in Glass-Forming Liquids. *Phys. Rev. X* **2011**, *1* (2), 21013.

(49) Simon, S. L.; Bernazzani, P. Structural Relaxation in the Glass: Evidence for a Path Dependence of the Relaxation Time. *J. Non. Cryst. Solids* **2006**, *352* (42–49), 4763–4768.

Chapter 4

Influence of Molecular Shape on the Thermal Stability and Molecular Orientation of Vapor-Deposited Organic Semiconductors

Diane M. Walters, M. D. Ediger

Department of Chemistry, University of Wisconsin-Madison, Madison, Wisconsin 53706

Lucas Anthony, Juan J. de Pablo

Institute for Molecular Engineering, University of Chicago, Chicago, IL 60637

Submitted to The Journal of Physical Chemistry Letters

4.1. Abstract

High thermal stability and anisotropic molecular orientation enhances the performance of vapor-deposited organic semiconductors, but controlling these properties is a challenge in amorphous materials. To understand the influence of molecular shape on these properties, vapor-deposited glasses of three disk-shaped molecules were prepared. Enhanced thermal stability is observed for glasses prepared over a wide range of substrate temperatures and anisotropic molecular orientation is observed at lower substrate temperatures. We also performed atomistic simulations of thin liquid films of two of the disk-shaped molecules and find anisotropic molecular orientation at the equilibrium liquid surface. We propose that the structure and thermal stability of vapor-deposited glasses results from high surface mobility and partial equilibration toward the structure of the equilibrium liquid surface during the deposition process. For the three molecules studied, molecular shape is a dominant factor in determining the anisotropy of vapor-deposited glasses.

4.2. Main Text

Vapor-deposited organic glasses are important materials in emerging technologies and for furthering our understanding of the amorphous state. Vapor deposition is commonly used to prepare amorphous active layers in organic electronics.[1–3] Amorphous films are desirable because they are macroscopically homogenous and their properties can be tuned by changing the preparation route. In addition, vapor deposition can produce glasses with high thermal stabilities and high densities, properties that are expected to improve lifetimes for organic electronic devices.[4–8] Furthermore, glasses produced by vapor-deposition can have very low

enthalpies, indicating a low position in the potential energy landscape that controls the structure and dynamics of amorphous systems.[9,10] These materials provide unique insight into fundamental glass behavior. For instance, it appears that secondary relaxations and tunneling two-level systems are significantly suppressed in these tightly-packed glasses.[11,12]

Controlling molecular packing in crystals is a long-standing goal for chemists but only in the last 15 years has it been recognized that packing can also be manipulated in the amorphous state through vapor deposition. While glasses prepared by more typical methods such as cooling a liquid inherit the isotropic structure of the liquid, early reports indicated horizontal molecular orientation in vapor-deposited glasses of several molecules.[13,14] Yokoyama and coworkers investigated how molecular shape and other factors influence molecular orienation.[1,15,16] They found that more anisotropic molecules produced more anisotropic glasses when deposited at room temperature. *Dalal, et. al.* systematically studied the effect of substrate temperature and found that the molecular orientation of rod-shaped molecules could be continuously controlled. [17] These trends persisted for two-component systems with rod-shaped molecules in an isotropic host.[18,19] Controlling molecular orientation in vapor-deposited active layers could improve device performance. For example, Yokoyama and coworkers reported that a glass with preferential horizontal orientation had three times higher electron mobility than an isotropic glass.[20] More recently, atomistic simulations of ethylbenzene have also shown how anisotropy can lead to improved charge transport properties.[21]

Understanding the mechanism responsible for high thermal stability and anisotropic molecular orientation in vapor-deposited glasses is important for improving organic electronic

devices. The remarkable stability of vapor-deposited glasses is believed to originate from enhanced mobility at the glass surface allowing molecules near the surface to partially equilibrate before being buried by subsequent deposition;[4] recent studies have shown diffusion at the surface of organic glasses can be up to 8 orders of magnitude faster than in the bulk.[22, 23] More equilibrated glasses are lower in the potential energy landscape and have higher barriers for rearrangement, resulting in enhanced thermal stability.[10] However, the role of surface equilibration in controlling anisotropic molecular orientation in vapor-deposited glasses is less clear. For rod-shaped organic semiconductors, it has been proposed that partial equilibration near the free surface during vapor-deposition forces molecules into anisotropic configurations that are characteristic of the those present at the surface of the equilibrium liquid.[17,24] While some studies of molecules outside of the "rod-like" designation can be interpreted in this manner,[1,25,26] there has been no systematic investigation to test the generality of this mechanism.

Here we investigate the thermal stability and molecular orientation of vapor-deposited glasses of three disk-shaped molecules used as organic semiconductors. This is the first time that vapor-deposited glasses of disk-shaped molecules have been prepared over a wide range of substrate temperatures. We find that the vapor-deposited glasses have high thermal stability. For all three molecules, glasses prepared at low substrate temperature are anisotropic with the unique symmetry axis having a tendency to be oriented perpendicular to the substrate. We simulate the equilibrium liquid of disk-shaped molecules and find there is a strong tendency for perpendicular orientation of the symmetry axis at the liquid surface. These findings suggest that the molecular orientation and thermal stability in these vapor-deposited

glasses are both derived from partial equilibration near the surface during deposition. This mechanism is expected to apply to a wide variety of organic molecules, thereby providing a major step towards establishing overarching design principles for engineering high thermal stability and molecular orientation in vapor-deposited organic glasses.

Vapor deposition was used to prepare glasses of the three disk-shaped molecules shown in Figure 1a. Also shown are three previously-studied rod-shaped molecules which we utilize for comparison. All six molecules are hole-transport materials or light emitters and are of interest for organic electronic applications. A previously described high-throughput protocol was utilized to efficiently prepare glasses of the disk-shaped molecules across a wide range of substrate temperatures ($T_{Substrate}$).[27] We confirmed through DFT calculations that the three disk-shaped molecules have a central core that is very nearly planar; x-ray crystallography of a similar molecule is consistent with this result.[28]

UV-vis absorption and spectroscopic ellipsometry were used to measure molecular orientation in the vapor-deposited glasses (see Methods). The molecules studied here have strong transition dipole moments in the plane of the disk (Figure 1a). Light polarized along the transition dipoles is more strongly absorbed than light polarized in a different direction. This leads to a change in absorbance depending on the molecular orientation of the molecules in the film, which is revealed by UV-vis absorption (Figure 1d) and spectroscopic ellipsometry.[1,19,29,30] Measuring samples prepared on a substrate with a temperature-gradient allows for rapid

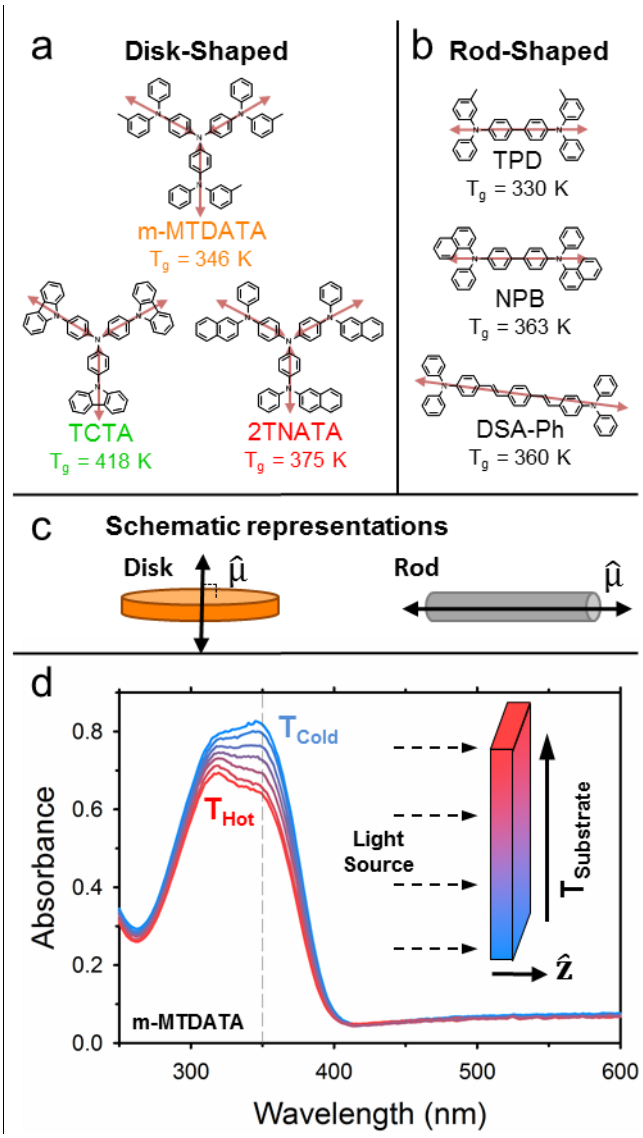

Figure 1. Molecular structures and glass transition temperatures of a) the three disk-shaped semiconductors studied here and b) previously studied rod-shaped compounds.[17] Arrows indicate the transition dipole(s). c) Schematic representations of disk- and rod-shaped molecules. Arrows indicate the unique symmetry axis $\hat{\mu}$. d) UV-vis absorbance of vapor-deposited glasses of m-MTDATA prepared at different substrate temperatures. S_z is calculated from the lowest energy absorbance, indicated with a dashed line. Inset: Schematic of the experiment.

characterization of glasses prepared at different substrate temperatures. The molecular orientation is quantified with an order parameter, S_z, defined in Equation 1:

$$S_z = \langle \frac{3}{2}(\hat{\mu} \cdot \hat{z})^2 - \frac{1}{2} \rangle \quad (1)$$

Here $\hat{z}$ is normal to the substrate and $\hat{\mu}$ is the axis used to describe the molecular orientation illustrated in Figure 1c. A S_z value of unity means $\hat{\mu}$ is perpendicular to the substrate, -0.5 means that $\hat{\mu}$ is parallel to the substrate, and 0 is consistent with the molecules having an isotropic distribution. Calculating S_z for $\hat{\mu}$, rather than for the transition dipoles, makes a fundamental connection with molecular shape and allows for disk- and rod-shaped molecules to be compared on the same scale.

Our results indicate that vapor-deposited glasses of disk-shaped molecules have high thermal stability. Ellipsometry was used to monitor the thickness of vapor-deposited glasses during thermal ramping (Figure 2a). On heating, film thickness increases due to thermal expansion. At T_{Onset} the film rapidly increases in thickness as the vapor-deposited glass transforms to the lower density supercooled liquid. T_{Onset} is higher than T_g indicating enhanced thermal stability. As shown in Figure 2b, vapor-deposited glasses of 2TNATA and m-MTDATA show enhanced stability when prepared over a wide range of substrate temperatures. Vapor-deposited glasses of TCTA also showed enhanced stability, but T_{Onset} values were above the range of our high-throughput heating stage and are not reported.

The molecular orientation of vapor-deposited disk-shaped molecules can be controlled using the substrate temperature during the deposition process. All three systems show similar trends when the substrate temperature ($T_{Substrate}$) is scaled by T_g, as shown in Figure 3. At

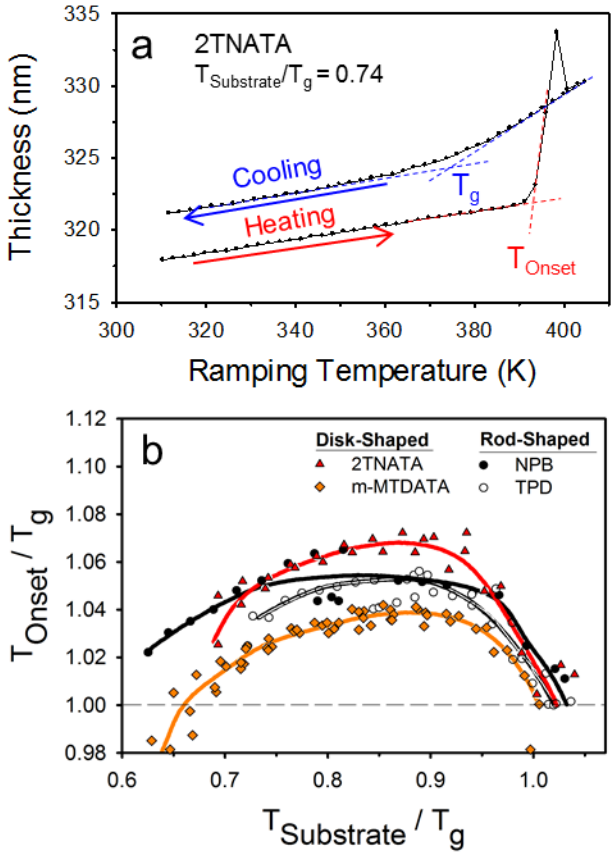

Figure 2. Thermal stability of vapor-deposited glasses of disk-shaped molecules with comparison to rod-shaped molecules**.** a) Ellipsometry monitors the thickness of a vapor-deposited glass of 2TNATA during temperature ramping. The vapor-deposited glass begins to transform into the supercooled liquid above T_g at T_{Onset}, indicating enhanced thermal stability. b) The thermal stability for vapor-deposited glasses of 2TNATA and m-MTDATA prepared at different substrate temperatures. T_{Onset} and $T_{Substrate}$ are normalized by T_g to compare different molecules. Also shown are T_{Onset} values for two rod-shaped molecules reported by *Dalal. et. al.*[17]

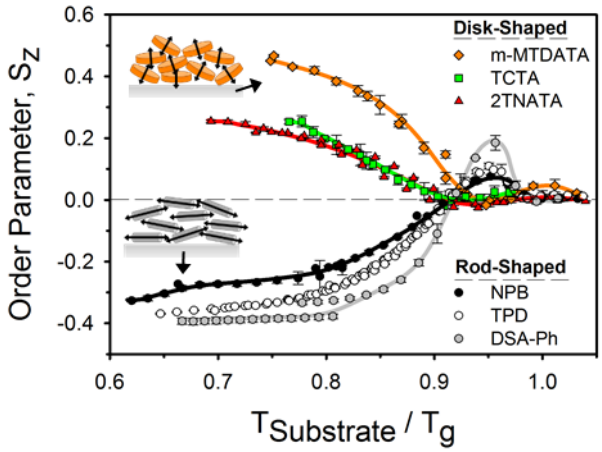

Figure 3. The order parameter, S_z, describing the average orientation of the molecular symmetry axis, $\hat{\mu}$, in vapor-deposited glasses as a function of substrate temperature during deposition. S_z is calculated from ellipsometry for 2TNATA and UV-vis for m-MTDATA and TCTA. Error bars represent 90 % confidence intervals for each substrate temperature for each sample and are typically smaller than the symbol size. Rod-shaped molecules NPB, TPD, and DSA-Ph are reproduced from *Dalal et. al.*[17] Inset cartoons illustrate the molecular orientations at low $T_{Substrate}$.

substrate temperatures above 0.9 T_g, glasses of the disk-shaped molecules have an order parameter value of approximately zero which is consistent with isotropic molecular orientation. For $T_{Substrate}$ below 0.9 T_g, the order parameter increases indicating a tendency for the symmetry axis to be oriented perpendicular to the substrate. The three disk-like molecules exhibit similar trends in molecular orientation when compared on the basis of $T_{Substrate}/T_g$.

The birefringence of the films, as measured by spectroscopic ellipsometry, provides an additional means to evaluate changes in the molecular orientation of vapor-deposited glasses. Birefringence is defined as the difference between the refractive index out-of-plane from the substrate, n_e, and in-plane, n_o. For vapor-deposited glasses of the three disk-shaped molecules, the birefringence can be controlled via the substrate temperature during the deposition, as shown in Figure 4. All three molecules show similar trends in birefringence when the substrate temperature is normalized by T_g. For these disk-shaped molecules, the birefringence and the order parameter are proportional to each other, as illustrated in the Figure 4 inset. Additionally, films with thicknesses ranging from 100 nm to 700 nm had birefringence values consistent with those reported in Figure 4, indicating that the molecular orientation is independent of film thickness and uniform within the film.

Before further discussion, we briefly comment on the glasses formed by disk- and rod-shaped molecules. Both disk- and rod-shaped molecules produce glasses with enhanced stability by vapor deposition over a considerable range of $T_{Substrate}/T_g$. Both disk- and rod-shaped molecules produce isotropic glasses for $T_{Substrate}/T_g$ very near unity, and glasses with significant anisotropy at lower values of $T_{Substrate}/T_g$. The observation that important patterns in

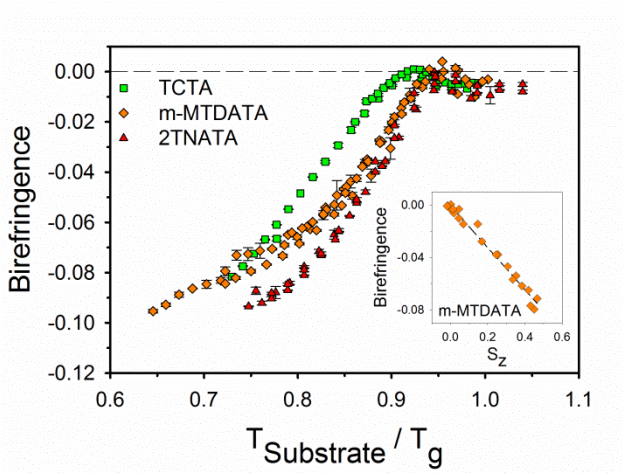

Figure 4. Birefringence of vapor-deposited glasses of three disk-shaped molecules from ellipsometric measurements. Error bars represent 90 % confidence intervals for each substrate temperature and are typically smaller than the symbol size. Inset: A comparison between the birefringence and the order parameter for m-MTDATA glasses

the data are revealed by dividing $T_{Substrate}$ by T_g immediately suggests a dominant role for molecular mobility in determining both the thermal stability and the anisotropic structure of the vapor-deposited glasses. Since bulk mobility is essentially negligible below T_g on the time scale of deposition,[22] it is reasonable to focus on the much faster surface mobility as the key influence for both disk- and rod-shaped molecules. Of course, the anisotropy of glasses formed by disk- and rod-shaped molecules show quite different dependences upon $T_{Substrate}/T_g$ in Figure 3, and a detailed mechanism must explain this difference, as we discuss below.

The enhanced thermal stability and anisotropic molecular orientation of rod-shaped molecules has been explained in terms of partial equilibration at the free surface during deposition.[17,24] *Dalal et. al.* and *Lyubimov et. al.* simulated the vapor-deposition of a coarse-grained, rod-shaped molecule at different substrate temperatures and reproduced the trends in stability and molecular orientation observed in experiments (and reproduced in Figure 2b and Figure 3).[17,24] High thermal stability was ascribed to increased equilibration at the glass surface. To test the extent that surface equilibration could explain anisotropic molecule orientation, they also simulated the equilibrium liquid and found anisotropic orientation near the free surface. The simulations indicated that high surface mobility during vapor deposition allowed molecules near the free surface to partially equilibrate towards the anisotropic structure of the free surface before being buried by subsequent deposition.

To test whether the above mechanism can be generalized to vapor-deposited glasses of disk-shaped molecules, we simulated the equilibrium liquid of disk-shaped molecules and calculated the molecular orientation near the free surface. Molecular dynamics simulations

were performed according to procedures described in the literature,[24] with further details given in Methods. For atomistic models of m-MTDATA and TCTA, Figure 5a shows the molecular orientation as a function of distance from the free surface of the equilibrium liquid at several temperatures. The free surface is defined as the distance where the film reaches 50% of its bulk density. At the free surface the equilibrium liquids have order parameter values between 0.2 to 0.4, indicating a strong tendency for $\hat{\mu}$ to orient perpendicular to the substrate. Farther away from the free surface the order parameter decreases and shows a small valley with S_z values from -0.05 to -0.1. In these simulations, S_z near the surface of the equilibrium liquid significantly increases with decreasing temperature. The simulated T_g is 388 K for m-MTDATA and 455 K for TCTA. As expected, these values are larger than the experimental T_g values due to the faster cooling rate utilized in simulations (10 K/ns vs. 1 K/min).

Partial equilibration at the free surface of the glass can explain the observed trends in thermal stability and molecular orientation for vapor-deposited glasses of disk-shaped molecules. At low substrate temperatures, surface mobility is low and only molecules very near the free surface can equilibrate. In the equilibrium liquid, molecules very near the free surface have positive order parameter values as shown in Figure 5a. Thus, molecules near the surface adopt molecular orientations with positive order parameter values and are then trapped by subsequent deposition. This happens many times until the net result is a bulk glass with a positive order parameter value. At higher substrate temperatures, greater surface mobility allows molecules located farther away from the free surface to equilibrate during deposition. As seen in Figure 5a, there is less anisotropy away from the free surface. Molecules therefore are trapped in the glass in less anisotropic molecular orientations. During deposition at

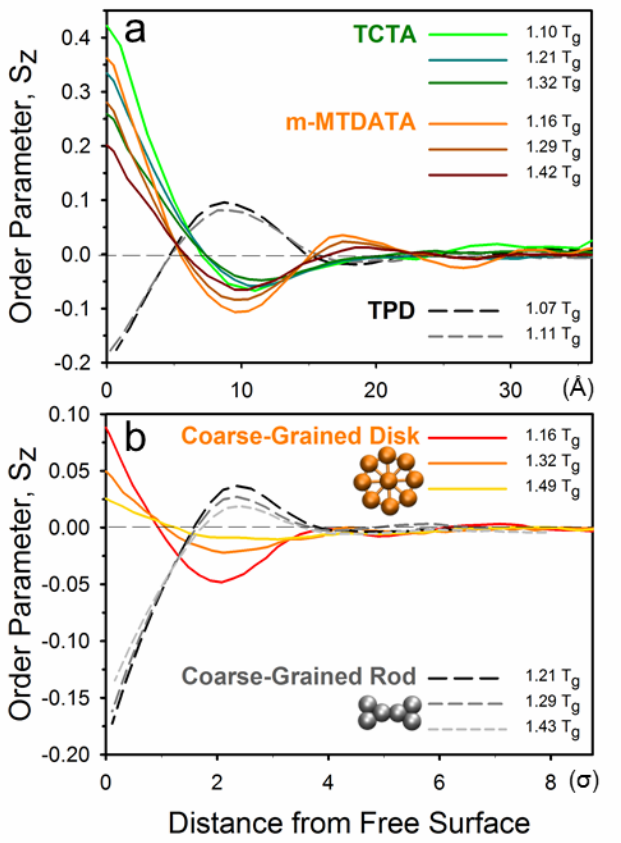

Figure 5. Molecular orientation as a function of distance from the free surface of equilibrium liquids of disk-shaped and rod-shaped molecules at different temperatures. Results for rod-shaped molecules are from ref. 17 and are included for comparison. a) Atomistic simulations. b) Simulations of coarse-grained models. Distance from the free surface is measured in terms of σ, the diameter of a Lennard Jones bead. Inset: Structures of the coarse-grained molecules.

substrate temperatures above 0.9 T_g, molecules equilibrate to depths where the equilibrium liquid exhibits a nearly isotropic molecular orientation, resulting in vapor-deposited glasses with an order parameter value of zero. The explanation given in this paragraph is consistent with the observation that molecular orientation is independent of film thickness (Figure 4). In addition, since the free surface controls the orientation eventually trapped into the glass, this mechanism predicts that the substrate chemistry is irrelevant; our experiments comparing glasses of m-MTDATA and TCTA deposited onto silicon and silica are consistent with this conclusion.

Knowledge of molecular orientation at the free surface of the equilibrium liquid allows us to understand how glasses with similarly high thermal stability (e.g., rod-like and disk-like molecules in Figure 2a) can have quite different dependences of S_z upon $T_{Substate}/T_g$. For comparison, Figures 2, 3, and 5 show results for rod-like molecules reported by *Dalal et. al.*[17] Vapor-deposited glasses of rod-shaped molecules also show enhanced thermal stability and anisotropic molecular orientation, but they show a different temperature dependence of molecular orientation upon $T_{Substate}/T_g$. As shown in Figure 5a, for TPD, the equilibrium liquid exhibits negative order parameter values near the free surface. Thus at low substrate temperatures, vapor deposition leads to glasses with a negative order parameter. During deposition near 0.95 T_g, TPD molecules are mobile down to a depth of about 10 Å where the equilibrium liquid of rod-shaped molecules exhibits a small positive order parameter; consequently vapor deposition generates glasses with a small positive order parameter. From the simulation results in Figure 5a, one might expect that deposition of disk-shaped molecules near 0.95 T_g, would result in glasses with a small negative order parameter. The data in Figures

3 and 4 show a slight tendency in this direction although this tendency does not exceed the uncertainty in S_z due to experimental errors.

To test the extent to which molecular shape alone controls molecular orientation in a vapor-deposited glass, we also simulated the equilibrium liquid of a coarse-grained model of a disk-like molecule. As shown in Figure 5b, the coarse-grained model consisted of a collection of nine Lennard-Jones sites connected by harmonic springs into a planar octagonal shape. Also in Figure 5b, we see that the equilibrium liquid of the coarse-grained disk shows trends in anisotropic surface structure similar to those observed in the atomistic simulations of m-MTDATA and TCTA: molecules near the surface have positive order parameter values and anisotropy at the free surface increases with decreasing temperature. Previous simulations with coarse-grained rods, reproduced in Figure 5b, show similar agreement with the atomistic model of TPD.[17,24] At a quantitative level, the simulations of coarse-grained molecules do not reproduce the magnitude of the anisotropic surface structure observed in atomistic simulations. However, the coarse-grained models do reproduce the qualitative features in the anisotropic surface structure. For the systems considered here, this suggests that molecular shape is the primary factor determining both the anisotropic surface structure of the equilibrium liquid and the anisotropic molecular orientation of the vapor-deposited glass.

These results show, for the first time, that vapor deposition of disk-shaped molecules used as organic semiconductors can prepare glasses exhibiting enhanced thermal stability and anisotropic molecular orientation over a wide range of substrate temperatures. Thermal stability and molecular orientation can be controlled by the choice of substrate temperature for

the deposition process. Vapor-deposited glasses of rod-shaped molecules also demonstrate high thermal stability, but they exhibit a different dependence of molecular orientation on substrate temperature. For both disk-like and rod-like molecules, we attribute these observations to efficient equilibration that occurs during deposition due to high surface mobility. Partial equilibration at the glass surface during vapor deposition allows molecules to find more thermodynamically stable packing configurations (leading to high thermal stability) and also to adopt molecular orientations that are favored near the free surface. Simulations show that disk- and rod-shaped molecules orient in different ways near the free surface, and this allows an understanding of the anisotropy of molecular orientation of the vapor-deposited glasses.

We suggest that the surface equilibration mechanism for vapor-deposited glasses described here will apply to a wide variety of organic molecules regardless of molecular shape, and also to two component systems. While molecular shape is a dominant factor in determining molecular orientation in the vapor-deposited glasses of the six molecules compared here, we expect that this will not always be the case. However, even for molecules where specific interactions might overwhelm the role of molecular shape and reduce surface mobility, we expect that the structure of the free surface of the equilibrium liquid will still allow a prediction of the anisotropic structure of vapor-deposited glasses. Deposition of a dilute guest molecule in a host material has been studied extensively because of the importance of emitter orientation in determining the efficiency of organic light emitting diodes. Much of the literature is in agreement with our view that the surface mobility of the host molecules is a key factor in determining emitter orientation in the glass.[19,31,25,32] However, for organometallic emitters,

some authors suggest that emitter orientation is slaved to host orientation,[33] while others suggest that the dilute emitter orientation is independent of the host material.[31] In contrast, we suggest that all of these systems might be well-described by the mechanism outlined here, i.e., we imagine that simulations of the free surface of a two-component liquid would allow an understanding of the anisotropic glasses produced by co-deposition of the components. For the first time, our work suggests a general mechanism for thermal stability and molecular orientation in vapor-deposited glasses of a wide variety of molecules, including systems commonly used in organic electronics. We expect this will guide the choice of molecule and deposition conditions for active layers in organic electronic devices.

4.3. Methods

Samples were prepared by physical vapor deposition onto silicon and fused silica substrates using a previously described high-throughput protocol.[27] Molecules obtained from Sigma-Aldrich (≥97% purity) were evaporated in a vacuum chamber with a base pressure of 10^{-7} torr at a rate of about 2 Å/s. A temperature gradient was applied to the substrate to efficiently prepare glasses over a wide range of substrate temperatures. Due to their low thermal conductivity, fused silica substrates were placed on a stainless steel bridge and a temperature gradient was applied to the bridge. Samples prepared at a single substrate temperature were used to calibrate the temperature of the high-throughput samples.

UV-Vis absorption at normal incidence was measured in transmission at many locations across samples (70-100 nm thick) deposited onto fused silica substrates with an imposed

temperature gradient. This procedure is a high-throughput version of a technique developed by Yokoyama and coworkers.[34] S_z was calculated from Equation 2:

$$S_z = 2\left(\frac{A}{A_{isotropic}} - 1\right) \quad (2)$$

Here A is the measured absorbance of the as-deposited glass and $A_{isotropic}$ is the absorbance of the liquid-cooled glass prepared by thermal cycling, which serves as an isotropic reference state.

Ellipsometry measurements were performed on glasses deposited onto silicon substrates using a J. A. Woollam M-2000U ellipsometer (245 – 1000 nm) at three angles.[27] For films over 100 nm, birefringence was calculated using an anisotropic Cauchy model as previously described.[5] For films with thickness ~ 100 nm, an anisotropic oscillator model meeting previous described requirements[17] was built for each material and used to determine the extinction coefficient out of the plane of the substrate (k_z) and the extinction coefficient in-plane (k_{xy}). S_z was then calculated using Equation 3:

$$S_Z = \frac{2(k_{xy} - k_z)}{k_z + 2k_{xy}} \quad (3)$$

Equations 2 and 3 are specific to disk-shaped molecules with a symmetric in-plane arrangement of transition dipoles; we verified with DFT calculations that these assumptions are met to an excellent approximation. For 2TNATA, the oscillator model provided a satisfactory description of all the vapor-deposited glasses, and the resulting values of S_z are shown in Figure 3. A satisfactory model of the ellipsometry data was not found for m-MTDATA and TCTA, but

different models agreed within ±0.05 S_z, and these results agree with the S_z values obtained by UV-Vis absorption (which are presented in Figure 3).

Molecular dynamics simulations of the equilibrium liquid were performed using the GROMACS 4.6.3 simulation package as previously described.[24] For the atomistic systems, a free standing film of about 800 molecules was prepared in a 8.5 nm x 8.5 nm x 28.0 nm box and the molecular orientation was averaged over both free surfaces. An all-atom optimized potential for liquid simulations (AA-OPLS) force field was used.[35,36] For the coarse-grained simulations, the liquid film was on a substrate consisting of 1000 LJ beads and the box size was 25 σ x 25 σ x 70 σ. The simulations were performed using the Large-Scale Atomic/Molecular Massively Parallel Simulator package (LAMMPS) in the NVT ensemble.[37] Stiff angles and bonds, where K =1000, were used to keep the octagonal shape with side length of 1 σ for the coarse-grained disk. The same pair coefficients were used as in the coarse-grained rod simulations.[17,24]

4.4. Acknowledgements

We would like to thank Noah Johnson and C. Travis Powell for helpful discussions about the experiments. The experimental measurements were supported by the US Department of Energy, Office of Basic Energy Sciences, Division of Materials Sciences and Engineering, Award DE-SC0002161. The simulations were supported by National Science Foundation DMR-1234320.

4.5. References

(1) Yokoyama, D. Molecular Orientation in Small-Molecule Organic Light-Emitting Diodes. *J. Mater. Chem.* **2011**, *21* (48), 19187.

(2) Semenza, P. OLEDs in Transition. *Inf. Disp.* **2011**, *27* (10), 14–16.

(3) Sasabe, H.; Kido, J. Recent Progress in Phosphorescent Organic Light-Emitting Devices. *European J. Org. Chem.* **2013**, *2013* (34), 7653–7663.

(4) Swallen, S. F.; Kearns, K. L.; Mapes, M. K.; Kim, Y. S.; McMahon, R. J.; Ediger, M. D.; Wu, T.; Yu, L.; Satija, S. Organic Glasses with Exceptional Thermodynamic and Kinetic Stability. *Science* **2007**, *315* (5810), 353–356.

(5) Dalal, S. S.; Ediger, M. D. Molecular Orientation in Stable Glasses of Indomethacin. *J. Phys. Chem. Lett.* **2012**, *3* (10), 1229–1233.

(6) Zhu, L.; Yu, L. Generality of Forming Stable Organic Glasses by Vapor Deposition. *Chem. Phys. Lett.* **2010**, *499*, 62–65.

(7) León-Gutierrez, E.; Garcia, G.; Clavaguera-Mora, M. T.; Rodríguez-Viejo, J. Glass Transition in Vapor Deposited Thin Films of Toluene. *Thermochim. Acta* **2009**, *492*, 51–54.

(8) Qiu, Y.; Antony, L. W.; De Pablo, J. J.; Ediger, M. D. Photostability Can Be Significantly Modulated by Molecular Packing in Glasses. *J. Am. Chem. Soc.* **2016**, *138* (35), 11282–11289.

(9) Ramos, S. L. L. M.; Oguni, M.; Ishii, K.; Nakayama, H. Character of Devitrification, Viewed from Enthalpic Paths, of the Vapor-Deposited Ethylbenzene Glasses. *J. Phys. Chem. B* **2011**, *115* (49), 14327–14332.

(10) Kearns, K. L.; Swallen, S. F.; Ediger, M. D.; Wu, T.; Sun, Y.; Yu, L. Hiking down the Energy Landscape: Progress toward the Kauzmann Temperature via Vapor Deposition. *J. Phys. Chem. B* **2008**, *112* (16), 4934–4942.

(11) Yu, H. B.; Tylinski, M.; Guiseppi-Elie, A.; Ediger, M. D.; Richert, R. Suppression of β Relaxation in Vapor-Deposited Ultrastable Glasses. *Phys. Rev. Lett.* **2015**, *115* (18), 1–5.

(12) Pérez-Castañeda, T.; Rodríguez-Tinoco, C.; Rodríguez-Viejo, J.; Ramos, M. A. Suppression of Tunneling Two-Level Systems in Ultrastable Glasses of Indomethacin. *Proc. Natl. Acad. Sci. U. S. A.* **2014**, *111* (31), 11275–11280.

(13) Lin, H. W.; Lin, C. L.; Chang, H. H.; Lin, Y. T.; Wu, C. C.; Chen, Y. M.; Chen, R. T.; Chien, Y. Y.; Wong, K. T. Anisotropic Optical Properties and Molecular Orientation in Vacuum-Deposited ter(9,9-Diarylfluorene)s Thin Films Using Spectroscopic Ellipsometry. *J. Appl. Phys.* **2004**, *95* (3), 881–886.

(14) Lin, H. W.; Lin, C. L.; Wu, C. C.; Chao, T. C.; Wong, K. T. Influences of Molecular Orientations on Stimulated Emission Characteristics of Oligofluorene Films. *Org. Electron. physics, Mater. Appl.* **2007**, *8*, 189–197.

(15) Yokoyama, D.; Sakaguchi, A.; Suzuki, M.; Adachi, C. Horizontal Molecular Orientation in Vacuum-Deposited Organic Amorphous Films of Hole and Electron Transport Materials. *Appl. Phys. Lett.* **2008**, *93* (17), 173302.

(16) Kim, J. Y.; Yokoyama, D.; Adachi, C. Horizontal Orientation of Disk-like Hole Transport Molecules and Their Application for Organic Light-Emitting Diodes Requiring a Lower

Driving Voltage. *J. Phys. Chem. C* **2012**, *116* (15), 8699–8706.

(17) Dalal, S. S.; Walters, D. M.; Lyubimov, I.; de Pablo, J. J.; Ediger, M. D. Tunable Molecular Orientation and Elevated Thermal Stability of Vapor-Deposited Organic Semiconductors. *Proc. Natl. Acad. Sci.* **2015**, *112* (14), 4227–4232.

(18) Yokoyama, D.; Sakaguchi, A.; Suzuki, M.; Adachi, C. Horizontal Orientation of Linear-Shaped Organic Molecules Having Bulky Substituents in Neat and Doped Vacuum-Deposited Amorphous Films. *Org. Electron.* **2009**, *10* (1), 127–137.

(19) Jiang, J.; Walters, D. M.; Zhou, D.; Ediger, M. Substrate Temperature Controls Molecular Orientation in Two-Component Vapor-Deposited Glasses. *Soft Matter* **2016**, *12*, 3265–3270.

(20) Yokoyama, D.; Setoguchi, Y.; Sakaguchi, A.; Suzuki, M.; Adachi, C. Orientation Control of Linear-Shaped Molecules in Vacuum-Deposited Organic Amorphous Films and Its Effect on Carrier Mobilities. *Adv. Funct. Mater.* **2010**, *20* (3), 386–391.

(21) Antony, L. W.; Jackson, N. E.; Lyubimov, I.; Vishwanath, V.; Ediger, M. D.; de Pablo, J. J. Influence of Vapor Deposition on Structural and Charge Transport Properties of Ethylbenzene Films. *ACS Cent. Sci.* **2017**. DOI: 10.1021/acscentsci.7b00041

(22) Zhu, L.; Brian, C. W.; Swallen, S. F.; Straus, P. T.; Ediger, M. D.; Yu, L. Surface Self-Diffusion of an Organic Glass. *Phys. Rev. Lett.* **2011**, *106* (25), 256103.

(23) Zhang, Y.; Fakhraai, Z. Invariant Fast Surface Diffusion on the Surfaces of Ultra-Stable and Aged Molecular Glasses. *Phys. Rev. Lett.* **2017**, *118*, 66101.

(24) Lyubimov, I.; Antony, L.; Walters, D. M.; Rodney, D.; Ediger, M. D.; de Pablo, J. J. Orientational Anisotropy in Simulated Vapor-Deposited Molecular Glasses. *J. Chem. Phys.* **2015**, *143* (9), 94502.

(25) Jurow, M. J.; Mayr, C.; Schmidt, T. D.; Lampe, T.; Djurovich, P. I.; Brütting, W.; Thompson, M. E. Understanding and Predicting the Orientation of Heteroleptic Phosphors in Organic Light-Emitting Materials. *Nat. Mater.* **2015**, *15*, 85–91.

(26) Lin, P.-H.; Lyubimov, I.; Yu, L.; Ediger, M. D.; de Pablo, J. J. Molecular Modeling of Vapor-Deposited Polymer Glasses. *J. Chem. Phys.* **2014**, *140* (20), 204504.

(27) Dalal, S. S.; Fakhraai, Z.; Ediger, M. D. High-Throughput Ellipsometric Characterization of Vapor-Deposited Indomethacin Glasses. *J. Phys. Chem. B* **2013**, *117* (49), 15415–15425.

(28) Shirota, Y. Organic Single Crystals for Electronic and Optoelectronic Devices. *J. Mater. Chem.* **2000**, *10*, 1–25.

(29) Shibata, M.; Sakai, Y.; Yokoyama, D. Advantages and Disadvantages of Vacuum-Deposited and Spin-Coated Amorphous Organic Semiconductor Films for Organic Light-Emitting Diodes. *J. Mater. Chem. C* **2015**, *3*, 11178–11191.

(30) Oelkrug, D.; Haiber, J. Electronic Spectra of Self-Organized Oligothiophene Films With “standing” and “lying” molecular Units. *Thin Solid Films* **1996**, *284–285*, 267–270.

(31) Mayr, C.; Brütting, W. Control of Molecular Dye Orientation in Organic Luminescent Films by the Glass Transition Temperature of the Host Material. *Chem. Mater.* **2015**, *27*, 2759–2762.

(32) Komino, T.; Tanaka, H.; Adachi, C. Selectively Controlled Orientational Order in Linear-Shaped Thermally Activated Delayed Fluorescent Dopants. *Chem. Mater.* **2014**, *26* (12), 3665–3671.

(33) Kim, K.-H.; Lee, S.; Moon, C.-K.; Kim, S.-Y.; Park, Y.-S.; Lee, J.-H.; Woo Lee, J.; Huh, J.; You, Y.; Kim, J.-J. Phosphorescent Dye-Based Supramolecules for High-Efficiency Organic Light-Emitting Diodes. *Nat. Commun.* **2014**, *5*, 4769.

(34) Sakai, Y.; Shibata, M.; Yokoyama, D. Simple Model-Free Estimation of Orientation Order Parameters of Vacuum-Deposited and Spin-Coated Amorphous Films Used in Organic Light-Emitting Diodes. *Appl. Phys. Express* **2015**, *8*, 96601.

(35) Jorgensen, W. L.; Maxwell, D. S.; Tirado-Rives, J. Development and Testing of the OLPS All-Atom Force Field on Conformational Energetics and Properties of Organic Liquids. *J. Am. Chem. Soc.* **1996**, *118* (15), 11225–11236.

(36) Kaminski, G. A.; Friesner, R. A.; Tirado-Rives, J.; Jorgensen, W. L. Evaluation and Reparametrization of the OPLS-AA Force Field for Proteins via Comparison with Accurate Quantum Chemical Calculations on Peptides. *J. Phys. Chem. B* **2001**, *105* (28), 6474–6487.

(37) Plimpton, S. Fast Parallel Algorithms for Short-Range Molecular Dynamics. *J. Comput. Phys.* **1995**, *117* (1), 1–19.

Chapter 5

Conclusions and Future Directions

In this final chapter, I summarize the contributions of this thesis to the larger body of knowledge. My conclusions in Section 1 focus on the two central themes of my work: the importance of equilibration at the glass surface during vapor deposition, and the benefits of using high-throughput experiments. I end with a discussion of how this work may shape the design of active layers for organic electronics and influence future studies of vapor-deposited glasses.

Additionally, I propose future experiments that could further our understanding of anisotropic molecular orientation and the transformation mechanism of vapor-deposited glasses. Section 2 describes experiments probing how strong intermolecular interactions, such as hydrogen bonding and strong electrostatic interactions, may influence molecular orientation in vapor-deposited glasses. Strong intermolecular interactions may limit mobility at the surface of the glass, but also could induce more ordered surface structures with the potential to create glasses with more anisotropic molecular orientation.

Sections 3-5 proposes experiments to understand the transformation of vapor-deposited glasses initiated in the bulk or at internal interfaces. Section 3 proposes studies of posaconazole, a molecule recently discovered to have a wide range of anisotropic molecular orientations and produces anisotropic glasses when prepared at substrate temperatures near T_g. Posaconazole studies are well suited to explore the role of the vapor-deposited glass structure in influencing the transformation behavior. I also propose studies of the

transformation behavior in sample geometries more applicable for organic electronics. Section 4 introduces studies of two-component systems, similar to active layers that serve as bulk heterojunctions in OPVs. Finally, in Section 5 I suggest a novel technique for initiating transformation in the bulk of a vapor-deposited glass. Understanding transformation behavior in the absence of a highly mobile free interface is of particular importance for applications in organic electronics, where vapor-deposited active layers are prepared in a stack and capped with a metallic anode. Through this work, I hope to better understand the important role of heightened mobility in controlling the transformation behavior.

5.1. Conclusions

The findings in this thesis highlight the importance of equilibration at the glass surface during vapor-deposition. Previously, it had been suggested that enhanced equilibration explained the high thermal stability in vapor-deposited glasses. Furthermore, the low mobility in the bulk results in the material transforming to the supercooled liquid via fronts initiated at highly mobile interfaces, like the free surface. My work supports this mechanism and shows it applies to molecules with different molecular shapes used in organic electronics. In Chapters 2 and 4, I show high thermal stability in rod- and disk-shaped organic semiconductors. In Chapter 3, I carefully characterize transformation fronts in one of these semiconductors.

My work illustrates that equilibration at the glass surface can also explain anisotropic molecular orientation in vapor-deposited glasses. I show that vapor-deposited glasses of the same molecule can have a wide range of molecular orientations when prepared at different substrate temperatures. Simulations reveal anisotropic structure at the surface of the

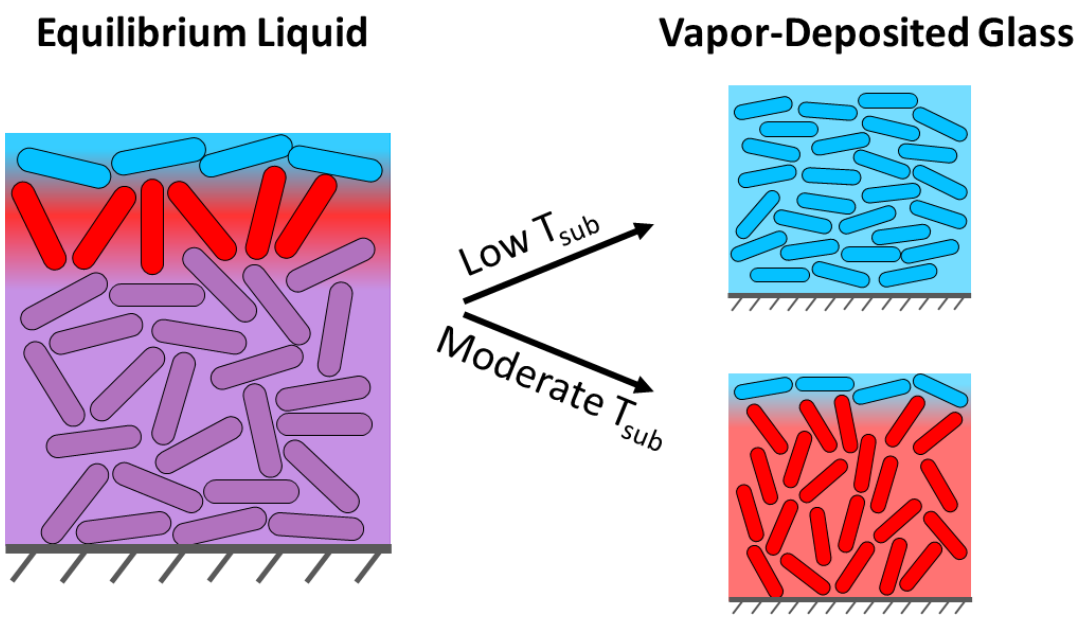

Figure 5.1. Schematic depiction of the origin of anisotropic molecular orientation in vapor-deposited glasses of rod-shaped organic semiconductors described in Chapter 2. The equilibrium liquid has anisotropic orientation near the free surface. At low substrate temperatures, T_{sub}, surface mobility is low and only molecules near the surface are able to rearranging. This leads to the horizontal orientation found at the free surface to be captured in the bulk vapor-deposited glass. At moderate substrate temperatures, surface mobility is higher and molecules near the free surface can partially equilibrate. Vertical orientation is favorable about one molecular layer from the free surface, and we observe that this orientation is trapped during the vapor deposition process.

equilibrium liquid that can explain the trend in the molecular orientation of the glass with substrate temperature. This is illustrated in Figure 5.1 for rod-shaped molecules. At low substrate temperatures, T_{sub}, only molecules near the free surface have sufficient mobility to equilibrate. This leads to the horizontal orientation found at the free surface of the equilibrium liquid to be captured in the bulk vapor-deposited glass. At moderate substrate temperatures, surface mobility is higher and molecules near the free surface can partially equilibrate. Vertical orientation is favorable about one molecular layer from the free surface, and we observe that this orientation is trapped during the vapor deposition process. Through this mechanism, anisotropic molecular orientation in vapor-deposited glasses is explained.

Furthermore, my work shows that this equilibration mechanism is general for molecules with different molecular shapes. Chapter 2 shows that it applies to rod-shaped semiconductors with a wide range of aspect ratios. Chapter 4 illustrates that the anisotropic molecular orientation of several disk-shaped molecules can also be explained by partial equilibration at the surface. Simulations of a coarse-grained model composed of Lennard-Jones beads illustrate that this behavior applies even for simple shapes mimicking the real molecules, as well as in the absence of specific molecular interactions, like π-π interactions. I hope my work will guide the choice of materials for active layers in organic electronics and the design of future experiments to expand our fundamental understanding of glasses.

My work also illustrates the power of using high-throughput experiments. By using a high-throughput sample preparation protocol and spectroscopic ellipsometry, I was able to characterize 19 different vapor-deposited glasses over a 100 K range of substrate temperatures

on a single sample. Efficiently preparing glasses over a wide variety of substrate temperature allowed me to rapidly characterize the influence of this variable on the stability and molecular orientation. Changing the substrate temperature allows me to change the mobility on the surface of the glass, allowing me to explore the role of surface equilibration in controlling glass properties. This high-throughput technique enabled me to discover that organic semiconductors can have a wide range of anisotropic molecular orientations. Before this work, nearly isotropic molecules like TPD were assumed to only form isotropic glasses. In contrast, my work in Chapter 2 shows that, by changing the substrate temperature, TPD fundamentally behaves like other rod-shaped molecules with higher aspect ratio and can form highly ordered glasses.

Additionally, I developed a high-throughput annealing protocol for characterizing the impact of annealing temperature on front velocity during the transformation of vapor-deposited glasses. Combined with the high-throughput sample preparation protocol, I was able to measure how a wide range of annealing temperatures changed the transformation front velocity in glasses prepared at many different substrate temperatures in Chapter 3. Obtaining this large amount of data allowed me to show that the substrate temperature during the sample preparation and the annealing temperature independently influenced the transformation front velocity. The annealing temperature controls the mobility of the supercooled liquid after it has been transformed and the substrate temperature controls the stability and structure of the glass. Illustrating that these components are independent simplifies our understanding of the transformation behavior; the mobility of supercooled liquids is well known, but how the structure of the glass influences the front velocity is not fully

understood. I propose further experiments to explore how the glass structure influences front velocity below.

5.2. Proposed Studies – Role of Strong Intermolecular Interactions

The work in this thesis focuses on studying systems with different molecular shapes but without strong intermolecular interactions. As was summarized above, I have found that for these systems the equilibration at the surface of the glass during the deposition controls the properties of the glass. Enhanced equilibration allows molecules to find lower energy packing configurations and adopt anisotropic structure favorable at the glass surface. This leads to glasses with enhanced thermal stability and anisotropic molecular orientation. In Chapters 2 and 4, I illustrated this mechanism for six organic molecules with different molecular shapes, and I expect it to be general even for systems with strong intermolecular interactions. However, strong intermolecular interactions may change the ability for molecules to equilibrate at the free surface of the glass, or they may change the equilibrium surface structure.

In the section below, I propose future experiments using molecules that have strong intermolecular interactions. Studying these systems will help us test the generality of the equilibration mechanism proposed in this thesis. Intermolecular interactions may also be useful in designing systems with improved orientation for applications in organic electronic devices.

5.2.1. Molecular Orientation of Dilute Organometallic Emitters

Organometallic emitters, such as Tris(2-phenylpyridinato)iridium(III) ($Ir(ppy)_3$), are of interests for use in OLEDs because they are phosphorescent and utilize both singlet and triplet

excitons, making them more efficient than traditional organic emitters that can use only singlets. However, controlling the molecular orientation of these emitters is needed to increase device efficiency. While the molecular orientation of organic emitters has been heavily studied in the last 10 year, less is known about how to control the molecular orientation of organometallic emitters and different molecular orientation mechanisms have been proposed.

Kim et. al. proposed that the organometallic emitter has strong electrostatic interactions with the host, inducing binding.[1] The orientation of the organometallic emitter was then controlled by the orientation of the host molecule. Different binding geometries may change the orientation of the emitter,[2] but typically the host molecules had horizontal molecular orientation and this is also the orientation of the emitters.[1]

In contrast, other authors have suggested that intermolecular interactions are not important.[3,4] Instead the organometallic emitters have preferential orientation at the interface that is trapped in the bulk and determines the molecule orientation of the emitters in the film. Specifically, they propose that for heteroleptic emitter with an acetylacetonate (acac) ligand, the acac ligand is preferentially aligned at the interface, resulted in preferential orientation.[3,4] It has been observed that this preferential orientation persists in several different host molecules, leading the authors to suggest that the organometallic emitters are too heavy to be equilibrate at the surface a glass regardless of the surface mobility of the host. Understanding the role of intermolecular interactions, or lack thereof, and the orientation of the emitters could lead to designing more efficient emission layers with these molecules.

To understand the role of electrostatic interactions and surface equilibration in the molecular orientation of organometallic emitters, I propose depositing organometallic emitters in hosts that enable and inhibit binding over a wide range of substrate temperatures. Fluorescence will be used to detect the orientation of a dilute emitter, such as the widely studied $Ir(ppy)_2(acac)$. Dilute concentrations are most relevant for applications in OLEDs, where the emitter is typically 3% of the film, and reduce the possibility of the emitter aggregating in the film. High-throughput sample preparation and characterization, such as what is discussed in Chapters 2-4, can be used to efficiently characterize glasses prepared at different substrate temperature. This assesses the role of equilibration in the glass properties, as preparing glasses at higher temperatures increases equilibration. Selecting hosts that could electrostatically bind to the emitter, such as NPB and TCTA, or cannot undergo binding, such as Alq_3, tests for the importance of intermolecular interactions.

I expect to find that molecular orientation is controlled by the equilibration at the surface of the equilibrium liquid. Recent results have shown that organometallic emitters can take on anisotropic molecular orientations even in hosts that have isotropic molecular orientation or unfavorable electrostatic interactions for binding.[2] This suggests that binding is not essential for anisotropic molecular orientation and another mechanism is needed to understand these materials. While it's been suggested that organometallic emitters are too heavy to reorient at the surface, films have not been prepared at high enough substrate temperatures or with a host with a low enough T_g to have high mobility at the surface during the deposition.[3] In my proposed study, I will prepare glasses over a wide range of substrate temperatures, including above the T_g of the host material, to see if high mobility will influence the molecular orientation

of the hosts. By using hosts with a wide range of T_g values (NPB = 336 K, TCTA = 418 K, Alq_3 = 450 K) I can further explore if this behavior just depends on $T_{Substrate}/T_g$ or if favorable electrostatic interactions between some of the hosts, NPB and TCTA, influence the orientation behavior of the organometallic emitter. Finding that surface equilibration controls the molecular orientation of organometallic emitter would greatly extend the range of molecules that this mechanism describes and further suggest that it is general for many systems.

5.2.2. Using Hydrogen Bonding to Engineer Molecular Orientation

Hydrogen bonding can be used to order molecules on a surface. This is seen in thin films that are up to a few monolayers thick.[5–7] However, the potential to use hydrogen bonding to direct molecular orientation in vapor deposited films has not been thoroughly explored. In a study by Yokoyama and coworkers, they found that molecules with increasing hydrogen bonding capability formed increasingly horizontally orientated films when vapor deposited.[8] A study by Schulze et. al. showed that vapor-deposited films of a hydrogen bonding system had 0.49% to 1.04% higher efficiency in an organic photovoltaic than similar systems that lacked hydrogen bonding.[9] These findings suggest that hydrogen bonding is a viable tool for engineering glasses with increased molecular orientation.

Hydrogen bonding has been shown to decrease mobility on the surface of a glass and could hinder the ability for molecule to equilibrate at the glass surface. Work by Yu and coworkers have shown for a series of molecules that greater hydrogen bonding capacity has slower surface diffusion.[10,11] In vapor-deposited glasses, Tylinski et. al. found that a series of alcohol molecules with hydrogen bonding capability formed glasses with only moderate thermal

stability, suggesting less equilibration at the surface of the glass during the deposition.[12] A similar decrease in thermal stability was seen in a series of triazine molecules with increasing hydrogen bonding capacity, although they still formed glasses with high density suggesting some degree of equilibration at the surface.[13] Limited surface mobility will hinder the ability for molecules to equilibrate and may be a challenge in designing hydrogen bonding systems with enhanced molecular orientation.

To understand how hydrogen bonding directing molecular orientation and slowly surface mobility and limiting equilibration at the glass surface contribute to the molecular orientation in vapor deposited glasses, I propose studying vapor deposited glasses of B2PyMPM, 4,6-Bis(3,5-di(pyridin-2-yl)phenyl)-2-methylpyrimidine, prepared with different deposition rates over a wide range of substrate temperatures. This system can form a hydrogen bonding network through C–H···N hydrogen bonds, it is a good glassformer, and when vapor-deposited at room temperature it prepares amorphous films with an order parameter value of -0.14, indicating small amount of preferential horizontal molecular orientation.[8]

Specifically, I am interested in systematically increasing equilibration at the surface by increasing the substrate temperature or by decreasing the deposition rate and measuring how this impacts the thermal stability and molecular orientation of B2PyMPM films. So far, B2PyMPM has only been prepared at the most common deposition rate, 2 Å/s, and at room temperature, which is just 0.77 T_g for this molecule. Previous work has indicated that hydrogen bonding systems form the most stable glasses when prepared at 0.90 – 0.95 T_g when deposited at 2 Å/s,[12,13] suggesting that B2PyMPM has not been prepared with conditions that allow it

sufficient time and mobility to equilibrate to its most stable configurations. I predict that increasing the equilibration during the deposition by changing in the preparation conditions I can compensate for the lowered surface mobility due to the hydrogen bonding and form highly stable and anisotropic glasses. This would provide evidence that the equilibration mechanism is relevant even in the presence of strong intermolecular interactions and offer a route for designing organic electronics with more anisotropic molecular orientation by harnessing intermolecular hydrogen bonding interactions.

The hydrogen bonding in B2PyMPM encourages a two-dimensional network, so I expect increased equilibration will allow for a hydrogen bonding network to form at the surface and result in horizontal molecular orientation in the films. While films vapor-deposited at room temperature show some horizontal molecular orientation (S_z = -0.14), IR absorption spectra show little peak shifting due to hydrogen bonding.[8] I believe a hydrogen bonding network was unable to form on the surface due to the low deposition temperature, 0.77 T_g. The small preference for horizontal molecular orientation is consistent with values observed for non-hydrogen bonding systems with similar shape and size.[14] I expect depositing at a slower rate and at slightly higher deposition temperature would increase equilibration at the surface and allow a hydrogen bonding network to form on the surface, resulting in increased horizontal molecular orientation.

5.3. Proposed Studies – Role of Glass Structure in Thermal Stability

To further investigate the role of the structure of vapor-deposited glasses in the transformation behavior, I propose studying the transformation behavior of posaconazole.

Vapor deposited glasses of posaconazole have been shown to have enhanced thermal stability, high density, and can be highly anisotropic.[15] Vapor deposited glasses of posaconazole have the largest range of anisotropic molecular orientations of any system without liquid crystalline states. In particular, posaconazole prepares anisotropic glasses when vapor-deposited at substrate temperatures near T_g. The huge range of molecular orientations for glass prepared at different substrate temperatures offers a route for investigating the role of molecular orientation on thermal stability and the transformation behavior for glasses of low stability prepared near T_g.

5.3.1. Role of Anisotropic Molecular Orientation

On heating above T_g, thin films of vapor-deposited glasses have been observed to transform to the supercooled liquid by fronts initiated at the free surface and other interfaces. The thermal stability of the film is determined by the velocity of these fronts. As discussed in Chapters 1 and 3, the influence of the structure of the glass on the front velocity is not well understood. Glasses of higher density generally have slower front velocities, but there is not a perfect correlation.[16] Rodgríguez-Viejo and coworkers have suggested that anisotropic molecular orientation influences front velocity, and glasses with more horizontal molecular orientation have faster fronts.[17,18] However, the range of anisotropic glasses explored is rather small and does not include glasses with significant vertical orientation.[17]

To further investigate the role of the structure of vapor-deposited glasses in the transformation behavior, I propose studying the transformation behavior of posaconazole. The huge range of molecular orientations for glass prepared at different substrate temperatures

offers a route for investigating the role of molecular orientation on thermal stability. For instance, glasses deposited with substrate temperatures below 0.88 T_g all have nearly the same birefringence but show over a 0.6% change in density.[15] Can the density predict the front velocity for these glasses? Or, does molecular orientation play a role, or is there a lower temperature regime where the fronts have different behavior? Posaconazole offers an opportunity to answer these fundamental questions about the front transformation mechanism for vapor-deposited glasses.

5.3.2. Transformation Behavior near T_g

I propose using spectroscopic ellipsometry to probe the fundamental connection between bulk and surface-initiated front transformation mechanisms in vapor-deposited glasses of posaconazole with low stability. Ordinary, liquid-cooled glasses transform via the bulk mechanism, while stable, vapor-deposited glasses transform via fronts. Directly observing both mechanisms in the same glass by using spectroscopic ellipsometry would allow us to fundamentally connect the two transformation mechanisms. I expect to see both transformation mechanisms in vapor deposited glasses deposited near T_g. As thermal stability increases, I expect that the bulk mechanism is delayed and the front mechanism dominates. I expect to also observe an increase in the crossover length as thermal stability increases. These observations would suggest a highly aged ordinary glass would transform via fronts and that stable glasses have the properties of highly aged materials.

Until recently, it has not been possible to characterize the transformation behavior of vapor-deposited glasses deposited near T_g using spectroscopic ellipsometry. Ellipsometry relies

on a contrast in the optical properties of the vapor-deposited glass and the supercooled liquid to characterize the transformation. However, glasses deposited near T_g typically share the optical properties of the equilibrium supercooled liquid.[19]Past studies have been unable to characterize glasses deposited near T_g because the materials are nearly isotropic like the liquid.[16,20] However, recently it was observed that posaconazole can form highly anisotropic glasses when deposited near T_g but has an isotropic supercooled liquid and does not have any liquid crystal states.[15] This makes it a promising candidate for studying the transformation behavior near T_g using ellipsometry. Ellipsometry could track the progression of a front through the film by using a two-layer model, and it could identify the onset of the bulk transformation by finding where the two-layer model breaks down and a homogenous model best describes the transformation.

Using ellipsometry, I will measure the front velocity for vapor-deposited films prepared with substrate temperatures near T_g. I expect to find that as I increase the substrate temperature to T_g, I will prepare glasses with increasingly lower stability and increasingly higher front velocity until I prepare glasses where I cannot observe a front. If stable glasses have the same transformation behavior as highly aged glasses, I expect this will be a smooth transition increase in front velocity. I am particularly interested in finding the highest substrate temperature where I am able to prepare a glass and observe a front; this will allow be to predict if it would be feasible to prepare a glass of equivalent stability by aging and attempt to measure a transformation front. Seeing a transformation front in an aged glass would illustrate that this transformation mechanism isn't unique to vapor-deposited glasses but instead is a feature of high stability.

5.4. Proposed Studies – Transformation behavior in two-component systems

Vapor-deposited films used as active layers in organic electronics can have multiple components. For instance, emitting layers in OLEDs contain a dilute light emitting molecule dispersed in a host. Bulk heterojunctions used in OPVs contain a mixture a hole transport material and an electron transport material. In Chapter 3 I show that a thin, vapor-deposited film composed of a single semiconductor transforms via front propagating from a free interfaces. However, the transformation mechanism has not been systematically studied in vapor-deposited films with two or more components.

I proposed preparing two-component films by vapor deposition and measuring the front velocity by spectroscopic ellipsometry. Ideally, the mixtures would be between two molecules that are relevant for applications in organic electronics, have previously been characterized, and have very different mobilities. To this end, I suggest characterizing mixtures of DSA-Ph, a blue light emitter with a T_g of 360 K, and TCTA, a hole transport material with a T_g of 418 K. The anisotropic molecular orientation and thermal stability have been investigated for a wide range of substrate temperatures in chapters 2 and 4 of this thesis. The nearly 60 K difference in glass transition temperatures suggest highly different mobilities.

For two-component glasses, I expect that the front velocity will be in part controlled by the mobility of the supercooled liquid of the mixture and structure of the underlying glass. Chapter 3 of this dissertation shows that these two factors can be considered independently. First, I expect the mobility of the supercooled liquid to depend on the T_g of the mixture. Jiang et. al. observed for two-component glasses of DSA-Ph and Alq_3 (Tris-(8-hydroxyquinoline)aluminum)

that the T_g of the mixture depended on the concentration of the high and low T_g components.[21] Furthermore, the trend in the molecular orientation of DSA-Ph depended on $T_{sub}/T_{g,mixture}$, rather than T_{sub}/T_g. This suggests T_g of the mixture described the mobility. I expect the T_g of the mixture will also predict the mobility of the supercooled liquid for a mixture. Front velocity will increase with increasing $T_{g,mixture}$.

Second, I expect the underlying glass structure to also influence the front velocity. Like what was observed in the study by Jiang, et. al. discussed above,[21] for a system without domains, I expect that the molecular orientation of each component is unperturbed and two-component films will transform with the same front velocity as the single-component films, once accounting for the different mobility of each system by normalizing by T_g of the mixture. I am particularly interested in studying very dilute concentrations of the emitter. These concentrations are most relevant for applications in OLEDs, where the emitter is typically 3% of the film. At low concentrations Jiang, et. al. reported some small changes in the molecular orientation of DSA-Ph in the film.[21] A similar change may persist to dilute concentrations and impact the structure of the film sufficiently to influence the transformation front velocity.

5.5. Proposed studies – Nucleating Transformation in the Bulk

Understanding the transformation behavior of glasses without free surfaces is important for applications in organic electronics. Vapor-deposited active layers are typically prepared in stacks that are capped with SiO_2/ITO, a metal anode, or another high T_g layer. These devices lack a free surface to initiate a transformation front, and further study is needed for the stacked film geometry to develop a microscopic understanding of the transformation mechanism in

these layers. In this section, I discuss experiments that use a novel technique described below for artificially nucleating areas with high mobility in the bulk of the film for characterizing the transformation behavior of vapor-deposited glasses.

I propose generating nucleation sites in a vapor-deposited film by co-depositing a dilute azobenzene and then exciting the azobenzene to disrupt the surrounding glass packing and generate a site with increased mobility. I expect these sites would nucleate the transformation of the vapor-deposited glass to the liquid and then propagate outward as growing bubbles, similar to what is expected for the bulk mechanism as was explained in Chapter 1, Section 1.3.3. I expect that transformation can be initiated in a bulk film a dilute emitter is excited in an emission layer repeatedly and eventually form a nucleation point; this technique is an exaggerated case of transformation mechanism. In particular, I suggest using the azobenzene Disperse Orange 37, 3-[[4-(2,6-dichloro-4-nitrophenyl)azo]-N-ethylanilino]-pro-pionitrile, which has previously been shown to disrupt the packing of vapor-deposited glasses when exposed to 532 nm light.[22] Most semiconductors are transparent at 532 nm, so the bulk of the vapor deposited glass by the exposure. By controlling the concentration of azobenzene in the film, I can change the number of sites with enhanced mobility in the film. I anticipate increasing the concentration of azobenzene will systematically decrease the transformation time of the film. Below, I propose studies that use this technique to understand transformation behavior initiated in the bulk of a vapor-deposited glass.

5.5.1. Transformation in a Capped Vapor-Deposited Layer

In my first experiment, I propose exploring the transformation behavior in the bulk of a vapor-deposited glass. I propose depositing a 150 nm layer of TPD, where the center 20 nm are co-deposited with Disperse Orange 37, an azobenzene, at about 3% concentration. TPD is a hole transport material and its transformation fronts velocities were characterized in Chapter 3 of this thesis. This makes TPD a relevant and well-studied system ideal for further study. TCTA will be vapor-deposited above and below this TPD layer so serve as a capping layer and prevent transformation via a front initiated at the free surface. TCTA has a significantly higher T_g than TPD (418 K vs 330 K), so it should effectively serve as an immobile interface even when annealing above T_g for TPD. Depositing a TCTA layer both above and below the TPD layer will eliminate any effects of the substrate. The possible substrate effects are explored in the following section.

I will expose the stacked layers to 532 nm light to excite the azobenzenes within the TPD layer and disrupt the packing, and then use spectroscopic ellipsometry to measure the transformation behavior of the TPD film on annealing. On annealing, I anticipate the 20 nm layer containing azobenzenes will transform homogenously according to an ellipsometry model. Even at a 3% concentration, there will be enough azobenzenes nucleating transformation within the 500 μm ellipsometry beam to not be able to distinguish individual nucleation points. There is a 1% volume increase during the transformation, and using ellipsometry I am interested in measuring the thickness change of each modeled layer so see if the film expands

or if other signatures of stress occur, such as changes in the refractive index of the neighboring glass layers.

Once the center 20 nm has transformed, I anticipate a front will propagate from this high mobility region. I am interested in studying the transformation time of the center 20 nm containing the azobenzenes and the transformation front velocity initiated from this layer. Is there an induction time in transformation from the nucleation sites? Will the front velocity be the same in when initiated from nucleation sites in the bulk as from a free surface? Previous SIMS studies show a front initiated from an internal ordinary glass interface has a similar velocity as a front from the free surface.[23] This finding leads me to expect that a front initiated from nucleation points to have the same velocity as fronts from the free surface, but my proposed study would be the first using small nucleation sites.

Ellipsometry is a good technique for this study because it is sensitive to the changes in the optical properties of the layers and can measure the propagation of a transformation front. To ensure sufficient optical contrast between the TPD vapor-deposited glass, the transformed supercooled liquid, and the capping TCTA layers, I will vapor-deposit the TCTA and TPD films with a substrate temperature of 280 K. At this substrate temperature, TPD films have an order parameter value of about -0.35, TCTA films have an anticipated order parameter value of -0.15, calculated for the transition dipoles, the supercooled liquid is isotropic, and a 3% concentration of azobenezene is not expected to perturb the optical properties of the film. This is sufficient optical contrast to distinguish the TPD and TCTA layers, as well as transformation of the TPD

glass to the supercooled liquid. Additionally, a substrate temperature of 280 K prepares TPD glasses with the maximum thermal stability, making these glasses the most interesting to study.

5.5.2. Transformation at the Substrate

My second experiment will use nucleated transformation sites to explore transformation in a bulk film near a substrate. The influence of the substrate on the transformation behavior of vapor-deposited glasses in poorly understood, but is particularly relevant for many applications. One challenge is that few techniques are independently sensitive to fronts originating from the substrate or other transformation behavior in very thin films. SIMS and ellipsometry are the only techniques that have been used to study the transformation behavior in glasses that can directly observe fronts, and the presence of multiple fronts can sometimes be inferred from bulk techniques such as nanocalorimetry.[24] In previous work, sometimes transformation fronts initiated from a substrate and in one study there seemed some dependence on the substrate temperature, but this behavior could not be predicted.[16,23–25] When fronts were initiated from the substrate, they were found to have the same velocity as fronts initiated from the free surface,[16] or about half the velocity.[25] Understanding the transformation behavior near an interface is important because films in organic electronics are often only 20-30 nm thick, so understanding transformation behavior near a substrate or another interface could allow for better devices to be designed.

Mimicking the design of the experiment above, I propose vapor-depositing a 150 TPD film, where the first 20 nm are co-deposited with Disperse Orange 37 at a dilute concentration. The film will be capped with a layer of TCTA. To test the effect of different interfaces on the

transformation behavior, the TPD layer can be vapor-deposited directly onto a silicon substrate or onto another TCTA layer to explore the effect of a stable organic layer. As described above, 532 nm light will be used to excite the azobenzenes in the glass and generate nucleation sites. The film will then be heated above T_g and the transformation behavior monitored using ellipsometry. I can compare the results to the experiment above to understand the impact of a very low mobility interface bordering the vapor-deposited glass on the transformation behavior. I would not expect a significant difference between the transformation front behavior near different low mobility interfaces. However, I hope these results will shed light on the surprising findings that glasses of lower stabilities initiated fronts from a substrate and could have just a fraction of the front velocity.[16,25] Understanding the transformation behavior near the substrate and other vapor-deposited glass interfaces is essential for increasing thermal stability in active layers.

5.6. References

(1) Kim, K.-H.; Lee, S.; Moon, C.-K.; Kim, S.-Y.; Park, Y.-S.; Lee, J.-H.; Woo Lee, J.; Huh, J.; You, Y.; Kim, J.-J. Phosphorescent Dye-Based Supramolecules for High-Efficiency Organic Light-Emitting Diodes. *Nat. Commun.* **2014**, *5*, 4769.

(2) Moon, C.-K.; Kim, K.-H.; Lee, J. W.; Kim, J.-J. Influence of Host Molecules on Emitting Dipole Orientation of Phosphorescent Iridium Complexes. *Chem. Mater.* **2015**, *27*, 2767–2769.

(3) Mayr, C.; Brütting, W. Control of Molecular Dye Orientation in Organic Luminescent Films by the Glass Transition Temperature of the Host Material. *Chem. Mater.* **2015**, *27*, 2759–

2762.

(4) Jurow, M. J.; Mayr, C.; Schmidt, T. D.; Lampe, T.; Djurovich, P. I.; Brütting, W.; Thompson, M. E. Understanding and Predicting the Orientation of Heteroleptic Phosphors in Organic Light-Emitting Materials. *Nat. Mater.* **2015**, *15*, 85–91.

(5) Xu, W.; Dong, M.; Gersen, H.; Rauls, E.; Vázquez-Campos, S.; Crego-Calama, M.; Reinhoudt, D. N.; Lægsgaard, E.; Stensgaard, I.; Linderoth, T. R.; et al. Influence of Alkyl Side Chains on Hydrogen-Bonded Molecular Surface Nanostructures. *Small* **2008**, *4*, 1620–1623.

(6) Meier, C.; Ziener, U.; Landfester, K.; Weihrich, P. Weak Hydrogen Bonds as a Structural Motif for Two-Dimensional Assemblies of Oligopyridines on Highly Oriented Pyrolytic Graphite: An STM Investigation. *J. Phys. Chem. B* **2005**, *109* (44), 21015–21027.

(7) Xu, W.; Zhang, C.; Gersen, H.; Sun, Q.; Kong, H.; Dong, L.; Sheng, K.; Tan, Q.; Laegsgaard, E.; Besenbacher, F. A Molecular Conformational Change Induced Self-Assembly: From Randomness to Order. *Chem. Commun.* **2013**, *49* (110), 5207–5209.

(8) Yokoyama, D.; Sasabe, H.; Furukawa, Y.; Adachi, C.; Kido, J. Molecular Stacking Induced by Intermolecular C-H···N Hydrogen Bonds Leading to High Carrier Mobility in Vacuum-Deposited Organic Films. *Adv. Funct. Mater.* **2011**, *21* (8), 1375–1382.

(9) Schulze, B. M.; Shewmon, N. T.; Zhang, J.; Watkins, D. L.; Mudrick, J. P.; Cao, W.; Bou Zerdan, R.; Quartararo, A. J.; Ghiviriga, I.; Xue, J.; et al. Consequences of Hydrogen Bonding on Molecular Organization and Charge Transport in Molecular Organic

Photovoltaic Materials. *J. Mater. Chem. A* **2014**, *2* (5), 1541–1549.

(10) Chen, Y.; Zhang, W.; Yu, L. Hydrogen Bonding Slows Down Surface Diffusion of Molecular Glasses. *J. Phys. Chem. B* **2016**, *120* (32), 8007–8015.

(11) Brian, C. W.; Yu, L. Surface Self-Diffusion of Organic Glasses. *J. Phys. Chem. A* **2013**, *117* (50), 13303–13309.

(12) Tylinski, M.; Chua, Y. Z.; Beasley, M. S.; Schick, C.; Ediger, M. D. Vapor-Deposited Alcohol Glasses Reveal a Wide Range of Kinetic Stability. *J. Chem. Phys.* **2016**, *145*, 174506.

(13) Laventure, A.; Gujral, A.; Lebel, O.; Pellerin, C.; Ediger, M. D. Influence of Hydrogen Bonding on the Kinetic Stability of Vapor-Deposited Glasses of Triazine Derivatives. *J. Phys. Chem. B* **2017**, *121*, 2350–2358.

(14) Yokoyama, D. Molecular Orientation in Small-Molecule Organic Light-Emitting Diodes. *J. Mater. Chem.* **2011**, *21* (48), 19187.

(15) Gómez, J.; Gujral, A.; Huang, C.; Bishop, C.; Yu, L.; Ediger, M. D. Nematic-like Stable Glasses without Equilibrium Liquid Crystal Phases. *J. Chem. Phys.* **2017**, *146* (5), 54503.

(16) Dalal, S. S.; Ediger, M. D. Influence of Substrate Temperature on the Transformation Front Velocities That Determine Thermal Stability of Vapor-Deposited Glasses. *J. Phys. Chem. B* **2015**, *119* (9), 3875–3882.

(17) Rodríguez-Tinoco, C.; Gonzalez-Silveira, M.; Ràfols-Ribé, J.; Lopeandia, A.; Rodriguez-Viejo, J. Transformation Kinetics of Vapor-Deposited Thin Film Organic Glasses: Role of

Stability and Molecular Packing Anisotropy. *Phys. Chem. Chem. Phys.* **2015**, *17*, 31195–31201.

(18) Rodríguez-Tinoco, C.; Ràfols-Ribé, J.; González-Silveira, M.; Rodríguez-Viejo, J. Relaxation Dynamics of Glasses along a Wide Stability and Temperature Range. *Sci. Rep.* **2016**, *6*, 35607.

(19) Dalal, S. S.; Fakhraai, Z.; Ediger, M. D. High-Throughput Ellipsometric Characterization of Vapor-Deposited Indomethacin Glasses. *J. Phys. Chem. B* **2013**, *117* (49), 15415–15425.

(20) Walters, D. M.; Richert, R.; Ediger, M. D. Thermal Stability of Vapor-Deposited Stable Glasses of an Organic Semiconductor. *J. Chem. Phys.* **2015**, *142* (13), 134504.

(21) Jiang, J.; Walters, D. M.; Zhou, D.; Ediger, M. Substrate Temperature Controls Molecular Orientation in Two-Component Vapor-Deposited Glasses. *Soft Matter* **2016**, *12*, 3265–3270.

(22) Qiu, Y.; Antony, L. W.; De Pablo, J. J.; Ediger, M. D. Photostability Can Be Significantly Modulated by Molecular Packing in Glasses. *J. Am. Chem. Soc.* **2016**, *138* (35), 11282–11289.

(23) Sepúlveda, A.; Swallen, S. F.; Ediger, M. D. Manipulating the Properties of Stable Organic Glasses Using Kinetic Facilitation. *J. Chem. Phys.* **2013**, *138* (12), 12A517.

(24) Tylinski, M.; Sepúlveda, A.; Walters, D. M.; Chua, Y. Z.; Schick, C.; Ediger, M. D. Vapor-Deposited Glasses of Methyl-M-Toluate: How Uniform Is Stable Glass Transformation? *J. Chem. Phys.* **2015**, *143* (24), 244509.

(25) Sepúlveda, A.; Swallen, S. F.; Kopff, L. a; McMahon, R. J.; Ediger, M. D. Stable Glasses of Indomethacin and A,α,β-Tris-Naphthylbenzene Transform into Ordinary Supercooled Liquids. *J. Chem. Phys.* **2012**, *137* (20), 204508.